



2012

DISRUPTIONS IN THE REGULATION OF EXTRACELLULAR GLUTAMATE IN THE RAT CENTRAL NERVOUS SYSTEM AFTER DIFFUSE BRAIN INJURY

Jason Michael Hinzman
University of Kentucky, jmhinz2@uky.edu

[Right click to open a feedback form in a new tab to let us know how this document benefits you.](#)

Recommended Citation

Hinzman, Jason Michael, "DISRUPTIONS IN THE REGULATION OF EXTRACELLULAR GLUTAMATE IN THE RAT CENTRAL NERVOUS SYSTEM AFTER DIFFUSE BRAIN INJURY" (2012). *Theses and Dissertations--Neuroscience*. 2.
https://uknowledge.uky.edu/neurobio_etds/2

This Doctoral Dissertation is brought to you for free and open access by the Neuroscience at UKnowledge. It has been accepted for inclusion in Theses and Dissertations--Neuroscience by an authorized administrator of UKnowledge. For more information, please contact UKnowledge@lsv.uky.edu.

STUDENT AGREEMENT:

I represent that my thesis or dissertation and abstract are my original work. Proper attribution has been given to all outside sources. I understand that I am solely responsible for obtaining any needed copyright permissions. I have obtained and attached hereto needed written permission statements(s) from the owner(s) of each third-party copyrighted matter to be included in my work, allowing electronic distribution (if such use is not permitted by the fair use doctrine).

I hereby grant to The University of Kentucky and its agents the non-exclusive license to archive and make accessible my work in whole or in part in all forms of media, now or hereafter known. I agree that the document mentioned above may be made available immediately for worldwide access unless a preapproved embargo applies.

I retain all other ownership rights to the copyright of my work. I also retain the right to use in future works (such as articles or books) all or part of my work. I understand that I am free to register the copyright to my work.

REVIEW, APPROVAL AND ACCEPTANCE

The document mentioned above has been reviewed and accepted by the student's advisor, on behalf of the advisory committee, and by the Director of Graduate Studies (DGS), on behalf of the program; we verify that this is the final, approved version of the student's dissertation including all changes required by the advisory committee. The undersigned agree to abide by the statements above.

Jason Michael Hinzman, Student

Dr. Greg A. Gerhardt, Major Professor

Dr. Wayne A. Cass, Director of Graduate Studies

DISRUPTIONS IN THE REGULATION OF EXTRACELLULAR GLUTAMATE IN THE
RAT CENTRAL NERVOUS SYSTEM AFTER DIFFUSE BRAIN INJURY

DISSERTATION

A dissertation submitted in partial fulfillment of the
requirements for the degree of Doctor of Philosophy in the
College of Medicine at the University of Kentucky

By
Jason Michael Hinzman

Lexington, Kentucky

Director: Dr. Greg A. Gerhardt, Professor of Anatomy and Neurobiology

Lexington, KY

2012

Copyright © Jason Michael Hinzman

ABSTRACT OF DISSERTATION

DISRUPTIONS IN THE REGULATION OF EXTRACELLULAR GLUTAMATE AFTER DIFFUSE BRAIN INJURY

By

Jason Michael Hinzman

Glutamate, the predominant excitatory neurotransmitter in the central nervous system, is involved in almost all aspects of neurological function including cognition, motor function, memory, learning, decision making, and neuronal plasticity. For normal neurological function, glutamate signaling must be properly regulated. Disrupted glutamate regulation plays a pivotal role in the acute pathophysiology of traumatic brain injury (TBI), disrupting neuronal signaling, initiating secondary injury cascades, and producing excitotoxicity. Increases in extracellular glutamate have been correlated with unfavorable outcomes in TBI survivors, emphasizing the importance of glutamate regulation.

The aim of this thesis was to examine disruptions in the regulation of extracellular glutamate after experimental TBI. In these studies, we used glutamate-sensitive microelectrode arrays (MEAs) to examine the regulation of extracellular glutamate two days after diffuse brain injury. First, we examined which brain regions were vulnerable to post-traumatic increases in extracellular glutamate. We detected significant increases in extracellular glutamate in the dentate gyrus and striatum, which correlated to the severity of brain injury. Second, we examined the regulation of extracellular glutamate by neurons and glia to determine the mechanisms responsible for post-traumatic increases in extracellular glutamate. In the striatum of brain-injured rats, we detected significant disruptions in release of glutamate by neurons and significant decreases in the removal of glutamate from the extracellular space by glia. Third, we examined if a novel therapeutic strategy, a viral-vector mediated gene delivery approach, could improve the regulation of extracellular glutamate. Infusion of an adeno-associated virus expressing a glutamate transporter into the rat striatum produced significant improvements in glutamate clearance, identifying a novel strategy to reduce excitotoxicity. Lastly, we examined the translational potential of MEAs as novel neuromonitoring device for clinical TBI research. Overall, these studies have demonstrated the translational potential of MEAs to aid in the diagnosis and treatment of TBI survivors.

KEYWORDS: midline fluid percussion injury, amperometry, excitatory amino acid transporters

DISRUPTIONS IN THE REGULATION OF EXTRACELLULAR GLUTAMATE IN THE
RAT CENTRAL NERVOUS SYSTEM AFTER DIFFUSE BRAIN INJURY

By

Jason Michael Hinzman

Dr. Greg A. Gerhardt
Director of Dissertation

Dr. Wayne A. Cass
Director of Graduate Studies

4/13/2012

Dedicated to my wife, our son, my parents and grandparents, and to all my friends and family who have helped me along the way

Acknowledgments

Completion of the following dissertation would not have been possible without the ongoing support, guidance, and assistance from several people. I am truly grateful for my parents and grandparents past and ongoing support, and a special gratitude for the time they spent with me to instill the skills, values, and desire necessary to pursue my goals. Also, I would like to thank my group of friends, whom I consider family, for their ongoing support and friendship over the years.

The successes of the outlined studies would not have been possible without the support and guidance of my mentor Dr. Greg Gerhardt, who started mentoring me as an undergraduate student. Dr. Gerhardt recruited me to join his lab for my thesis work and has played an instrumental role in shaping my scientific thinking. I am truly grateful for his mentorship throughout the years and look forward to continuing our friendship and scientific endeavors throughout the upcoming years. Also, I would like to thank Dr. Jonathan Lifshitz, who has shouldered much of my professional development and is greatly responsible for the success of these studies. Next, I wish to thank my dissertation committee, Dr. Jim Geddes, Dr. Ed Hall, and Dr. Nada Porter who provided insight, guided my research project, and also challenged my thinking along the way. Also I would like to thank Dr. Bret Smith for taking the time to be my outside examiner.

I need to thank Dr. Brandon Harvey for his guidance and expertise allowing completion of the viral studies. Jason Burmeister for his assistance with data analysis, electrode coatings, and calibrations that made completion of these studies possible. Dr. Theresa Currier Thomas, a past and present lab member, for guidance and review of my thesis work. Dr. Jorge Quintero for his countless answers to my questions and discussion about my research projects, completion of these studies would not have been possible without his guidance. I am truly grateful for his wisdom and advice throughout the years. Francois Pomerleau, Robin Lindsay, and Peter Huettl for their assistance and guidance in the laboratory, having help in the time of need is greatly appreciated. My classmate, Dr. Meagan Littrell, who shared with me the trials and tribulations of graduate school. Amanda Lisembee for assistance with fluid percussion brain injury. Ad-Tech Medical Instrument Corporation for providing devices used in this thesis. Kevin Hascup, Erin Hascup, David Price, Martin Lundbland, Josh Fuqua, for their friendship and scientific mentoring, which made success of these studies possible and means a great deal to me. Thanks to the past and present members of the Gerhardt and Lifshitz lab, for your support and providing an enjoyable environment for completion of these studies. I would also like to thank the students who I had the opportunity to mentor and made completion of this work possible, Laura Crawford, Emily Cottrell, Kawthar Suleiman, and Seth Batten. I hope I was able to teach them as much as they taught me.

Most importantly, I would like to thank my wonderful wife, Ashley, who has provided unlimited love, support, encouragement, and understanding during my thesis work. Lastly, I would like to thank our son, Henry, for his unlimited love, toothless grins, and giggles providing the best reward when I come home at the end of the day. And once again, a special thanks to my wife who had to take care of Henry while I was writing this dissertation.

Table of Contents

Acknowledgments	iii
List of Tables.....	viii
List of Figures.....	ix
Chapter One: Introduction.....	1
Traumatic Brain Injury	1
Glutamate's Role as a Neurotransmitter in the Central Nervous System.....	2
Glutamate's Role in the Pathophysiology of TBI	4
Chapter One: Figures	8
Chapter One: Tables	11
Preface to Chapter Two	14
Chapter Two: Diffuse Brain Injury Elevates Tonic Glutamate Levels and Potassium- Evoked Glutamate Release in Discrete Brain Regions at Two Days Post-Injury: an Enzyme-Based Microelectrode Array Study	14
Abstract	14
Introduction.....	15
Methods.....	17
Animals	17
Midline Fluid Percussion Injury	17
Enzyme-Based Microelectrode Arrays.....	18
MEA Calibration	19
MEA/Micropipette Assembly	20
<i>In Vivo</i> Anesthetized Recording.....	20
Data Analysis	21
Results.....	21
Prefrontal Cortex: Tonic and Evoked Glutamate Release	21
Dentate Gyrus: Tonic and Evoked Glutamate Release	22
Striatum: Tonic and Evoked Glutamate Release	22
Tonic Glutamate Levels Correlate with Injury Force	23

Discussion	24
Chapter Two: Figures	28
Chapter Two: Tables	34
Preface to Chapter Three.....	35
Chapter Three: Disruptions in the Regulation of Extracellular Glutamate by Neurons and Glia in the Rat Striatum Two Days after Diffuse Brain Injury.....	35
Abstract	35
Introduction.....	36
Materials and Methods	38
Animals	38
Midline fluid percussion injury (FPI)	38
Enzyme-based microelectrode arrays	39
MEA calibration.....	40
MEA/micropipette assembly	40
<i>In vivo</i> anesthetized recordings of extracellular glutamate	41
Quantitative gene expression (rtPCR)	42
Statistical analyses	42
Results.....	42
Increased extracellular glutamate in the striatum of brain-injured rats.....	43
Reduced calcium channel-dependent glutamate release in the striatum of brain- injured rats	43
Activation of mGluR _{2/3} failed to reduce extracellular glutamate in the striatum of sham and brain-injured rats	44
Inhibition of the glial x_c^- failed to reduce extracellular glutamate in the striatum of sham and brain-injured rats	44
Increased glutamate spillover from the inhibition of glutamate uptake in the striatum of brain-injured rats	44
Decreased glutamate clearance in the striatum of brain-injured rats.....	45
Discussion	46
Chapter Three: Figures	54
Chapter Three: Tables.....	59
Preface to Chapter Four.....	60

Chapter Four: Targeted expression of the glutamate transporter, GLT-1, in the rat striatum using a viral vector-mediated gene delivery approach	60
Abstract	60
Introduction.....	61
Materials and Methods	62
Animals	62
Construction, packaging, purification and titering of AAV vectors.....	63
Intracerebral AAV injections.....	63
Enzyme-based microelectrode arrays	64
MEA/micropipette assembly	64
<i>In vivo</i> anesthetized recordings of extracellular glutamate	65
Data analysis	66
Histology	66
Quantitative gene expression (rtPCR)	66
Results.....	67
Single infusion of AAV- GLT-1/RFP increases expression of functional GLT-1 in the rat striatum	67
Multiple infusions of AAV- GLT-1 within the striatum failed to express functional GLT-1	68
Discussion	69
Chapter Four: Figures	73
Chapter Four: Tables.....	80
Preface to Chapter Five	81
Chapter Five: Development of a novel neuromonitor for clinical TBI research: enzyme-based microelectrode arrays for real-time <i>in vivo</i> detection of neurochemicals.....	81
Abstract	81
Introduction.....	82
Materials and Methods	84
Animals	84
Continuous recordings of extracellular glutamate for 72 hours in awake animals ...	84
Multiple Analyte Calibrations.....	85
Modification of FDA-approved device (AD-TECH® Epilepsy/LTM macro-micro depth electrode) for <i>in vivo</i> detection of glutamate	86

Results.....	87
MEAs can continuously measure extracellular glutamate for the initial 72 hours after implantation.....	87
Detection of multiple analytes of interest using a single MEA (glutamate, lactate, pyruvate, or glucose)	88
Modification of FDA approved device (AD-TECH® Epilepsy/LTM macro-micro depth electrode) for <i>in vivo</i> detection of glutamate	90
Discussion	92
Chapter Five: Figures	97
Chapter Six: Overall Conclusions	104
Chapter Six: Figures.....	110
References.....	111
VITA	129

List of Tables

Table 1.1 Glasgow Coma Scale (GCS)	11
Table 1.2 Ionotropic Glutamate Receptors	11
Table 1.3 Metabotropic Glutamate Receptors	12
Table 1.4 Excitatory Amino Acid Transporters (EAATs)	13
Table 2.1 Clearance Parameters of KCl-Evoked Glutamate Release.....	34
Table 3.1 Effect of local application of drugs on extracellular glutamate in sham and traumatic brain injured (TBI) animals	59
Table 4.1 Comparison of glutamate clearance between the AAV-GFP and AAV-GLT-1 treated hemispheres	80

List of Figures

Figure 1.1 Schematic of a glutamate synapse	8
Figure 1.2 Schematic and diagram depicting glutamate's role in the initiation, propagation, and amplification of secondary brain injury	10
Figure 2.1 Methods for microelectrode array glutamate recordings.....	28
Figure 2.2 Tonic and KCl-evoked release of glutamate in the prefrontal cortex of the urethane anesthetized rat	30
Figure 2.3 Tonic and KCl-evoked release of glutamate in the dentate gyrus in the hippocampus of the urethane anesthetized rat	31
Figure 2.4 Tonic and KCl-evoked release of glutamate in the striatum of the urethane anesthetized rat.....	32
Figure 2.5 Correlations of tonic glutamate levels with force of injury in the rat prefrontal cortex, dentate gyrus, and striatum.....	33
Figure 3.1 Increased extracellular glutamate in the striatum of brain-injured rats at two days after midline fluid percussion brain injury	54
Figure 3.2 Reduced calcium channel-dependent glutamate release in the striatum of brain-injured rats	55
Figure 3.3 Increased glutamate spillover from inhibition of glutamate uptake in the striatum of brain-injured rats	56
Figure 3.4 Decreased glutamate clearance in the striatum of brain-injured rats.....	57
Figure 3.5 Schematic depicting the regulation of extracellular glutamate in the rat striatum in sham and brain-injured animals	58
Figure 4.1 Representation of the sites for the viral infusion and glutamate recordings in the rat striatum	73
Figure 4.2 Representation of the sites for the viral infusion, glutamate recordings, and tissue punches for gene expression in the rat striatum.....	74
Figure 4.3 Representative in vivo recording from a glutamate-oxidase site and sentinel site of the MEA.....	75
Figure 4.4 Faster glutamate clearance in AAV-GLT-1 treated hemisphere compared to AAV-GFP hemisphere.....	76

Figure 4.5 Expression of green and red fluorescent protein in the striatum three weeks after infusion of AAV-GFP and AAV-GLT-1/RFP	77
Figure 4.6 Similar rates of glutamate clearance in the AAV-GFP and AAV-GLT-1 treated hemispheres.....	78
Figure 4.7 Similar amounts of GLT-1 gene expression between the AAV-GFP and AAV-GLT-1 treated hemispheres	79
Figure 5.1 MEAs can continuously measure extracellular glutamate for the initial 72 hours after implantation.....	97
Figure 5.2 MEAs can detect multiple analytes of interest on a single device (glutamate, lactate, pyruvate, and glucose)	99
Figure 5.3 Modification of FDA-approved device AD-TECH [®] Epilepsy/LTM macro-micro depth electrode for real-time glutamate measures using constant potential amperometry	100
Figure 5.4 <i>In vivo</i> detection of extracellular glutamate using modified AD-TECH [®] Epilepsy/LTM macro-micro depth electrode.....	101
Figure 5.5 MEA prototypes for clinical use.....	103
Figure 6.1 Schematic depicting the disruptions in the regulation of extracellular glutamate in the rat striatum two days after diffuse brain injury	110

Chapter One: Introduction

Traumatic Brain Injury

Recent estimates indicate that traumatic brain injury (TBI) produces 50,000 deaths, 235,000 hospitalizations, and 1.1 million visits to the emergency department annually in the United States. Nationally, the top three causes of TBI are falls (28%), motor vehicle crashes (20%), and being struck by an object or person (19%) (Corrigan, et al. 2010). TBI is a heterogeneous disorder producing a wide range of symptoms based on the severity of the injury. The Glasgow coma scale (GCS) was developed to reliably classify the severity of a TBI based on the patient's eye, verbal, and motor responses with a total GCS score of (≥ 13) for mild injury, (9-12) for moderate injury, and (≤ 8) for severe injury (Table 1.1) (Narayan, et al. 2002). TBI results in various anatomical changes within the central nervous system including hemorrhage (subarachnoid and intraventricular), hematoma (epidural, subdural, and parenchymal), diffuse axonal injury, and contusion (Saatman, et al. 2008). Presently, there are no approved therapeutics for the treatment of TBI, instead current medical care focuses on maintaining proper physiological parameters such as intracranial pressure and blood pressure (Wang, et al. 2006).

Traumatic brain injury contains two distinct pathophysiological processes, primary injury and secondary injury (McIntosh, et al. 1996). Primary injury is the result of mechanical forces producing tissue deformation at the time of injury that damages blood vessels, shears axons, and produces cellular damage (Reilly and Bullock 1997, Gaetz 2004). Secondary injury, a consequence of the primary tissue damage, propagates damage through complex biochemical and cellular pathways (McIntosh, et al. 1996, Reilly and Bullock 1997). Secondary injury, which occurs in the hours to days after injury, is the target of therapies to reduce or limit damage to improving outcomes in TBI survivors (Bullock, et al. 1995, Myseros and Bullock 1995, Reilly and Bullock 1997). Recent evidence suggests that TBI is more than a single event; instead, it involves a complex disease process with the long term consequences including an increased risk for epilepsy, sleep disorders, neurodegenerative diseases, neuroendocrine disorders, psychiatric disorders, and reduced life expectancy (Masel and DeWitt 2010).

Glutamate's Role as a Neurotransmitter in the Central Nervous System

Glutamate, the predominant excitatory neurotransmitter in the central nervous system, is involved in almost all aspects of neurological function including cognition, motor function, memory, learning, decision making, and neuronal plasticity (McEntee and Crook 1993). In nerve terminals, glutamate is synthesized from multiple sources for neurotransmission. Glutamate can be synthesized from glucose via the Krebs cycle, transamination of α -oxoglutarate by alanine transaminase, and conversion of glutamine by glutaminase (Cooper, et al. 2003). High concentrations of glutamate are packaged into synaptic vesicles by vesicular glutamate transporters (vGluTs) using a proton-dependent electrochemical gradient across the vesicle membrane to transport glutamate against the concentration gradient (Takamori 2006). Glutamate is released into the extracellular space by two mechanisms. First, classical release of glutamate by neurons involves the opening of voltage-gated calcium channels after neuronal depolarization, permitting calcium influx into the nerve terminal. Calcium influx induces membrane fusion of the vesicles and exocytosis of glutamate into the extracellular space (Danbolt 2001, Cooper, et al. 2003). Second, glutamate is released into the extracellular space via carrier mediated exchange with other amino acids (Jabaudon, et al. 1999, Jensen, et al. 2000). Once in the extracellular space glutamate binds to ionotropic and metabotropic glutamate receptors for signal propagation (Fig 1.1).

There are three major types of ionotropic glutamate receptors (iGluRs), named after the agonist that would selectively activate them: N-methyl-D-aspartate (NMDA), α -amino-3-hydroxy-5-methyl-4-isoazolepropionic acid (AMPA), and 2-carboxy-3-carboxymethyl-4-isopropenylpyrrolidine (Kainate, KA) (Table 1.2). The iGluRs are ligand-gated ion channels responsible for modulating post-synaptic excitability and plasticity (Kew and Kemp 2005). AMPA and KA receptors are involved in fast excitatory neurotransmission; glutamate binding produces a conformational change in both receptors permitting sodium influx into the post-synaptic neuron (Greene and Greenamyre 1996). Compared to AMPA and KA receptors, the NMDA receptor requires multiple steps for activation. First, the NMDA receptor requires binding of two ligands, glutamate and glycine. Second, because the NMDA receptor is a voltage-sensitive ion channel, it requires depolarization to release the magnesium block and permit calcium influx. Glutamate binding to AMPA and KA receptors permits sodium influx into the cell, responsible for depolarizing the post-synaptic neuron and removing the magnesium block. Binding of glutamate and glycine, while the post-synaptic neuron is in a

depolarized state, will then open the ion channel of the NMDA receptor permitting calcium influx (Gardoni and Di Luca 2006).

There are a total of eight metabotropic glutamate receptors (mGluRs), organized into three groups (Table 1.3). mGluRs are G-protein coupled receptors using second messenger responses for signal transduction. mGluRs regulate the release of glutamate, post-synaptic excitability, packaging of glutamate into vesicles, and uptake of glutamate from the extracellular space (Schoepp 2001, Swanson, et al. 2005). Since mGluRs use secondary messenger systems for signal propagation, signaling is generally slower compared to activation of iGluRs. mGluRs contain seven alpha-helical transmembrane domains with a ligand binding site located on the extracellular N-terminus (Kew and Kemp 2005). Group I (mGluR₁ and mGluR₅) are excitatory localized on the post-synaptic terminals of glutamatergic neurons. Group II (mGluR₂ and mGluR₃) receptors are inhibitory with mGluR₂ localized primarily on pre-synaptic glutamatergic terminals, while mGluR₃ is expressed on glial as well as pre- and post-synaptic glutamatergic neurons. Group III (mGluR₄, mGluR₆, mGluR₇ and mGluR₈) are inhibitory with mGluR₄ and mGluR₇ receptors localized pre- and post-synaptically (Schoepp 2001) (Refer to Table 1.2 for localization and function of mGluRs).

For normal neurological function, extracellular concentrations of glutamate must be properly regulated. Appropriate activation of glutamate receptors requires the extracellular concentration of glutamate to remain low, producing a high signal-to-noise ratio during synaptic release of glutamate. Since there are no extracellular enzymes to degrade glutamate, low concentrations of extracellular glutamate are maintained by the uptake of glutamate via five high affinity sodium-dependent excitatory amino acid transporters (EAATs) (EAAT1, GLAST) (EAAT2, GLT-1), (EAAT3, EAAC), EAAT4, and EAAT5 (Danbolt 2001)(Table 1.4). Glutamate uptake is an electrogenic process using the negative membrane potential maintained by the sodium/potassium adenosine triphosphatase to transport glutamate. Uptake of glutamate by the EAATs requires both sodium and potassium ions; sodium for glutamate binding and potassium for glutamate transport. During glutamate transport, one molecule of glutamate, three sodium ions, and one hydrogen ion are transported into the cell, while one potassium ion is transported out of the cell (Danbolt 2001). A majority (~90%) of glutamate uptake is performed by two glial transporters in the rat forebrain, GLAST and GLT-1 (Rothstein, et al. 1996, Tanaka, et al. 1997, Danbolt 2001).

Glutamate's Role in the Pathophysiology of TBI

While glutamate normally functions as an excitatory neurotransmitter, increases in extracellular glutamate can lead to excessive stimulation of glutamate receptors producing cell death by a mechanism termed "excitotoxicity" (Lucas and Newhouse 1957, Olney and de Gubareff 1978). Excitotoxicity was described as a phenomenon whereby the excitatory action of glutamate becomes transformed into a neuropathological process that rapidly kills neurons (Olney and de Gubareff 1978). Excitotoxicity involves the activation of complex biochemical and cellular pathways that produce prolonged depolarization of neurons, increased concentrations of intracellular calcium, and activation of enzymatic and nuclear mechanisms of cell death (Doble 1999). Increases in extracellular glutamate have been shown to play a pivotal role in the initiation and propagation of secondary brain injury (Fig 1.2). The mechanical forces of the primary brain injury compromise the blood-brain barrier and cellular membranes releasing glutamate into the extracellular space (Schmidt and Grady 1993, Bullock, et al. 1998, Farkas, et al. 2006). Also, redistribution of ions from the primary injury creates a massive depolarization leading to neuronal release of glutamate (Katayama, et al. 1990). The massive increase in extracellular glutamate at the initial time of injury has been well characterized in experimental models of traumatic brain injury (Faden, et al. 1989, Katayama, et al. 1990, Nilsson, et al. 1990, Palmer, et al. 1993, Globus, et al. 1995, Kato, et al. 1997, Stoffel, et al. 1997, Matsushita, et al. 2000, Rose, et al. 2002, Stoffel, et al. 2002).

The initial surge of glutamate at the time of injury leads to excessive activation of iGluRs and mGluRs, and increases glutamate uptake by the EAATs to restore the extracellular glutamate concentration. The above processes lead to increase ionic flux into the cell. First, increases in extracellular glutamate activate AMPA and KA receptors permitting sodium influx into the cell and depolarizing the cell (Greene and Greenamyre 1996). Second, depolarization opens voltage-sensitive calcium channels and removes the magnesium block from the NMDA receptor, which allows further calcium influx into the cell (Gardoni and Di Luca 2006). Third, activation of Group I mGluRs by glutamate leads to the opening of voltage-gated calcium channel permitting calcium influx (Mao and Wang 2002). Lastly, uptake of glutamate by the EAATs results in sodium influx into the cell (Danbolt 2001). To maintain ionic equilibrium in the cell, chloride ions passively diffuse into the cell along with water creating osmotic swelling of the cell. Cytotoxic edema

directly contributes to raising the intracranial pressure (ICP), one of the most common sequelae of secondary brain injury (Marmarou 2004).

To restore ionic equilibrium in the cell, the sodium-potassium pump actively transports sodium out of the cell. Since the sodium-potassium pump is driven by the hydrolysis of adenosinetriphosphate (ATP), reestablishing the ionic equilibrium can deplete ATP levels in the cell (Tavalin, et al. 1997). After TBI, there is an increase in glucose transport to facilitate glycolysis and ATP generation (Kawamata, et al. 1995). Restoring the ATP concentration through oxidative phosphorylation leads to mitochondrial dysfunction as the mitochondria attempt to maintain the energy supply (Sullivan, et al. 2005). Mitochondrial dysfunction leads to the production of reactive oxygen species (ROS) and oxidative damage that includes protein nitration and lipid peroxidation (Braughler and Hall 1992, Hall, et al. 1994, Singh, et al. 2006). Mitochondrial dysfunction and oxidative damage are well established sequelae of secondary brain injury (Braughler and Hall 1992, McIntosh, et al. 1996, Sullivan, et al. 2005). Mitochondrial dysfunction in a state of increased glycolysis leads to anaerobic glycolysis and the production of lactate as an alternate energy supply. TBI produces significantly higher levels of lactate in the brain, with a correlation between lactate levels and reduced outcomes in TBI survivors (Reilly and Bullock 1997, Makoroff, et al. 2005).

A pivotal process in the secondary injury cascade is calcium influx into the cell, the ability of the cell to survive depends on the buffering capacity of the mitochondria and endoplasmic reticulum to sequester cytosolic calcium (Doble 1999). If the cell is unable to buffer the calcium influx, calcium overload can trigger many irreversible neurotoxic cascades, including the uncoupling mitochondrial electron transfer from ATP synthesis, the activation and overstimulation of enzymes such as calpains and other proteases, protein kinases, nitric oxide synthase, calcineurins, and endonucleases (Nasr, et al. 2003, Arundine and Tymianski 2004, Lifshitz, et al. 2004, Sullivan, et al. 2005). The above processes lead to cellular damage and dysfunction, responsible for the activation of apoptotic/necrotic mechanisms of cell death (Nicholls and Budd 2000, Sattler and Tymianski 2000). Reducing or preventing increases in cytosolic calcium and the activation of neurotoxic cascades has been the therapeutic target of multiple compounds to provide neuroprotection and improved outcomes after TBI (Okonkwo, et al. 1999, Sullivan, et al. 2004, Geddes and Saatman 2010, Saatman, et al. 2010).

Increases in extracellular glutamate not only initiate secondary injury cascades, but the downstream consequences of secondary injury lead to further increases in

extracellular glutamate that amplify and propagate damage. First, increased ionic flux can depolarize neurons and enhance vesicular glutamate release. Second, structural damage to the cell can lead to a loss of membrane fidelity allowing glutamate to leak into the extracellular space (Yi and Hazell 2006). Third, release of inflammatory cytokines can activate microglia, which release glutamate into the extracellular space via the glutamate/cystine exchanger (Barger, et al. 2007). Fourth, disruptions in the ionic equilibrium and oxidative damage to the EAATs can inhibit the ability of the EAATs to uptake glutamate from the extracellular space (Trotti, et al. 1998). Overall, increases in the release of glutamate and decreases in the ability to uptake glutamate can increase the extracellular concentrations of glutamate diffusing to nearby neurons amplifying and propagating secondary damage.

Clinically, a multitude of studies have detected significant increases in extracellular glutamate levels in the days following injury with some reports correlating increases in extracellular glutamate with unfavorable outcomes (Persson and Hillered 1992, Bullock, et al. 1995, Bullock, et al. 1998, Koura, et al. 1998, Vespa, et al. 1998, Yamamoto, et al. 1999, Reinert, et al. 2000, Hutchinson, et al. 2002, Hlatky, et al. 2004, Chamoun, et al. 2010, Lakshmanan, et al. 2010, Timofeev, et al. 2011a). Based on the large body of clinical evidence supporting a role for increased glutamate release and excessive glutamate receptor activation in pathophysiology of TBI, many compounds have been developed to modulate aspects of glutamate signaling. The NMDA receptor has been the primary therapeutic target to reduce excitotoxicity (Muir 2006). Unfortunately, NMDA antagonists have failed to reach their primary endpoints in randomized controlled trials in head-injured patients (Willis, et al. 2004). One of the major problems encountered with the NMDA antagonists trials were adverse effects that include hallucinations, catatonia, ataxia, nightmares, and memory deficits (Blanke and VanDongen 2009).

Unlike the clinical studies, multiple animals studies report increases in extracellular glutamate at the time of the injury, which returns to baseline concentrations within the first hour after injury (Faden, et al. 1989, Katayama, et al. 1990, Nilsson, et al. 1990, Palmer, et al. 1993, Globus, et al. 1995, Katoh, et al. 1997, Stoffel, et al. 1997, Matsushita, et al. 2000, Rose, et al. 2002, Stoffel, et al. 2002). Since experimental TBI has failed to model glutamate dysregulation seen in the clinic, the role of glutamate excitotoxicity in the acute pathophysiology of TBI has been challenged and remains unclear (Carbonell and Grady 1999, Obrenovitch 1999). All of the prior studies have

used microdialysis, a common method for neurochemical sampling in vivo. However, microdialysis suffers from methodological limitations that restrict the ability of microdialysis to sample glutamate near the synapse, due to poor spatial and temporal resolution and extensive damage from implantation of the probe (Obrenovitch, et al. 2000, Borland, et al. 2005, Diamond 2005, Hillered, et al. 2005, Jaquins-Gerstl and Michael 2009).

In this thesis, we will re-examine glutamate dysregulation in the acute pathophysiology of experimental brain injury using a novel technique, enzyme-based microelectrode arrays (MEAs). MEAs have improved upon some methodological limitations inherent to microdialysis allowing measures of extracellular glutamate closer to the synapses (Burmeister and Gerhardt 2001, Burmeister, et al. 2002, Day, et al. 2006, Hascup, et al. 2010). We will use MEAs to examine disruptions in the regulation of extracellular glutamate in brain regions that may be responsible for post-traumatic deficits in behavioral, cognitive, and motor function. The overall goal of this thesis is to examine the regulation of extracellular glutamate after a TBI, identify novel therapeutic targets to improve the regulation of extracellular glutamate, and examine possible therapeutic approaches to improve regulation of extracellular glutamate.

Copyright © Jason Michael Hinzman 2012

Chapter One: Figures

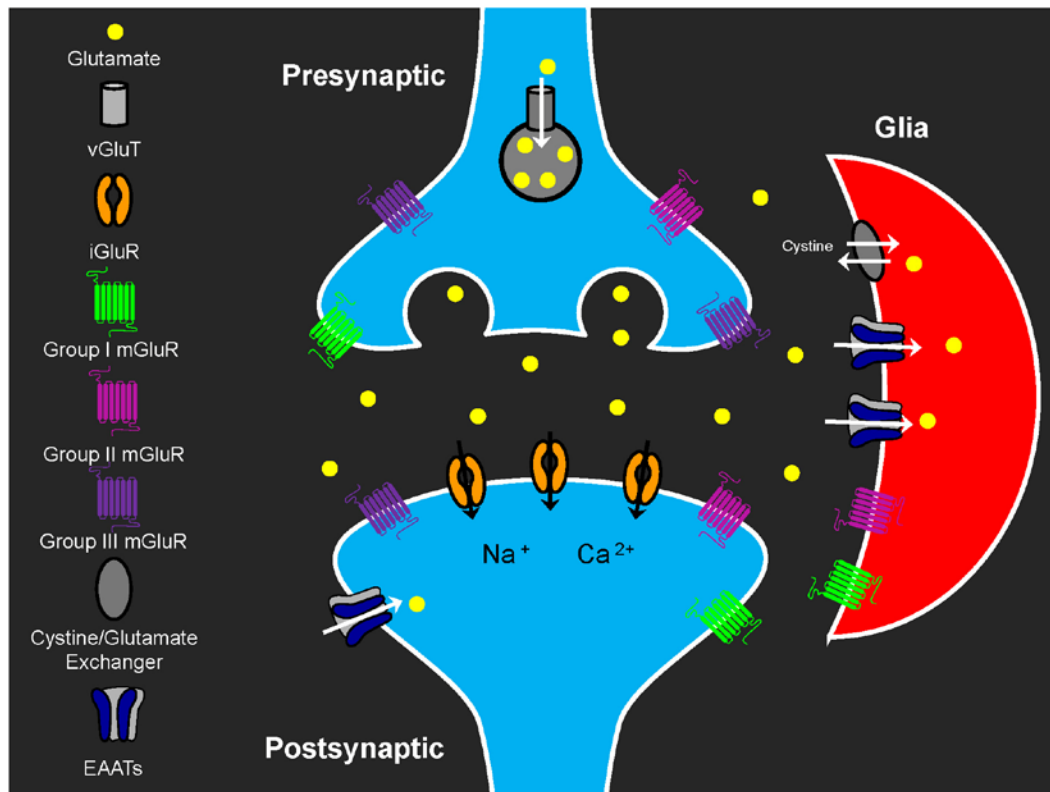
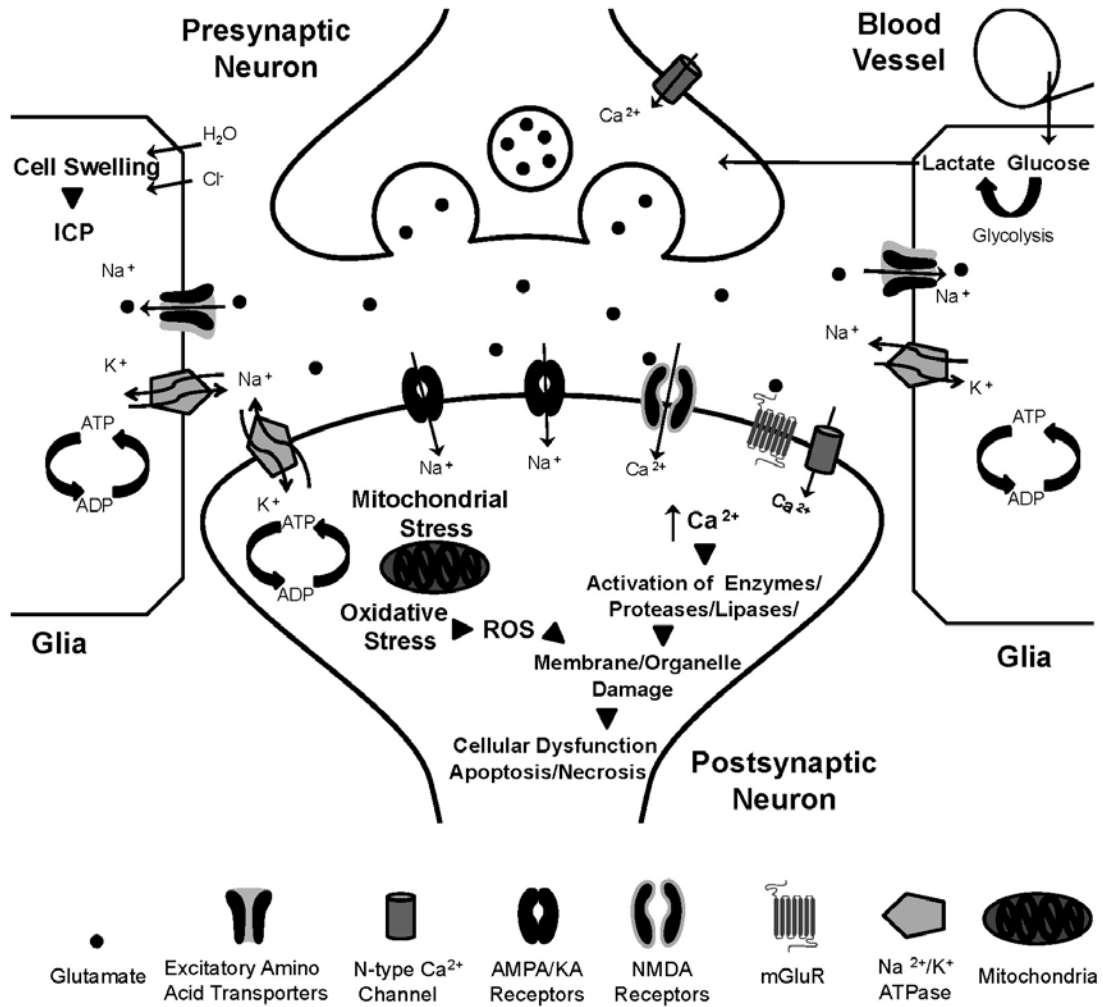
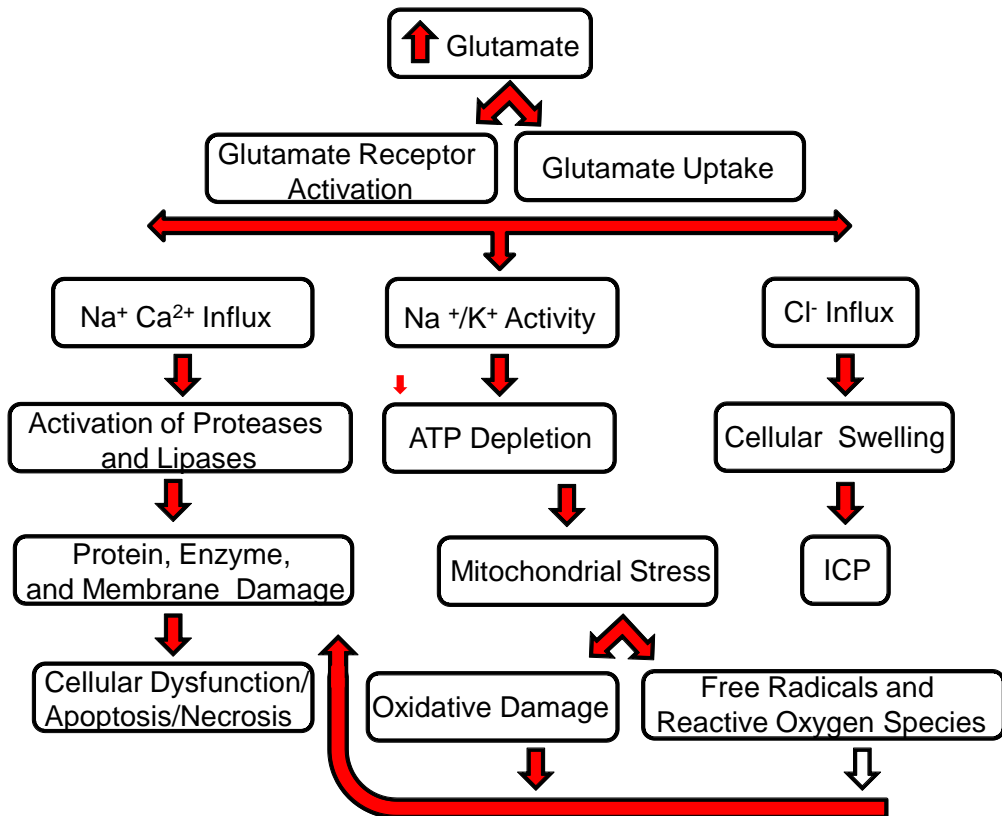


Figure 1.1 Schematic of a glutamate synapse

Several aspects of glutamate neurotransmission are depicted in the diagram of a glutamate synapse. Glutamate is packaged into vesicles by vesicular glutamate transporters (vGluT). Glutamate is released in the extracellular space in a Ca²⁺-dependent mechanism upon membrane depolarization. Glutamate can also be released from non-neuronal sources, such as the cystine/glutamate exchanger. Once in the extracellular space, glutamate propagates downstream signaling by binding to both metabotropic glutamate receptors (mGluRs) and ionotropic glutamate receptors (iGluRs). Glutamate is removed from the extracellular space by sodium-dependent, high affinity excitatory amino acid transporters (EAATs), regulating the extracellular glutamate concentration and activation of glutamate receptors.

A





Chapter One: Tables

Table 1.1 Glasgow Coma Scale (GCS)

Score	1	2	3	4	5	6
Eyes	Does not open eyes	Opens eyes to painful stimuli	Opens eyes to voice	Opens eyes spontaneously		
Verbal	Does not make sound	Incomprehensible sound	Sounds inappropriate words	Confused or disoriented	Converses normally	
Motor	Does not move	Extension to painful stimuli	Abnormal flexion to painful stimuli	Flexion withdrawal to painful stimuli	Localizes painful stimuli	Obeys commands

Severity	GCS (Total Score)
Minor	≥ 13
Moderate	9-12
Severe	≤ 8

Table 1.2 Ionotropic Glutamate Receptors

	NMDA	AMPA	Kainate
Receptor Subunits	NR1, NR2A, NR2B NR2C, NR2D NR3A, NR3B	GluR1, GluR2, GluR3, GluR4	GluR5, GluR6 GluR7, KA-1 KA-2
Signal Transduction	Ca ²⁺ , Na ⁺	Na ⁺ (Ca ²⁺)	Na ⁺ (Ca ²⁺)

Table 1.3 Metabotropic Glutamate Receptors

	Receptor	Localization	Function
Group I	mGluR1	Pre-synaptic Post-synaptic	Enhances excitability Synaptic plasticity, LTP/LTD
	mGluR5	Post-synaptic and glia	Synaptic plasticity, LTD
Group II	mGluR2	Pre-synaptic	LTD
	mGluR3	Pre/Post-synaptic and glia	Neurotrophin release
Group III	mGluR4	Pre/Post-synaptic	Motor learning
	mGluR6	Retina	Visual acuity
	mGluR7	Pre/Post-synaptic	Autoreceptor
	mGluR8	Pre-synaptic	Regulation of lateral perforant path

Table 1.4 Excitatory Amino Acid Transporters (EAATs)

Human Nomenclature	Rodent Nomenclature	Localization
EAAT1	Glutamate aspartate transporter (GLAST)	Astrocytes
EAAT2	Rat glutamate transporter (GLT-1)	Astrocytes
EAAT3	Rabbit glutamate transporter (EAAC)	Postsynaptic neurons
EAAT4		Cerebellar Purkinje neurons (human)
EAAT 5		Retina (human)

Preface to Chapter Two

The aim of the experiments in Chapter Two was to examine if an experimental model of diffuse traumatic brain injury (TBI) produced post-traumatic disruptions in the regulation of tonic glutamate and potassium-evoked glutamate release in brain regions that may be responsible for post-traumatic deficits in behavioral, cognitive, and motor function. Using glutamate-sensitive microelectrode arrays (MEAs), I detected discrete regional changes in tonic glutamate and potassium-evoked glutamate release that were dependent on the severity of injury. In the end, I demonstrated that glutamate-sensitive MEAs were able to detect disruptions in the regulation of extracellular glutamate two-days after diffuse brain injury.

Chapter Two: Diffuse Brain Injury Elevates Tonic Glutamate Levels and Potassium-Evoked Glutamate Release in Discrete Brain Regions at Two Days Post-Injury: an Enzyme-Based Microelectrode Array Study

Abstract

Traumatic brain injury (TBI) survivors often suffer from a wide range of post-traumatic deficits including impairments in behavioral, cognitive, and motor function. Regulation of glutamate signaling is vital for proper neuronal excitation in the central nervous system. Without proper regulation, increases in extracellular glutamate can contribute to the pathophysiology and neurological dysfunctions seen in TBI. In the present studies, enzyme-based microelectrode arrays (MEAs) that selectively measure extracellular glutamate at 2 Hz enabled the examination of tonic glutamate levels and potassium chloride (KCl)-evoked glutamate release in the prefrontal cortex, dentate gyrus, and striatum of adult male rats two days after mild or moderate midline fluid percussion brain injury. Moderate brain injury significantly increased tonic extracellular glutamate levels by 256% in the dentate gyrus and 178% in the dorsal striatum. In the dorsal striatum, mild brain injury significantly increased tonic glutamate levels by 200%. Tonic glutamate levels were significantly correlated with injury severity in the dentate gyrus and striatum. The amplitudes of KCl-evoked glutamate release were increased significantly only in the striatum after moderate injury, with a 249% increase seen in the dorsal striatum. Thus, with MEAs, we measured discrete regional changes in both tonic and KCl-evoked glutamate signaling, which were injury severity dependent. Future studies may reveal the specific mechanisms responsible for glutamate dysregulation in

the post-traumatic period, providing novel therapeutic targets to improve outcomes after TBI.

Introduction

Approximately 1.5 million Americans suffer from a traumatic brain injury (TBI) each year, with mild TBI accounting for as many as 75% of all the injuries (Centers for Disease Control and Prevention, 2003). Survivors of TBI often suffer from a wide variety of neurological deficits that impair quality of life (Baddeley 1992, Capruso and Levin 1992, McAllister 1992, Levine, et al. 2002). Glutamate signaling in the central nervous system (CNS) plays a pivotal role in the acute pathophysiology of TBI. Primary mechanical forces of the initial injury can compromise the blood-brain barrier and cellular membranes allowing increased glutamate release into the extracellular space (Schmidt and Grady 1993, Bullock, et al. 1998, Farkas, et al. 2006). The redistribution of ions after injury can further depolarize neurons and augment the release of glutamate (Katayama, et al. 1990). Excessive glutamate receptor activation can promote cellular damage through secondary injury cascades by disrupting ionic homeostasis in the cell, activating calcium-dependent proteases and phospholipases, uncoupling mitochondrial ATP synthesis, promoting oxidative stress, producing reactive oxygen species, depleting glutathione levels, and increasing the energy demand of the cell (Faden, et al. 1989, Hall, et al. 1994, McIntosh, et al. 1996, Yi and Hazell 2006). Further, clinical reports have reported increases in extracellular glutamate up to four days after injury that correlated with increased intracranial pressure and unfavorable outcomes (Bullock, et al. 1995). These prior studies emphasize the consequences of CNS glutamate dysregulation, and the need to examine changes in glutamate signaling in the post-traumatic period after TBI that may be responsible for aberrant neuronal signaling and the contribution to neurological deficits.

Glutamate is released constantly into the extracellular space via stimulated and spontaneous exocytosis of synaptic vesicles and by carrier mediated exchange with other amino acids (Jabaudon, et al. 1999, Jensen, et al. 2000). Because there is no enzyme in the extracellular fluid to degrade glutamate, the synaptic concentration of glutamate is lowered by diffusion away from the synapse and through glutamate uptake. Since diffusion of glutamate is limited by the extrasynaptic anatomy, glutamate uptake is the primary mechanism to maintain the extracellular concentration of glutamate. In the

central nervous system, almost all of the glutamate clearance is achieved by the sodium-dependent excitatory amino acid transporters (EAATs) GLAST and GLT-1, predominantly located on glia (Danbolt 2001).

Previous studies have reported several fold increases in the extracellular concentration of glutamate initiated by a TBI, which subside within two hours (Faden, et al. 1989, Katayama, et al. 1990, Nilsson, et al. 1990, Matsushita, et al. 2000). These studies employed microdialysis, a common method for neurochemical sampling in vivo. However, microdialysis suffers from spatial and temporal limitations that restrict the ability to sample dynamic fluctuations of glutamate near the synapse (Obrenovitch, et al. 2000, Hillered, et al. 2005). The large sampling area of the microdialysis membrane (1-4 mm length) and extensive damage from implantation of the microdialysis probe limit the ability to detect neuronal release (Borland, et al. 2005, Jaquins-Gerstl and Michael 2009). Furthermore, the low temporal resolution of microdialysis (1-20 min) is inadequate to sample the fast dynamics of glutamate release and clearance that occurs on the order of milliseconds to seconds (Diamond 2005).

Interestingly, experimental TBI has yet to produce pathological extracellular concentrations of glutamate, even immediately post-injury (Katayama, et al. 1990, Matsushita, et al. 2000), which raises doubt about glutamate excitotoxicity after TBI (Carbonell and Grady 1999, Obrenovitch 1999). In this study, we used midline fluid percussion injury (FPI), a model of a diffuse closed head injury that affects both hemispheres equally and shares pathological features of human head injuries (Dixon, et al. 1987, McIntosh, et al. 1987), to examine changes in glutamate signaling two days after mild or moderate diffuse brain injury. To study injury-induced alterations in glutamate neurotransmission, we employed a novel technique, in vivo amperometry coupled to enzyme-based microelectrode arrays (MEAs), with high temporal resolution (2 Hz), low limit of detection ($< 1 \mu\text{M}$), and high spatial resolution to selectively measure extracellular glutamate closer to synapses (Burmeister and Gerhardt 2001, Burmeister, et al. 2002). The improved spatial and temporal resolution of the MEAs allowed us to examine injury-induced alterations in tonic glutamate levels and potassium chloride (KCl)-evoked glutamate release in the prefrontal cortex, dentate gyrus of the hippocampus, and striatum; brain regions known to play a role in the behavioral, cognitive, and motor deficits suffered by TBI survivors (Baddeley 1992, Capruso and Levin 1992, McAllister 1992, Levine, et al. 2002).

Methods

Animals

Male Sprague-Dawley rats (350-400g; Harlan Laboratories Inc., Indianapolis, IN) were used for all experiments. The animals were housed in a 12 h light/dark cycle with food and water *ad libitum* according to the Association for Assessment and Accreditation of Laboratory Animal Care International. Animals were acclimated to their environment for at least 1 week before any experiments. After surgery, animals were monitored daily for post-operative care. Animal care was approved by the University of Kentucky Institutional Animal Care and Use Committee.

Midline Fluid Percussion Injury

Animals were subjected to midline FPI as previously described (Lifshitz 2008). Rats were anesthetized with isoflurane at 4% for five minutes and placed in a stereotaxic frame in a sterile surgery hood with continuously delivered isoflurane at 2%. The head was shaved and a 70% alcohol and betadine solution was applied. Eyes were treated with artificial tears and body temperature was maintained with a delta-phase heating pad (Braintree Scientific, Braintree, MA). A midline incision was made and fascia removed from the skull. A 4.7 mm trephine was used for the craniotomy, centered on the sagittal suture between bregma and lambda without disrupting the underlying dura or superior sagittal sinus. Anchoring screws were secured into pilot holes remote from the craniotomy. An injury hub was constructed from a Luer-Loc hub. The outer diameter of the hub was beveled to match the craniotomy. The injury hub was fitted into the craniotomy and cyanoacrylate gel was applied to seal the skull-hub interface. To secure the injury hub to the anchoring screws, methyl-methacrylate (Hygenic Corp., Akron, OH) was applied. The hub was filled with sterile saline and the wound sutured to prevent tearing. The animals were allowed to recover for 30-60 minutes until ambulatory and then re-anesthetized with 5% isoflurane for 5 minutes. The incision was opened and the injury hub was inspected. The female Luer-Loc injury hub was connected to the male Luer-Loc hub of the injury device (Custom Design and Fabrication, Virginia Commonwealth University, Richmond, VA). Before reflexive responses returned, the pendulum hammer was dropped onto the fluid-filled piston to induce either a mild or moderate injury. Sham injured animals underwent the same procedure without induction of injury. The fluid pressure pulse for mild injury was 1.1 ± 0.01 atm, and 2.0 ± 0.02 atm

for moderate injury. The injury hub was removed and any bleeding controlled with Gelfoam (Pharmacia, Kalamazoo, MI). The incision was closed with staples. Righting reflex recovery times were recorded for the injury group, from the time of impact to the time when animals' spontaneously righted. Mild injured animals had righting reflex times of 144 ± 34 seconds ($n=10$), and moderate injured animals had times of 606 ± 85 seconds ($n=11$). Sham injured animals had righting reflex less than 15 seconds ($n=10$). No animals died from complications caused by the injury.

Enzyme-Based Microelectrode Arrays

Ceramic-based MEAs, consisting of four platinum recording sites ($15 \times 333 \mu\text{m}$) arranged in dual pairs, were prepared and selected for in vivo recordings as previously described (Burmeister, et al. 2002, Day, et al. 2006). Glutamate-oxidase (GluOX) covered one pair of recording sites to allow for the enzymatic conversion of glutamate to α -ketoglutarate and the generation of the reporter molecule H_2O_2 . An inactive protein matrix covered the other pair of recording sites (sentinel sites). The two different coatings allowed the use of a self-referencing technique, in which the background current of the sentinel sites can be subtracted from the current of the glutamate-oxidase sites, thereby producing a more selective glutamate measure (Burmeister and Gerhardt 2001, Burmeister, et al. 2002). A size exclusion layer of 1,3-phenylenediamine (mPD) restricted the passage of large molecules that can be oxidized, such as ascorbic acid (AA) and dopamine (DA). Small molecules, such as H_2O_2 , diffuse through the exclusion layer, reaching the platinum recording sites (Fig 2.1A).

A $10 \mu\text{L}$ solution of 1% bovine serum albumin (BSA) (Sigma-Aldrich, St. Louis, MO), 0.125% glutaraldehyde (Glut) (Sigma-Aldrich), and 1% glutamate-oxidase (Seikagaku America, East Falmouth, MA) was prepared. Using a dissecting microscope, a microsyringe was used to manually apply a small drop ($\sim 0.1 \mu\text{L}$) of the glutamate-oxidase solution onto the bottom pair of platinum recording sites. Three enzyme coats were applied onto the platinum recording sites with a one minute drying period between each coat. The same procedure was used to coat the top pair of platinum recording sites (sentinel sites) with a solution containing 1% BSA and 0.125% glutaraldehyde. After coating, the MEAs were cured for at least 48 hours in a low humidity environment. The coated MEAs were connected to the FAST-16 mkII system (Fast Analytical Sensor Technology Mark II; Quanteon, L.L.C., Nicholasville, KY) and the tips of the MEAs were

placed in a 5 mM mPD solution (Acros Organics, Morris Plains, NJ). Electroplating software was used to apply a potential as a triangular wave with an offset of -0.5V, peak to peak amplitude equal to 0.25V, at a frequency of 0.05 Hz, for a period of 20 minutes to electroplate the mPD on all platinum recording sites. MEAs were cured for an additional 24 hours in a low humidity environment before use.

MEA Calibration

Calibrations were conducted to test the capability of the MEAs to measure glutamate and generate a standard curve for the conversion of current to glutamate concentration. Constant potential amperometry was performed with the MEAs using a FAST-16 mkII system. A potential of + 0.7 V versus a Ag/AgCl reference was applied to oxidize the reporter molecule, H₂O₂, which is a 2-electron oxidation reaction that occurs at the platinum recording sites of the MEA. The resulting current was amplified and digitized by the FAST-16 mkII system. The platinum recording sites of the MEA were placed in a continuously stirred 40 ml solution of 0.05 M phosphate buffered saline (PBS) maintained at 37 °C with a re-circulating water bath (Gaymar Industries Inc., Orchard Park, NY). The MEAs were exposed to final concentrations of 250 μM AA, 20, 40, 60 μM glutamate, 2 μM DA, and 8.8 μM H₂O₂ (Fig 2.1B). Parameters tested were limit of detection (LOD), selectivity for glutamate over ascorbic acid, slope of the electrode (sensitivity), and linearity of the glutamate response (R²). The average LOD was 0.8 ±0.1 μM, selectivity was 167 ±19:1 (glutamate: ascorbic acid), and slope was 3.4 ±0.3 pA/μM (n=51 GluOX recording sites).

In a separate study, we examined MEA performance after in vivo recordings. The post-implantation calibrations demonstrated that the parameters were not different (pre vs. post-implantation, n=24 glutamate-oxidase recording sites, paired t-test): limit of detection (1.1 ±0.1 μM vs. 1.5 ±0.4 μM, p=0.37), selectivity (93 ±21 vs. 83 ±26, p=0.77), and slope (2.1 ±0.2 pA/μM vs. 2.2 ±0.1 pA/μM, p=0.68).

Oxygen is a required co-factor of glutamate-oxidase for the production of the reporter molecule, H₂O₂. Therefore, we examined if low oxygen concentrations would affect MEA performance. Glutamate responses were minimally affected by oxygen concentration and the performance even at 0 μM oxygen was within 80% of the MEA response obtained in air saturated buffer (200 μM).

MEA/Micropipette Assembly

For local application of solutions in the rat brain, glass micropipettes (1 mm o.d. 0.58 mm i.d., A-M Systems, Inc., Everett, WA) were pulled (Kopf Instruments, Tujunga, CA), and the tips of the micropipettes were bumped to create a tip with an i.d. of 10-15 μm . The micropipettes were placed centrally among all four platinum recording sites and mounted 50-100 μm above the MEA. Micropipettes were filled with sterile filtered (0.20 μm) isotonic KCl solution (70 mM KCl, 79 mM NaCl, 2.5 mM CaCl_2 or 120 mM KCl, 29 mM NaCl, 2.5 mM CaCl_2 , pH 7.4) concentrations previously used to elicit reproducible KCl-evoked glutamate release in the brain regions of interest (Burmeister et al., 2002; Day et al., 2006; Stephens et al., 2009). The micropipette was attached to a Picospritzer III (Parker-Hannifin, Cleveland, OH) with settings adjusted to consistently deliver volumes between 50-100 nl. Pressure was applied from 2-20 p.s.i. for 1 sec. Volume displacement was monitored with the use of a stereomicroscope fitted with a reticule (Friedemann and Gerhardt 1992).

***In Vivo* Anesthetized Recording**

Two days after midline FPI, rats were anesthetized with urethane (1.25 g/kg i.p.) (Sigma-Aldrich) and prepared for *in vivo* electrochemical recordings as previously described (Burmeister, et al. 2002, Pomerleau, et al. 2003, Day, et al. 2006). Briefly, animals were placed in a stereotaxic frame and body temperature was maintained at 37 $^{\circ}\text{C}$ with a water pad connected to a recirculating water bath. A craniotomy was performed to provide access to the prefrontal cortex (AP: +3.2 mm, ML: +0.8 mm, DV: -4.5 mm), dentate gyrus (AP: -4.3 mm, ML: +2.1 mm, DV -4.2), and striatum (AP: +1.0 mm, ML: +2.5 mm, DV: -4.0, -4.5, -5.0 mm) (Paxinos and Watson, 1998) (Fig 2.1C). A Ag/AgCl reference wire was implanted into the lateral parietal cortex in the opposite hemisphere from the recording areas. The MEA was lowered into the brain using a microdrive (MO-10, Narishige International, East Meadow, NY). All MEA recordings were performed at a frequency of 2 Hz using constant potential amperometry. After the MEA reached a stable baseline (10-15 min), tonic glutamate levels (μM) were calculated by averaging extracellular glutamate levels over 10 seconds. Local application of KCl produced glutamate signals that were reproducible every 30 s. Each signal was analyzed by the following parameters: amplitude (μM), T_{80} (s) the time for the signal to decay by 80% from the peak amplitude, and k_{-1} (sec^{-1}) the slope of the linear regression

of the natural log transformation of the decay over time (Fig 2.1D) (Thomas, et al. 2009). Approximately eight reproducible signals were evoked at each location and then averaged into a representative signal for comparisons between injury groups. After recording from all locations, a MEA with an attached micropipette was used to locally apply green waterproof drawing ink (Higgins, Eberhard Faber Inc., Lewisburg, TN), which was used to confirm MEA placement during brain sectioning.

Data Analysis

Amperometric data were analyzed using custom Microsoft Excel™ - based software to determine the tonic levels and KCl-evoked signal parameters. To determine tonic levels of glutamate in the different brain regions, the background current from the sentinel site was subtracted from the current of the glutamate-oxidase site. Then, the resulting current (pA) was divided by the slope ($\mu\text{M}/\text{pA}$) obtained during the calibration to determine the tonic glutamate concentration in a given brain region. Data from the dentate gyrus and prefrontal cortex were analyzed by a one-way ANOVA followed by a Bonferonni post-hoc test. For the striatum, data were analyzed by a repeated measures two-way ANOVA followed by a Bonferonni post-hoc test (injury severity vs. depth). Data are presented as mean \pm SEM. Statistical significance was defined as $p < 0.05$.

Results

Prefrontal Cortex: Tonic and Evoked Glutamate Release

Tonic glutamate levels were not significantly changed in the prefrontal cortex two days after mild or moderate diffuse brain injury [ANOVA: $F(2,18)=0.8$, $p=0.43$] (Fig 2.2A). Tonic levels averaged $4.1 \pm 1.4 \mu\text{M}$ (sham), $4.2 \pm 1.3 \mu\text{M}$ (mild), and $6.2 \pm 2.5 \mu\text{M}$ (moderate). Local application of ~ 50 nL of 120 mM KCl produced reproducible glutamate release in the prefrontal cortex. Representative recordings demonstrate similar evoked-glutamate signals from local application of KCl between the sham and injury groups (Fig 2.2B). The amplitudes of KCl-evoked glutamate release in the prefrontal cortex were not significantly changed after diffuse brain injury [ANOVA $F(2,15)=0.49$, $p=0.62$] (Fig 2.2C). The amplitudes of KCl-evoked glutamate release in the sham, mild and moderate brain-injured rats were 5 to 10 times larger than the corresponding tonic levels of glutamate.

Amplitudes averaged $31.9 \pm 4.5 \mu\text{M}$, $40.2 \pm 11.5 \mu\text{M}$, and $27.8 \pm 9.6 \mu\text{M}$ in the sham, mild and moderate brain-injured groups, respectively. Clearance parameters (T_{80} and k_{-1}) of the KCl-evoked glutamate signal back to tonic levels were equivalent between all groups (Table 2.1). Thus, mild or moderate midline FPI did not produce significant changes in the tonic glutamate concentration, the amplitude of KCl-evoked glutamate release, or glutamate clearance parameters in the prefrontal cortex.

Dentate Gyrus: Tonic and Evoked Glutamate Release

Tonic glutamate levels in the hippocampal dentate gyrus were significantly elevated after brain injury [ANOVA $F(2,21)=4.9$, $p=0.018$]. Tonic levels averaged $1.6 \pm 0.4 \mu\text{M}$ (sham), $4.3 \pm 1.4 \mu\text{M}$ (mild), and $5.7 \pm 2.3 \mu\text{M}$ (moderate). Moderate brain-injured animals exhibited a significant 256% increase in tonic glutamate levels compared to sham controls (Fig 2.3A). Tonic glutamate levels in mild brain-injured animals were not significantly different from either sham or moderate brain-injured animals. Local application of $\sim 75 \text{ nL}$ of 70 mM KCl produced reproducible glutamate release in the dentate gyrus. Representative recordings demonstrate similar evoked-glutamate signals from local application of KCl between the sham and brain injury groups (Fig 2.3B). Amplitudes of evoked-glutamate release in the dentate gyrus were not significantly different between groups [ANOVA $F(2,18)=0.41$, $p=0.67$] (Fig 2.3C). The amplitude of KCl-evoked glutamate release in the sham, mild and moderate injured rats were 4 to 15 times larger than the tonic glutamate levels, as amplitudes averaged $25.1 \pm 4.9 \mu\text{M}$, $19.1 \pm 4.9 \mu\text{M}$, and $24.7 \pm 5.9 \mu\text{M}$ in the sham, mild and moderate brain-injured groups, respectively. Clearance parameters (T_{80} and k_{-1}) of the KCl-evoked glutamate signal back to tonic levels were equivalent between all groups (Table 2.1). Thus, tonic levels of extracellular glutamate were significantly increased after moderate midline FPI, with no significant changes in the amplitude of KCl-evoked glutamate release or glutamate clearance parameters in the dentate gyrus after mild or moderate midline FPI.

Striatum: Tonic and Evoked Glutamate Release

With the high spatial resolution of the platinum recording sites, glutamate responses were sampled from multiple depths of the large heterogeneous structure of the rat striatum (DV: -4.0 mm , -4.5 mm , -5.0 mm). Tonic glutamate levels were significantly affected by brain injury severity [$F(2,42)=9.26$, $p=0.0005$] and by recording

depth in the striatum [$F(2,42)=4.87$, $p=0.0183$]. At -4.0 mm in the striatum, tonic levels averaged $2.3 \pm 0.6 \mu\text{M}$ (sham), $6.9 \pm 1.2 \mu\text{M}$ (mild) and $6.4 \pm 1.2 \mu\text{M}$ (moderate). Mild and moderate brain injury produced a significant increase in tonic glutamate levels at a depth of -4.0 mm compared to sham control animals, with a significant 200% increase after mild brain injury and a significant 178% increase after moderate brain injury (Fig 2.4A). The injury-induced increases in tonic glutamate levels after mild and moderate brain injury compared to sham animals at recording depths of -4.5 mm and -5.0 mm did not reach significance.

Local application of ~100 nL of 70 mM KCl produced reproducible glutamate release in all depths of the striatum. Representative recordings of KCl-evoked glutamate release in the dorsal striatum (-4.0 mm) demonstrate the significantly elevated amplitude of glutamate release after moderate brain injury (Fig 2.4B). At -4.0 mm in the striatum, the amplitude of KCl-evoked glutamate release were 10-25 times larger than the tonic glutamate concentration, as amplitudes averaged $14.9 \pm 2.4 \mu\text{M}$, $16.1 \pm 1.9 \mu\text{M}$ and $52.0 \pm 16.6 \mu\text{M}$ in the sham, mild or moderate brain-injured animals, respectively. The amplitude of evoked-glutamate release was significantly affected by brain injury severity [$F(2,42)=24.96$, $p<0.0001$], but not by recording depth of the MEA [$F(2,42)=0.02$, $p=0.97$]. Amplitudes of KCl-evoked glutamate release after moderate brain injury were significantly elevated by 249%, 302%, 153% at -4.0, -4.5, and -5.0 mm, respectively (Fig 2.4C). Clearance parameters (T_{80} and k_{-1}) of the KCl-evoked glutamate signal back to tonic levels were equivalent in all depths of the striatum between all groups (Table 2.1). Thus, the striatum exhibits significantly elevated tonic glutamate levels after mild and moderate midline FPI, whereas the amplitude of KCl-evoked glutamate release was elevated significantly only after moderate brain injury.

Tonic Glutamate Levels Correlate with Injury Force

To examine if injury force (atm) is predictive of tonic glutamate levels, linear correlations were calculated for the three brain regions. The correlation was not significant in the prefrontal cortex (Pearson $r^2=0.05$ $p=0.30$). However, tonic glutamate levels were significantly correlated with injury force in the dentate gyrus (Pearson $r^2=0.29$; $p=0.006$) and in the striatum, when the three recording depths were averaged into a single value (Pearson $r^2=0.22$; $p=0.019$) (Fig 2.5). Thus, injury force was predictive

of elevated tonic glutamate levels in the dentate gyrus and the striatum at two days after diffuse brain injury.

Discussion

We examined the extent of glutamate dysregulation two days after diffuse brain injury, which may contribute to aberrant neuronal signaling and the propagation of secondary injury cascades. The present study was a first attempt to use enzyme-based MEAs to examine regional changes in glutamate signaling after TBI. First, the prefrontal cortex exhibited no significant alterations in glutamate signaling two days after diffuse injury. Second, tonic glutamate levels in the dentate gyrus and striatum were significantly increased after midline FPI. Third, moderate midline FPI produced significant increases in the amplitudes of evoked-glutamate release in multiple depths of the striatum. Finally, tonic glutamate levels in the dentate gyrus and striatum were significantly correlated to the mechanical forces of injury.

MEAs have improved upon some limitations inherent to microdialysis for sampling glutamate in vivo. The high spatial resolution of the platinum recording sites allowed glutamate measurements from discrete regions, which is vital in studying local glutamate regulation. Also, the 2 Hz sampling rate of the MEAs records the fast dynamics of glutamate signaling that may be susceptible to TBI pathophysiology. The improved spatial resolution and limited damage to the surrounding tissue (Rutherford, et al. 2007) allow MEAs to sample glutamate spillover from nearby synapses that are TTX sensitive (Day, et al. 2006, Hascup, et al. 2008). In contrast, microdialysate samples of glutamate are largely TTX independent and poorly correlated with the concentration of glutamate near synapses (Timmerman and Westerink 1997, Obrenovitch 1999). Moreover, the small recording sites of the MEAs require little tissue oxygen utilization and the electrochemical oxidation of H_2O_2 produces oxygen as supplementary substrate for glutamate-oxidase. In anoxic tissue, such as stroke, MEA performance may be compromised.

Tonic glutamate levels in the dentate gyrus and striatum are positively correlated with injury severity. However, the concentrations do not appear to reach excitotoxic levels, as a continuous infusion of 1.8 M glutamate at 0.5 μ L/hr was insufficient to produce a neuropathological lesion (Mangano and Schwarcz 1983). The present study was carried out under urethane anesthesia, which can decrease tonic glutamate levels by 60-80% (Rutherford, et al. 2007). Therefore, the values reported here may represent

only a fraction of the tonic glutamate concentration in the awake animal. Still, the increased tonic glutamate levels may contribute to the development or maintenance of diffuse brain injury pathophysiology. The observed tonic glutamate levels may explain elevated neuronal calcium levels, altered calcium regulation, which result in calpain mediated spectrin proteolysis reported after midline FPI (Sun, et al. 2008, McGinn, et al. 2009). With regard to secondary injuries, increased tonic glutamate levels after the initial injury may produce increased susceptibility to excitotoxic damage or provide neuroprotection via preconditioning. Future work should examine the effect of increased tonic glutamate levels on a secondary insult and identify alternate sources of glutamate contributing to the increased tonic glutamate levels.

Tonic glutamate levels seem independent of evoked-glutamate release as we report significant increases in tonic glutamate levels in the presence and absence of alterations in KCl-evoked glutamate release, depending on brain region. Evoked-glutamate release, unlike the graded response in tonic glutamate levels, exhibited an all-or-none response with injury severity. Local application of isotonic KCl depolarized local axons and pre-synaptic terminals, evoking neurotransmitter release. The increase in extracellular glutamate was transient as glutamate uptake rapidly restores the glutamate concentration back to tonic levels. Although transient, elevated evoked-glutamate release may prolong secondary injury cascades, by excessively activating ionotropic receptors, increasing calcium influx, and activating proteases (McIntosh, et al. 1996). Elevated evoked-glutamate release could arise from several different mechanisms. First, the pre-synaptic terminal could release more glutamate vesicles or vesicles with higher glutamate concentrations. Lateral FPI produces transient changes in the synaptic machinery, specifically complexin I and II, up to one week after injury, which could alter neurotransmitter packaging and synaptic release (Yi and Hazell 2006). Furthermore, free radicals can increase KCl-evoked glutamate release (Pellegrini-Giampietro, et al. 1990). Second, reduced glutamate transporter function would increase the extracellular glutamate concentration. Controlled cortical impact decreases the expression of GLT-1 and GLAST, the EAATs which mediate most of the glutamate uptake in the rat brain (Rothstein, et al. 1996, Rao, et al. 1998). Third, synaptic reorganization may alter synaptic structure and function. Future work could explore clearance of locally applied glutamate into the extracellular space to evaluate EAATs surface expression (Nickell, et al. 2007).

Midline FPI produces a diffuse, multi-focal pathology with significant neurological impairments after mild and moderate injury, without overt cavitation (McIntosh, et al. 1987, Schmidt and Grady 1993, Hamm 2001, Kelley, et al. 2007). In addition, physiological disturbance may contribute to observed post-traumatic deficits (Lyeth, et al. 1990, Delahunty, et al. 1995). The spectrum of deficits includes behavioral, cognitive and motor impairments ascribed to the prefrontal cortex, hippocampus, and striatum (Baddeley 1992, Capruso and Levin 1992, McAllister 1992, Levine, et al. 2002, Khan, et al. 2003).

The medial prefrontal cortex receives glutamatergic projections from the mediodorsal nucleus of the thalamus, hippocampus, and amygdala (Steketee 2003). Post-traumatic impairments in working memory have been linked to damage in the medial prefrontal cortex (Baddeley 1992, Delatour and Gisquet-Verrier 2000, Levine, et al. 2002). Here, we report no significant changes in tonic glutamate levels or evoked glutamate release in the medial prefrontal cortex, likely due to the injury type or the selected time point. Few reports have examined the prefrontal cortex after midline FPI, reporting blood-brain barrier disruption within 24 hours post-injury (McIntosh, et al. 1987, Schmidt and Grady 1993). After controlled cortical impact, impairments in working memory have been attributed to excessive GABA-mediated inhibition weeks post-injury (Kobori, et al. 2006, Kobori and Dash 2006). Thus, diffuse brain injury in the medial prefrontal cortex retains glutamate regulation at two days post-injury.

The dentate gyrus of the hippocampus receives glutamate projections from the entorhinal cortex and projects to area CA3 (Andersen 2007). Survivors of TBI suffer from impairments in learning and memory attributed to hippocampal damage (Tate and Bigler 2000). Midline FPI produces significant deficits in the Morris water maze memory tests 11-15 days after injury (Hamm, et al. 1993, Liu, et al. 1994). In the absence of significant neuronal cell death, physiological changes in the hippocampus may contribute to the functional deficits (Lyeth, et al. 1990, Delahunty, et al. 1995, Grady, et al. 2003). The significantly elevated tonic glutamate levels after moderate brain injury may provide a potential substrate for the increased hippocampal excitability reported two days after midline FPI (Reeves, et al. 1995) and ensuing cognitive deficits.

The striatum receives glutamatergic projections from the thalamus and virtually all regions of the neocortex (Fonnum, et al. 1981). Survivors of TBI suffer motor and cognitive impairments (Khan, et al. 2003), as reported with glutamate and dopamine dysregulation in the striatum (Canales, et al. 2002). Injury-induced increases in tonic and

evoked-glutamate release in the striatum at two days post-injury may underlie the motor deficits within five days post-injury and the memory deficits within 11-15 days post-injury (Liu, et al. 1994, Hamm 2001). Two weeks after controlled cortical impact, dopamine neurotransmission in the striatum exhibited decreased electrically-induced dopamine overflow, decreased levels of the dopamine transporter, and decreased dopamine uptake from the extracellular space (Wagner, et al. 2005). Activation of ionotropic glutamate receptors reduces evoked-dopamine release in the striatum (Wu, et al. 2000). The glutamate-dopamine interactions underlying motor and cognitive function warrant further investigation to explain the neurological deficits observed in experimental and clinical TBI.

In conclusion, we used MEAs in combination with midline FPI to examine how diffuse brain injury alters glutamate signaling without the influence of tissue destruction seen in focal injury models. Our results demonstrate that elevated glutamate signaling contributes to the pathophysiology of diffuse brain injury, establishing a basis for further functional deficits. The specific mechanisms responsible for the elevations in tonic glutamate levels and evoked-glutamate release *in vivo* should be explored over a more complete time course to identify novel therapeutic targets to improve outcomes after TBI.

Chapter Two has been published in the following manuscript:

Hinzman JM, Thomas TC, Burmeister JJ, Quintero JE, Huettl P, Pomerleau F, Gerhardt GA and Lifshitz J. (2010). Diffuse brain injury elevates tonic glutamate levels and potassium-evoked glutamate release in discrete brain regions at two days post-injury: an enzyme-based microelectrode array study. J Neurotrauma. 27:889-899.

This is a copy of an article published in the [Journal of Neurotrauma] © [2010] [copyright Mary Ann Liebert, Inc.]; [Journal of Neurotrauma] is available online at: <http://online.liebertpub.com>.

Copyright © Jason Michael Hinzman 2012

Chapter Two: Figures

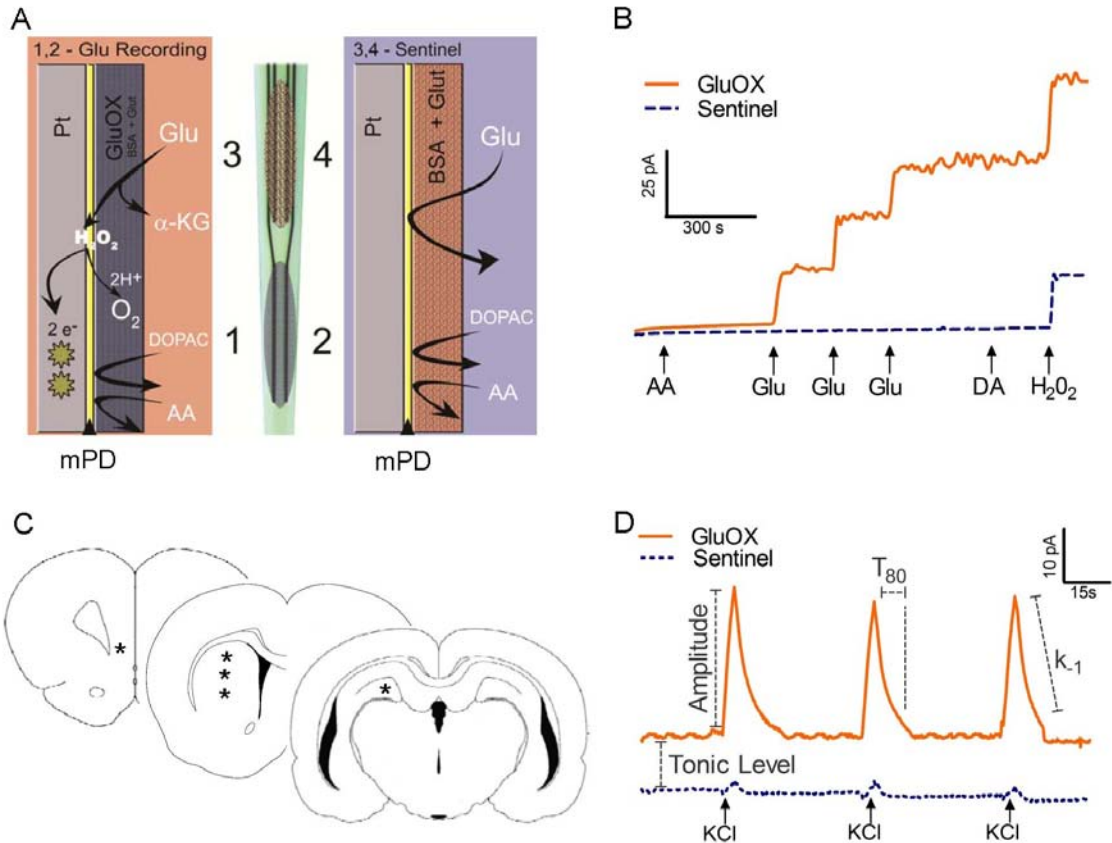


Figure 2.1 Methods for microelectrode array glutamate recordings

(A) Schematic diagram showing the configuration and coatings applied to the MEA. The lower pair of platinum sites were prepared with a mixture of glutamate-oxidase (GluOX), bovine serum albumin (BSA), and glutaraldehyde (Glut), illustrated at left. While the upper pair of platinum sites were prepared only with BSA and Glut, illustrated at right. A layer of m-phenylenediamine (mPD) is electroplated onto the recording sites providing a size exclusion layer to block major interferents, ascorbic acid (AA) and dopamine (DA). (B) MEA *in vitro* calibration measuring the change in current on a GluOX site (solid line) and a sentinel site (dashed line) with addition of multiple analytes. Additions of interferents such as AA and DA produced no change in current on the GluOX or sentinel sites. Three glutamate (Glu) additions showed a stepwise increase of current on the GluOX site with no response on the sentinel site. Addition of H_2O_2 produces an increase

in current on both the GluOX and sentinel sites. (C) Illustrations of coronal sections of the rat brain (Paxinos and Watson, 1998) highlight the regions of interest for glutamate recordings (*) in the prefrontal cortex (PFC, AP: 3.2 mm), striatum (STR, AP: 1.0 mm), and dentate gyrus (DG, AP: -4.3 mm). (D) Representative *in vivo* recording from a GluOX site and sentinel site. Local application of KCl (†) produced reproducible glutamate release, highlighting the fast kinetics of glutamate release and uptake. Tonic glutamate was calculated in each brain region after the microelectrode had reached a stable baseline. KCl-evoked glutamate release was analyzed using the following parameters: amplitude, T_{80} , and k_{-1} for each signal. Parameters are shown separately for clarity.

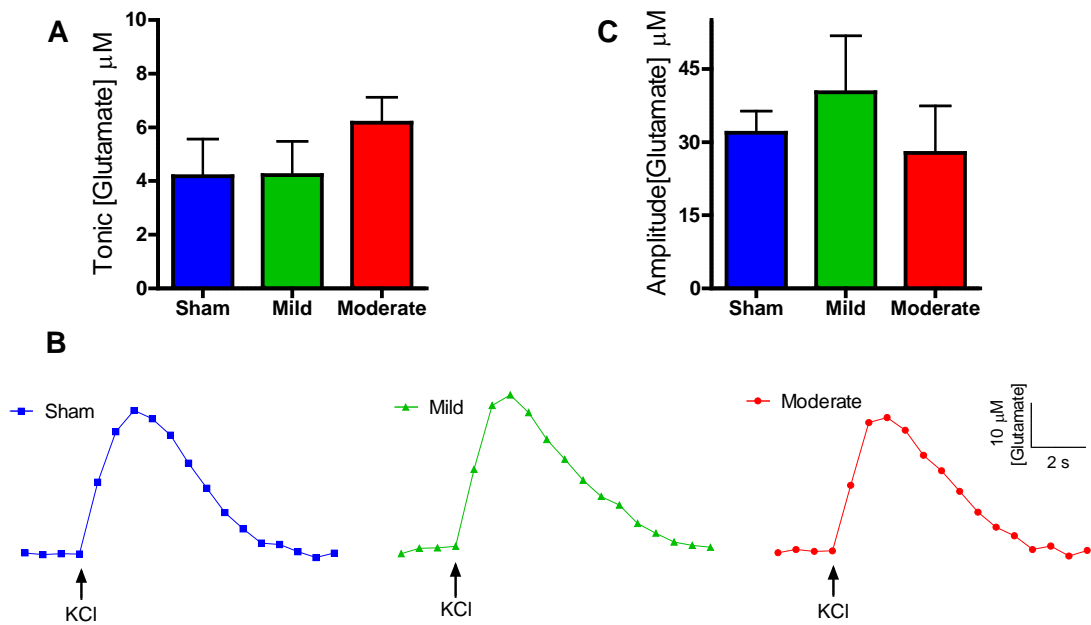


Figure 2.2 Tonic and KCl-evoked release of glutamate in the prefrontal cortex of the urethane anesthetized rat

(A) Tonic glutamate levels were not significantly different after mild or moderate midline FPI ($n= 7$). (B) Baseline-matched representative recordings exhibit no significant change in KCl-evoked glutamate release after midline FPI. Local application of KCl (↑) produced a robust increase in extracellular glutamate that rapidly returned to tonic levels. (C) The average amplitudes of KCl-evoked glutamate release were not significantly different after mild or moderate midline FPI ($n= 6$).

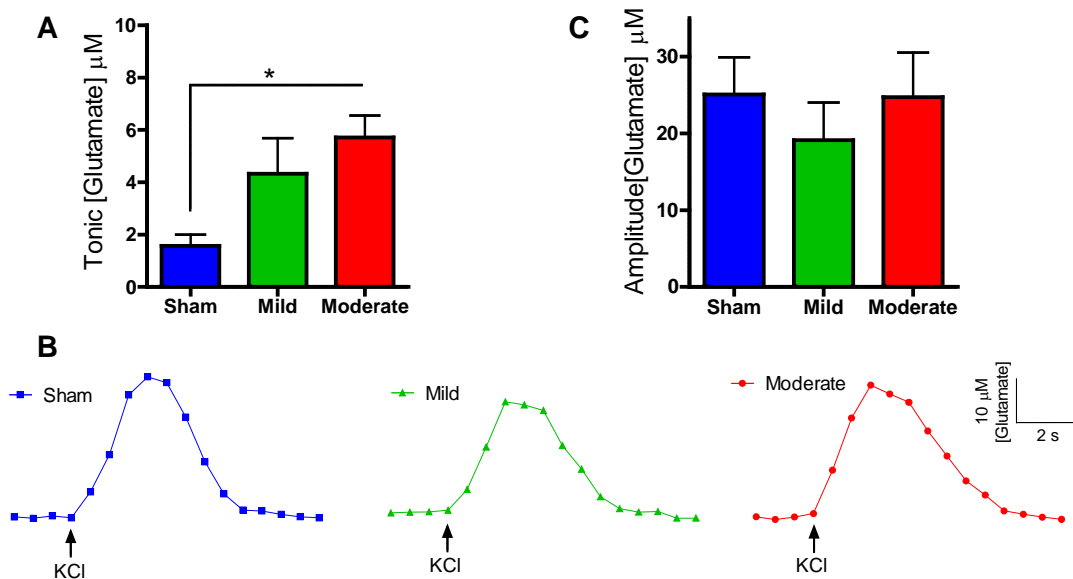


Figure 2.3 Tonic and KCl-evoked release of glutamate in the dentate gyrus in the hippocampus of the urethane anesthetized rat

(A) Tonic glutamate levels were significantly increased after moderate midline FPI in the dentate gyrus (* $p < 0.05$, $n = 8$). (B) Baseline-matched representative recordings exhibit no significant change in KCl-evoked glutamate release after midline FPI. (C) The average amplitudes of KCl-evoked glutamate release were not significantly different after mild or moderate injury ($n = 7$).

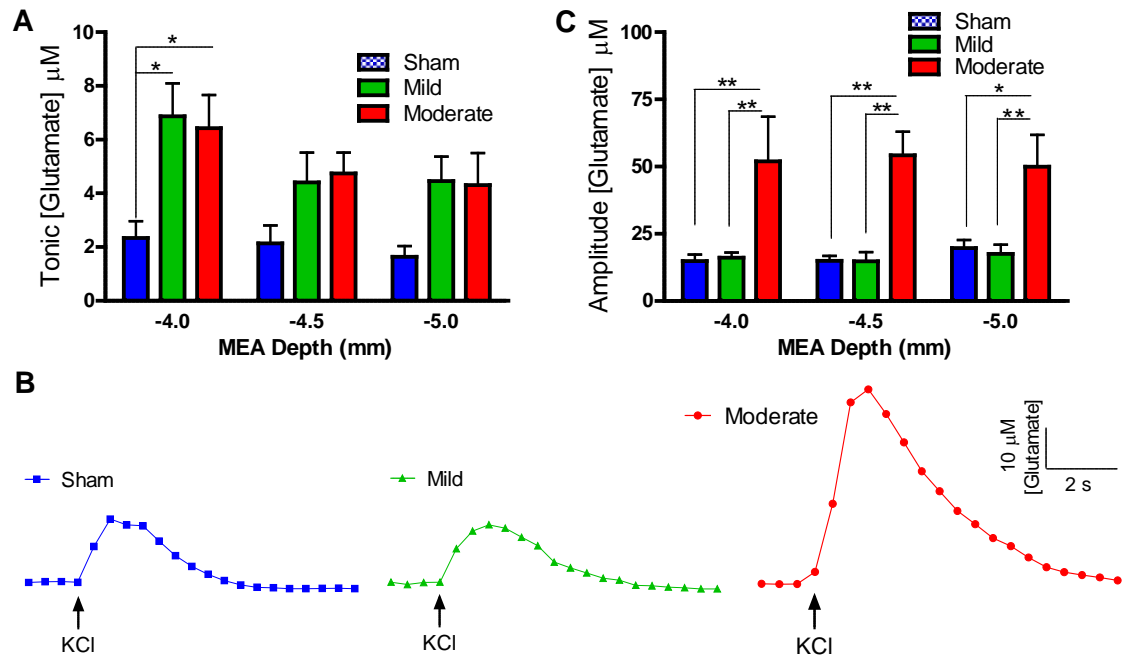


Figure 2.4 Tonic and KCl-evoked release of glutamate in the striatum of the urethane anesthetized rat

(A) Tonic glutamate levels were significantly increased after mild or moderate injury in the striatum at a depth of -4.0 mm with no significant changes at -4.5 mm or -5.0 mm (* $p < 0.05$, $n = 8$). (B) Baseline-matched representative recordings of KCl-evoked glutamate release showed that there was a significant increase in the amplitude of glutamate release after moderate midline FPI. Local application of KCl (produced a robust increase in extracellular glutamate that rapidly returned to tonic levels. (C) The average amplitudes of KCl-evoked glutamate release in the rat striatum at -4.0 mm, -4.5 mm, -5.0 mm were significantly increased after moderate midline FPI from local application of 100 nL of 70 mM KCl, compared to sham or mild injury animals (* $p < 0.05$, ** $p < 0.01$, $n = 8$).

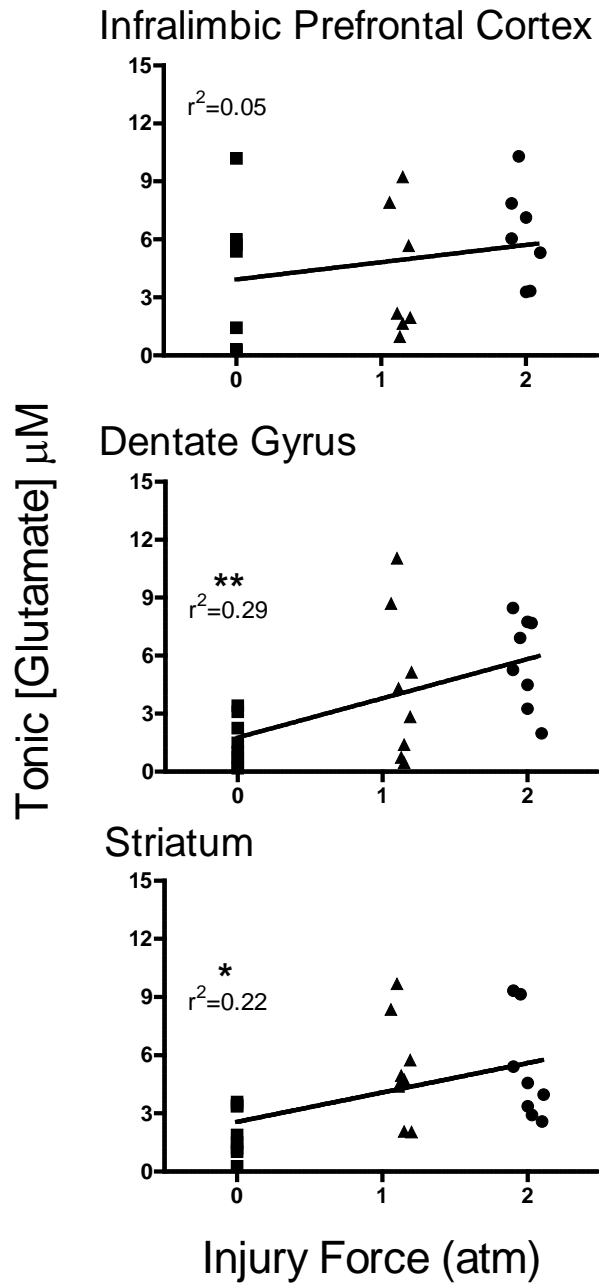


Figure 2.5 Correlations of tonic glutamate levels with force of injury in the rat prefrontal cortex, dentate gyrus, and striatum

Tonic glutamate levels were not significantly correlated with injury force in the prefrontal cortex ($n= 7$), but were significantly correlated in the dentate gyrus (** $p < 0.01$, $n= 8$), and in the striatum (* $p < 0.05$, $n= 8$).

Chapter Two: Tables

Table 2.1 Clearance Parameters of KCl-Evoked Glutamate Release

	T₈₀ (sec)			k₋₁ (sec⁻¹)		
	Sham	Mild	Moderate	Sham	Mild	Moderate
Prefrontal Cortex	7.0 ±0.6	8.7 ±1.5	7.4 ±1.6	0.11 ±0.02	0.11 ±0.02	0.15 ±0.01
Dentate Gyrus	5.5 ±0.8	7.1 ±1.3	5.6 ±0.6	0.17 ±0.03	0.17 ±0.03	0.16 ±0.05
Striatum (-4.0 mm)	5.4 ±0.4	6.0 ±0.6	6.9 ±0.8	0.14 ±0.02	0.14 ±0.03	0.13 ±0.02
Striatum (-4.5 mm)	4.3 ±0.3	5.3 ±1.2	5.1 ±0.8	0.21 ±0.04	0.19 ±0.05	0.25 ±0.02
Striatum (-5.0 mm)	4.4 ±0.6	5.9 ±1.5	5.9 ±1.1	0.27 ±0.06	0.18 ±0.04	0.21 ±0.03

Mean ±SEM; Prefrontal Cortex *n*= 6; Dentate Gyrus *n*= 7; Striatum *n*= 8

Preface to Chapter Three

The aim of the experiments in Chapter Three was to examine how neurons and glia regulate extracellular glutamate to determine the source of increased extracellular glutamate after diffuse traumatic brain injury. Using glutamate-sensitive microelectrode arrays (MEAs) coupled with targeted pharmacological agents, I developed a model on the regulation of extracellular glutamate by neurons and glia. Furthermore, I detected disruptions in the release and regulation of extracellular glutamate by both neurons and glia after diffuse brain injury. Overall, this study uncovers specific targets to try to improve the regulation of extracellular glutamate with therapeutics after TBI.

Chapter Three: Disruptions in the Regulation of Extracellular Glutamate by Neurons and Glia in the Rat Striatum Two Days after Diffuse Brain Injury

Abstract

Disrupted regulation of extracellular glutamate in the central nervous system contributes to and can exacerbate the acute pathophysiology of traumatic brain injury (TBI). Previously, we reported increased extracellular glutamate in the striatum of anesthetized rats at two days after diffuse brain injury. To determine the mechanism(s) responsible for increased extracellular glutamate, we used enzyme-based microelectrode arrays (MEAs) coupled with specific pharmacological agents targeted at *in vivo* neuronal and glial regulation of glutamate. After TBI, extracellular glutamate was significantly increased in the striatum by ~90% averaging $4.1 \pm 0.6 \mu\text{M}$ compared to sham $2.2 \pm 0.4 \mu\text{M}$. Calcium-dependent neuronal glutamate release, investigated by local application of a N-type calcium channel blocker, was no longer a significant source of extracellular glutamate after TBI compared to sham. In brain-injured animals, inhibition of glutamate uptake with local application of an excitatory amino acid transporter inhibitor produced significantly greater increase in glutamate spillover (~65%) from the synapses of brain-injured animals compared to sham. Furthermore, glutamate clearance measured by locally applying glutamate into the extracellular space revealed significant reductions in the glutamate clearance parameters in brain-injured animals compared to sham. Taken together, these data indicate disruptions in calcium-mediated glutamate

release and glial regulation of extracellular glutamate contribute to increased extracellular glutamate in the striatum two days after diffuse brain injury. Overall, these data suggest that therapeutic strategies used to regulate glutamate release and uptake may improve excitatory circuit function and possibly outcomes following TBI.

Introduction

The central nervous system requires strict regulation of extracellular glutamate to guard against aberrant neuronal signaling and possible excitotoxicity. Disrupted glutamate regulation plays a pivotal role in the acute pathophysiology of traumatic brain injury (TBI) through the initiation of secondary injury cascades (McIntosh, et al. 1996, Bullock, et al. 1998). The primary physical and mechanical forces of a TBI disrupt the blood-brain barrier and cellular membranes leading to a release of intracellular contents into the extracellular space (Schmidt and Grady 1993, Bullock, et al. 1998). Furthermore, disruptions in ionic regulation after TBI create a massive depolarization or wave of depolarizations that promotes excessive neuronal glutamate release (Katayama, et al. 1990). Moreover, post-traumatic reductions in the expression of excitatory amino acid transporters (EAATs) responsible for removing glutamate from the extracellular space leads to further increases in extracellular glutamate levels (Rao, et al. 1998, van Landeghem, et al. 2001, Yi, et al. 2005, van Landeghem, et al. 2006, Yi and Hazell 2006). High extracellular glutamate propagates secondary injury cascades through the activation of glutamate receptors, increasing ionic flux, disrupting ionic homeostasis, activating calcium-dependent proteases and phospholipases, uncoupling ATP synthesis, and producing reactive oxygen species (Faden, et al. 1989, Hall, et al. 1994, McIntosh, et al. 1996, Yi and Hazell 2006).

Glutamate is normally released into the extracellular space by both neuronal and non-neuronal sources (Jabaudon, et al. 1999, Jensen, et al. 2000). Once in the extracellular space, glutamate binds to both ionotropic glutamate receptors and metabotropic glutamate receptors (mGluRs) for signal propagation. For removal of glutamate from the extracellular space, five high affinity sodium-dependent excitatory amino acid transporters (EAATs), GLAST, GLT-1, EAAC, EAAT4, and EAAT5, are expressed throughout the central nervous system (Danbolt 2001). Glutamate uptake is driven by electrochemical gradients across neurons and glia with the majority (~90%) of

glutamate uptake performed by two glial transporters in the rat striatum, GLAST and GLT-1 (Rothstein, et al. 1996, Tanaka, et al. 1997, Danbolt 2001).

Clinically, a multitude of studies have detected significant increases in extracellular glutamate levels in the days following injury with some reports correlating increases in extracellular glutamate with unfavorable outcomes (Persson and Hillered 1992, Bullock, et al. 1995, Bullock, et al. 1998, Koura, et al. 1998, Vespa, et al. 1998, Yamamoto, et al. 1999, Reinert, et al. 2000, Hutchinson, et al. 2002, Hlatky, et al. 2004, Chamoun, et al. 2010, Lakshmanan, et al. 2010, Timofeev, et al. 2011a). These studies emphasize the significance of glutamate dysregulation in the acute pathophysiology and consequences of TBI. Unlike the clinical studies, multiple animals studies report increases in extracellular glutamate at the time of the injury, which returns to baseline concentrations within a few hours (Faden, et al. 1989, Katayama, et al. 1990, Nilsson, et al. 1990, Palmer, et al. 1993, Globus, et al. 1995, Katoh, et al. 1997, Stoffel, et al. 1997, Matsushita, et al. 2000, Rose, et al. 2002, Stoffel, et al. 2002). Because experimental TBI has failed to model glutamate dysregulation seen in the clinic, the role of glutamate excitotoxicity in the acute pathophysiology of TBI has been challenged and remains unclear (Carbonell and Grady 1999, Obrenovitch 1999).

Using novel enzyme-based microelectrode arrays (MEAs) to measure extracellular glutamate, we previously reported significant increases in extracellular glutamate and evoked glutamate release in the striatum two days after midline fluid percussion brain injury (Hinzman, et al. 2010). The purpose of this study was to examine the regulation of extracellular glutamate by both neurons and glia to identify specific mechanism(s) responsible for the increased extracellular glutamate in the rat striatum two days after diffuse brain injury. Using targeted pharmacological agents, we examined how both neurons and glia release and regulate extracellular glutamate. First, we examined the contribution of calcium-mediated neuronal glutamate release to extracellular glutamate by locally applying an N-type calcium channel blocker (ω -conotoxin). Second, we examined if transient activation of the group II mGluRs (mGluR_{2/3}) would improve neuronal regulation of extracellular glutamate by locally applying a mGluR_{2/3} agonist (LY 379268). Third, we examined non-neuronal sources of extracellular glutamate such as the glial expressed cystine/glutamate exchanger (x_c^-) by locally applying a x_c^- blocker ((S)-4-carboxyphenylglycine: CPG). Fourth, we examined how glia regulate extracellular glutamate by inhibiting glutamate uptake with a competitive non-transportable EAATs blocker (*D,L*-threo- β -benzyloxyaspartate: TBOA).

Finally, we directly tested the ability of glia to clear glutamate from the extracellular space.

Materials and Methods

Animals

Male Sprague-Dawley rats (300-400g; Harlan Laboratories Inc., Indianapolis, IN) were used for all experiments (n =45). The animals were housed in a 12 h light/dark cycle with food and water available *ad libitum* according to the Association for Assessment and Accreditation of Laboratory Animal Care International. Animals were acclimated to their environment for at least one week before any experiments. After surgery, animals were evaluated daily for post-operative care by a physical examination of the rat screening the animals breathing, gait, coat appearance, dehydration, body appearance, locomotion, and food and water intake. Animal care was approved by the University of Kentucky Institutional Animal Care and Use Committee.

Midline fluid percussion injury (FPI)

Animals were subjected to midline FPI as previously described (Lifshitz 2008, Hinzman, et al. 2010, Thomas, et al. 2011). Rats were initially anesthetized with isoflurane at 5% for five minutes and placed in a stereotaxic frame in a sterile surgery hood with continuously delivered isoflurane at 2%. The head was shaved and a 70% alcohol and betadine solution was applied to the skin. Eyes were treated with artificial tears and body temperature was maintained with a delta-phase heating pad at ~37°C (Braintree Scientific, Braintree, MA). A midline incision was made and fascia removed from the skull. A 4.7 mm trephine was used for the craniotomy, centered on the sagittal suture between *bregma* and *lambda* without disrupting the underlying dura or superior sagittal sinus. Anchoring screws were secured into pilot holes remote from the craniotomy. An injury hub was constructed from a Luer-Loc hub (20 gauge needle). The outer diameter of the hub was beveled to match the craniotomy. The injury hub was fitted into the craniotomy and cyanoacrylate gel was applied to seal the skull-hub interface. To secure the injury hub to the anchoring screws, methyl-methacrylate (Hygenic Corp., Akron, OH) was applied. The hub was filled with sterile saline and the

wound sutured to prevent tearing. The female Luer-Loc injury hub was connected to the male Luer-Loc hub of the injury device (Custom Design and Fabrication, Virginia Commonwealth University, Richmond, VA). Before reflexive responses returned, the pendulum hammer of the injury device was dropped onto the fluid-filled piston to induce a moderate injury. Sham injured animals underwent the same procedure without induction of injury. The fluid pressure pulse for the brain injury was 2.0 ± 0.01 atm. The injury hub was removed and any bleeding controlled with Gelfoam (Pharmacia, Kalamazoo, MI). The incision was closed with staples. Righting reflex recovery times were recorded for the injury group, from the time of impact to the time when animals' spontaneously righted. Brain injured animals had righting times of 437 ± 19 seconds ($n = 23$). Sham injured animals had righting reflex less than 15 seconds ($n = 22$). No animals died from complications caused by the injury.

Enzyme-based microelectrode arrays

Ceramic-based MEAs, consisting of four platinum recording sites ($15 \times 333 \mu\text{m}$) arranged vertically in dual pairs, were prepared and selected for *in vivo* recordings as previously described (Burmeister, et al. 2002, Day, et al. 2006, Hascup, et al. 2007, Stephens, et al. 2009, Hinzman, et al. 2010). Briefly, a glutamate-oxidase solution covered one pair of recording sites to allow for the enzymatic conversion of glutamate to α -ketoglutarate and the generation of the reporter molecule, H_2O_2 . The small amount of H_2O_2 generated by glutamate-oxidase on the surface of the MEA will have a minimal impact on the production of reactive oxygen species in the local area due to the small amount of glutamate-oxidase coated on the surface of the MEA, the oxidation of H_2O_2 by the MEA, and the limited time of the MEA in the tissue. An inactive protein matrix covered the other pair of recording sites (sentinel sites). The two different coatings allowed the use of a self-referencing technique, in which the background current of the sentinel sites could be subtracted from the current of the glutamate-oxidase sites, thereby producing a more selective glutamate measure allowing the determination of tonic levels of glutamate (Burmeister and Gerhardt 2001, Burmeister, et al. 2002). Furthermore, a size exclusion layer of 1,3-phenylenediamine (mPD) was electroplated onto the platinum recording sites to restrict the passage of large molecule interferents (ascorbic acid and dopamine) from reaching the platinum recording sites to further improve the selectivity of the MEA's for glutamate detection (Hinzman, et al. 2010).

MEA calibration

Constant potential amperometry was performed with the MEAs using the FAST-16 mkII system (Quanteon Inc., LLC, Nicholasville, KY). A potential of +0.7 V versus an Ag/AgCl reference was applied to oxidize the reporter molecule, H₂O₂. The resulting current was amplified and digitized by the FAST-16 mkII system. Calibrations were conducted to test the capability of the MEA to selectively measure glutamate and to generate a standard curve for the conversion of current to concentration of glutamate. The parameters tested were limit of detection (three times the standard deviation of the baseline noise), selectivity (ability of the MEA to measure glutamate compared to a major interferent, ascorbic acid), and slope of the electrode (the linear increase in current due to additions of glutamate). The average limit of detection was 0.99 ±0.1 μM, selectivity was 301 ±57 (glutamate: ascorbic acid), and slope was 8.7 ±0.6 pA/μM (*n*=113 glutamate recording sites). Calibrations were conducted before *in vivo* experimentation to ensure MEAs were functional before implantation and prior results have shown similar performance of the MEAs between pre- and post-experimental testing (Hinzman, et al. 2010).

MEA/micropipette assembly

For local application of solutions into the rat brain, glass micropipettes (1 mm o.d. 0.58 mm i.d., A-M Systems, Inc., Everett, WA) were pulled (Kopf Instruments, Tujunga, CA), and the tips of the micropipettes were bumped to create a tip with an i.d. of 10-15 μm. The micropipettes were placed centrally among all four platinum recording sites and mounted 50-100 μm above the MEA. Micropipettes were filled with (1) 10 μM ω-conotoxin GVIA, N-type calcium channel blocker, (Alomone Labs, Jerusalem, Israel); (2) 100 μM LY 379268, mGluR_{2/3} receptor agonist, (Tocris, Ellisville, MO); (3) 50 μM (S)-4-carboxyphenylglycine (CPG), x_c⁻ blocker, (Tocris, Ellisville, MO); (4) 100 μM D,L-threo-β-benzyloxyaspartate (TBOA), EAATs competitive inhibitor, (Tocris, Ellisville, MO); (5) 500 μM glutamate (Sigma-Aldrich, St. Louis, MO); or (6) physiological saline (Day, et al. 2006, Hascup, et al. 2010). All drugs were dissolved to their final concentrations in physiological saline. Solutions were sterile filtered (0.20 μm) and adjusted to a pH of 7.4. The micropipette was connected to a Picospritzer III (Parker-Hannifin, Cleveland, OH)

with settings adjusted to consistently deliver volumes between 12.5-350 nL. Pressure was applied from 2-30 psi for 0.3-3 sec. Volume displacement was monitored with the use of a stereomicroscope fitted with a reticule to determine and control the volume of solution that was locally applied by pressure ejection. (Friedemann and Gerhardt 1992).

***In vivo* anesthetized recordings of extracellular glutamate**

Two days after midline FPI, rats were anesthetized with urethane (1.25 g/kg i.p.) (Sigma-Aldrich) and prepared for *in vivo* electrochemical recordings as previously described (Day, et al. 2006, Hascup, et al. 2007, Stephens, et al. 2009, Thomas, et al. 2009, Hinzman, et al. 2010, Thomas, et al. 2011). Briefly, animals were placed in a stereotaxic frame and body temperature was maintained at ~37 °C with a water pad connected to a recirculating water bath. A craniotomy was performed to provide access to the striatum (AP: +1.0 mm, ML: +/- 2.5 mm, DV: -3.5, -4.0, -4.5, -5.0 mm), (Paxinos and Watson, 1998). A Ag/AgCl reference wire was implanted into the lateral parietal cortex. The MEA was lowered into the brain using a microdrive (MO-10, Narishige International, East Meadow, NY). All MEA recordings were performed at a frequency of 2 Hz.

To measure tonic extracellular glutamate, the background current from the sentinel site was subtracted from the current of the enzyme site. Then, the resulting current (pA) was converted to glutamate concentration by dividing the current by the slope (pA/ μ M) obtained during the calibration. To examine the effect of drugs on extracellular glutamate, 100 nL of physiological saline was locally applied to assess potential dilution effects. Then, the solution in the micropipette was exchanged and 100 nL of the drug of interest was locally applied into the striatum using the same application parameters. The maximum increase/decrease in extracellular glutamate and area above/below the curve (to examine the extent of changes in extracellular glutamate with respect to time) were calculated for both local application of saline and the drugs of interest. To examine glutamate clearance, varying volumes of 500 μ M glutamate were applied into the extracellular space. Glutamate signals with amplitudes in the 5-50 μ M range were analyzed as this was the physiological range of KCl-evoked glutamate release seen in sham and brain injured rats (Hinzman, et al. 2010). Glutamate clearance was analyzed for the following parameters: (1) amplitude (μ M); (2) T_{rise} (s), the time for the signal to reach the peak amplitude; (3) T_{80} (s), the time for the signal to decay by

80% from the peak amplitude; (4) and k_{-1} (sec^{-1}), the slope of the linear regression of the natural log transformation of the decay over time (Nickell, et al. 2007, Thomas, et al. 2009, Hinzman, et al. 2010).

Quantitative gene expression (rtPCR)

Two days post-injury, sham and brain-injured animals were transcardially perfused with cold saline, the brains rapidly removed from the skull, dissected into 2 mm slices using a chilled rat brain matrix, and a 1 mm diameter biopsy was removed from the dorsal striatum. The mRNA content was stabilized (RNAlater, Qiagen Corp) and stored frozen. Isolated mRNA (RNeasy, Qiagen Corp) was quantified (NanoDrop ND-1000 spectrophotometer), converted to complementary DNA (cDNA; High Capacity cDNA Archive Kit, Applied Biosystems Inc.) and then used as a template for selected commercially-available gene expression assays for quantitative real-time PCR (StepONE, Applied Biosystems). The Applied Biosystems TaqMan[®] Gene Expression Assays (GLT-1: Rn00568080_m1; GLAST: Rn00570130_m1; 18s rRNA: 4352930E) were used for EAAT gene expression. Within each animal, relative gene expression was normalized to the 18s rRNA endogenous control and the expression level in the sham/vehicle group using the $2^{-\Delta\Delta CT}$ method (Livak and Schmittgen 2001), which relates gene expression to the PCR cycle number at which the fluorescence signals exceed a threshold above baseline. Relative gene expression was compared between sham and brain-injured animals using a two-tailed t-test.

Statistical analyses

Amperometric data were analyzed using custom MATLAB[®] - based software. For both resting extracellular glutamate and analysis of glutamate clearance, multiple depths in the striatum were averaged per animal as there were no sub-regional differences detected. All data were analyzed using a two-tailed t-test. Data are presented as mean \pm SEM, and statistical significance was defined as $p < 0.05$.

Results

Increased extracellular glutamate in the striatum of brain-injured rats

Previously, our laboratory has reported increased extracellular glutamate in the striatum two days after midline fluid percussion injury (Hinzman, et al. 2010). Here, we confirm the original finding detecting significantly higher extracellular glutamate after TBI than in sham [$t_{30} = 2.681$, $p = 0.012$] (Fig 3.1). Extracellular glutamate averaged 2.2 ± 0.4 μM (Sham) vs. 4.1 ± 0.6 μM (TBI). Since we detected significant increases in extracellular glutamate after TBI, we set out to pharmacologically manipulate the regulation of glutamate by both neurons and glia to determine the possible mechanism(s) responsible for the increased extracellular glutamate after TBI.

Reduced calcium channel-dependent glutamate release in the striatum of brain-injured rats

By applying a N-type calcium channel blocker (ω -conotoxin) into the extracellular space, we examined the contribution of calcium-mediated vesicular glutamate release on extracellular glutamate. In sham, local application of ω -conotoxin produced a significant (~80 %) decrease in extracellular glutamate and reduced glutamate for a longer period of time (area under curve) compared to local application of saline (Table 3.1). After TBI, local application of ω -conotoxin failed to reduce the extracellular glutamate concentration compared to local application of saline (Table 3.1). Averaged group responses to the local application of ω -conotoxin into the striatum in both sham and TBI groups demonstrate the reduced efficacy of ω -conotoxin on reducing extracellular glutamate after TBI (Fig 3.2A). The maximum decrease in extracellular glutamate in the presence of ω -conotoxin was significantly smaller after TBI compared to sham [$t_6 = 2.901$, $p = 0.028$] (Fig 3.2B). Also, the extent of reduced glutamate with respect to time (area under curve) was significantly reduced after TBI as compared to sham [$t_6 = 3.113$, $p = 0.021$] (Fig 3.2C). Thus, in sham animals calcium-mediated neuronal glutamate release was a significant source to extracellular glutamate. Whereas, calcium-mediated neuronal glutamate release was no longer a significant source to extracellular glutamate in brain-injured animals. Consequently, increased calcium-dependent glutamate release is unlikely to be a predominant mechanism for increased extracellular glutamate after TBI.

Activation of mGluR_{2/3} failed to reduce extracellular glutamate in the striatum of sham and brain-injured rats

Additional studies were carried out to investigate other potential presynaptic changes in glutamate regulation after TBI. By applying an mGluR_{2/3} agonist (LY 379268) into the extracellular space, we examined if transient activation of the glutamate autoreceptors, mGluR_{2/3}, would reduce neuronal glutamate release and thereby improve regulation of extracellular glutamate. Local application of LY 379268 failed to produce a significant decrease in extracellular glutamate compared to local application of saline in sham and after TBI (data not shown). Thus, insufficient mGluR_{2/3} activation is unlikely to be responsible for increased extracellular glutamate after TBI.

Inhibition of the glial x_c^- failed to reduce extracellular glutamate in the striatum of sham and brain-injured rats

Another glial source of extracellular glutamate may be derived from the x_c^- , predominantly localized to glia. Considerable attention has recently been paid to the x_c^- and its possible role in glutamate dysregulation by glia in drug abuse (Kalivas 2009). By applying a x_c^- blocker (CPG) into the extracellular space, we examined the contribution of glutamate release through the x_c^- on extracellular glutamate. Local application of CPG failed to produce a significant decrease in glutamate compared to local application of saline in sham and after TBI (data not shown). Thus, glial glutamate release through the x_c^- is not a significant source of extracellular glutamate in sham and TBI animals, and glutamate release through the x_c^- unlikely to be a mechanism for increased extracellular glutamate after TBI.

Increased glutamate spillover from the inhibition of glutamate uptake in the striatum of brain-injured rats

We further examined if disruptions in the regulation of extracellular glutamate by glia were responsible for the increased extracellular glutamate after TBI. Glutamate uptake through the EAATs, predominantly localized to glia, is the primary mechanism for regulating extracellular glutamate. By locally applying a competitive non-transportable EAAT blocker (TBOA) into the extracellular space, we examined how transient inhibition of glutamate uptake alters the extracellular glutamate concentration. In sham, local

application of TBOA produced a rapid and significant increase in the extracellular glutamate concentration and produced higher levels of glutamate for a longer period of time (area under curve) compared to local application of saline (Table 3.1). After TBI, local application of TBOA produced a rapid and significant increase in the extracellular glutamate concentration and produced higher levels of glutamate for a longer period of time (area under curve) compared to local application of saline (Table 3.1). Averaged group responses from the local application of TBOA within the striatum in both sham and TBI groups demonstrate increased amounts of glutamate spillover from inhibition of glutamate uptake after TBI (Fig 3.3A). The maximum increase in extracellular glutamate from local application of TBOA was significantly greater after TBI than sham [$t_6 = 3.391$, $p = 0.015$] (Fig 3.3B). Also, after TBI more glutamate remained in the extracellular space for a longer period of time (area under curve) than in sham [$t_6 = 2.521$, $p = 0.045$] (Fig 3.3C). Thus, the increased glutamate spillover from the transient inhibition of glutamate uptake in brain-injured animals suggests decreased glutamate uptake may play a role in the increase in extracellular glutamate after TBI.

Using quantitative real-time PCR, we examined if decreased gene expression of glial EAATs (GLAST and GLT-1) was responsible for the increased sensitivity to the inhibition of the EAATs to TBOA. In the dorsal striatum, the relative expression of GLAST and GLT-1 was decreased, but not significantly after TBI compared to sham; (sham: TBI), GLAST (1.02 ± 0.13 : 0.80 ± 0.06) [$t_6 = 1.58$, $p = 0.164$], GLT-1 (1.01 ± 0.06 : 0.84 ± 0.16) [$t_6 = 0.95$, $p = 0.378$]. Thus, any injury-related changes in glial glutamate transporters are not evident as changes in gene expression.

Decreased glutamate clearance in the striatum of brain-injured rats

We further explored post-traumatic decreases in glutamate uptake by examining how sham and brain-injured animals were able to clear exogenous applications of glutamate within the striatum. Local application of small volumes of glutamate into the extracellular space, allowed us to mimic endogenous glutamate release and examine clearance of glutamate back to baseline values. The primary mechanism for removing glutamate from the extracellular space is glutamate uptake via EAATs. Diffusion of glutamate also plays a role in lowering the extracellular glutamate concentration, but is limited by the extracellular anatomy (Danbolt 2001). Representative recordings demonstrate slower glutamate clearance after TBI than sham (Fig 3.4A). Since the

amplitude of the glutamate signals were similar between sham ($30.4 \pm 1.6 \mu\text{M}$) and TBI ($32.4 \pm 1.9 \mu\text{M}$) [$t_{14} = 0.8139$, $p = 0.429$] (Fig 3.4B), we compared specific parameters of glutamate clearance (Nickell, et al. 2007, Thomas, et al. 2009, Thomas, et al. 2011). After local application of glutamate, glutamate levels spike and rapidly returned to baseline concentrations as glutamate diffused from the local area and through uptake of glutamate from the extracellular space. We calculated the T_{rise} , the time for the signal to reach the maximum amplitude, to examine if injury altered diffusion of glutamate in the extracellular space. The T_{rise} was not significantly altered after TBI ($1.8 \pm 0.1 \text{ s}$) compared to sham ($1.9 \pm 0.1 \text{ s}$) [$t_{14} = 1.129$, $p = 0.278$] (Fig 3.4C). Since, no differences in diffusion were detected after injury, any reductions in glutamate clearance likely result from decreases in glutamate uptake. TBI produced a significant decrease in k_{-1} , a measure of glutamate uptake, ($0.31 \pm 0.05 \text{ s}^{-1}$), compared to sham ($0.48 \pm 0.07 \text{ s}^{-1}$) [$t_{14} = 2.166$, $p = 0.048$] (Fig 3.4D). Also, TBI produced a significantly longer T_{80} , time for the signal to decay by 80% from the peak amplitude ($4.5 \pm 0.6 \text{ s}$), compared to sham ($3.2 \pm 0.2 \text{ s}$) [$t_{14} = 2.184$, $p = 0.047$] (Fig 3.4E). Thus, TBI produced significant decreases in glutamate clearance, without altering diffusion rates of extracellular glutamate between sham and TBI. Functional decreases in glutamate uptake are likely to be a primary mechanism responsible for increased extracellular glutamate after TBI.

Discussion

The purpose of this study was to examine the regulation of extracellular glutamate by both neurons and glia to determine the specific mechanism(s) responsible for the increase in extracellular glutamate in the rat striatum two days after diffuse brain injury. By combining glutamate-sensitive MEAs with targeted pharmacological agents, we were able to examine the neuronal and glial contributions to the release and regulation of extracellular glutamate. In sham animals, presynaptic calcium channel-dependent neuronal glutamate release significantly contributed to extracellular glutamate. Glia were also found to regulate extracellular glutamate as inhibition of EAATs produced a significant increase in extracellular glutamate. Two days after diffuse brain injury, we detected significant post-traumatic disruptions in the regulation of extracellular glutamate by both neurons and glia. In brain-injured animals, the contribution of presynaptic calcium channel-dependent neuronal glutamate release to extracellular glutamate was significantly decreased compared to sham. In addition, TBI

produced increased glutamate spillover from the inhibition of glutamate uptake in the striatum of brain-injured rats. Furthermore, brain-injured animals exhibited slower clearance of extracellular glutamate due primarily to decreases in glutamate uptake, yet not necessarily due to decreases in GLAST and GLT-1 gene expression. These results are depicted in schematic format to highlight possible sites of dysregulation in the injury-induced increase in extracellular glutamate (Fig 3.5).

Calcium channel-dependent neuronal glutamate release contributes extracellular glutamate in sham animals

In sham animals, local application of ω -conotoxin produced a significant ~80% decrease in extracellular glutamate, suggesting that a majority of extracellular glutamate measured by MEAs is of a neuronal origin. This result is similar to another study using MEAs, where local application of ω -conotoxin (mixed channel type) produced a significant ~50% decrease in the extracellular glutamate concentration in awake freely moving animals (Hascup, et al. 2010). Collectively, these results confirm that MEAs measure extracellular glutamate derived, in part, from calcium-dependent neuronal release. In contrast to the MEA studies, extracellular glutamate sampled by microdialysis is insensitive to sodium/calcium channel blockers; suggesting the extracellular pool of glutamate sampled with microdialysis is of a non-neuronal origin (Timmerman and Westerink 1997). The discrepancy that MEAs detect neuronally derived glutamate, whereas microdialysis samples extracellular glutamate derived from non-neuronal origins, may be due to inherent differences in the methodologies. The extensive damage to the local brain area during implantation of the microdialysis probe and the large area of tissue sampled (1-4 mm in length), restricts microdialysis measurements of glutamate to large regions far beyond synapses (Timmerman and Westerink 1997, Obrenovitch 1999, Obrenovitch, et al. 2000, Borland, et al. 2005, Hillered, et al. 2005, Jaquins-Gerstl and Michael 2009). Furthermore, the inadequate temporal resolution of microdialysis (~1-20 min) prevents microdialysis from detecting the rapid dynamic changes in extracellular glutamate that occur in the order of milliseconds to seconds (Diamond 2005). The improved spatial resolution (333 μ m in length), limited damage to the local area from implantation of the device and fast temporal resolution (2 Hz) allow MEAs to detect the fast dynamics of glutamate closer to synapses and detect extracellular glutamate that is neuronally derived (Day, et al. 2006, Hascup, et al. 2007, Rutherford, et al. 2007, Hascup, et al. 2009, Hascup, et al. 2010).

Reduced calcium channel-dependent neuronal glutamate release in brain-injured rats

In contrast to sham animals, local application of ω -conotoxin failed to significantly reduce the extracellular glutamate concentration compared to saline after TBI. This shift in the source of glutamate release from neuronal sources in sham to non-neuronal sources after TBI could be explained by two different mechanisms. First, there could be a post-traumatic decrease in neuronal glutamate release with a concurrent increase in non-neuronal sources of glutamate. Non-neuronal sources of extracellular glutamate can include: One, micropores in cellular membranes from the primary injury forces can release glutamate into the extracellular space due to the higher concentrations of glutamate found in the cytosol or blood (Schmidt and Grady 1993, Koizumi, et al. 1997). Two, activated microglia can release glutamate into the extracellular space in response to inflammatory cytokines after TBI (Brown and Neher 2010). Three, glutamate can be released from the x_c^- , which may be enhanced after injury for the production of glutathione, a major cellular anti-oxidant (Baker, et al. 2002, Domercq, et al. 2007). Four, EAATs can reverse due to ionic and metabolic disruptions after TBI transporting glutamate into the extracellular space (Gemba, et al. 1994, Phillis, et al. 2000, Hamann, et al. 2002). Overall, the observed reduction in presynaptic calcium channel-dependent vesicular glutamate release after TBI may be a compensatory mechanism for increases in non-vesicular sources of glutamate.

A second mechanism that may contribute to the decrease in presynaptic calcium channel-dependent glutamate release after TBI is a post-traumatic alteration in the mechanism of vesicular glutamate release that is independent of calcium entry through the N-type calcium channel. Neurons are capable of vesicular release independent of calcium entry from the extracellular space, as internal calcium stores can mobilize from the mitochondria and endoplasmic reticulum for vesicular release (Ryglewski, et al. 2007, Neher and Sakaba 2008). After midline FPI, neurons have exhibited disrupted calcium regulation with increasing intracellular calcium levels (Sun, et al. 2008, McGinn, et al. 2009). The disrupted internal calcium regulation and a post-traumatic shift utilizing internal calcium stores for vesicular glutamate release may explain why blocking the N-type calcium channel with ω -conotoxin failed to reduce extracellular glutamate in brain-injured animals.

Neuronal regulation of extracellular glutamate (mGluR_{2/3})

Transient activation of the glutamate autoreceptors (mGluR_{2/3}) has been reported to regulate neuronal glutamate release (Bond, et al. 1999), potentially restoring extracellular glutamate levels in the injured brain. The mGluR_{2/3}s are G-protein linked receptors that negatively regulate adenylate cyclase and decrease levels of cyclic adenosine monophosphate (Danbolt 2001). The mGluR_{2/3} act as negatively coupled autoreceptors providing presynaptic inhibition of glutamate release (Nakanishi 1994, Di Iorio, et al. 1996, Battaglia, et al. 1997, Allen, et al. 1999, Schoepp 2001). In sham animals, local application of LY 379268 failed to significantly reduce extracellular glutamate compared to saline. Whereas, a previous study in awake animals detected a significant ~20% decrease in the extracellular glutamate from local application of LY 379268 (Hascup, et al. 2010). The discrepancy between our results and the aforementioned study may be due to confounding effects of anesthesia, as urethane has been shown to dramatically reduce extracellular glutamate by ~60-80% (Rutherford, et al. 2007).

We hypothesized that local transient activation of mGluR_{2/3} would reduce excessive synaptic glutamate release and lower extracellular glutamate, as we have previously shown increased amounts of neuronal glutamate release from local depolarization in the rat striatum two days after TBI (Hinzman, et al. 2010). Furthermore, multiple reports have shown LY 379268 to be neuroprotective in ischemia and TBI models (Cai, et al. 1999, Bond, et al. 2000, Stover, et al. 2003, Movsesyan and Faden 2006). However, in brain-injured animals transient local application of LY 379268 failed to reduce extracellular glutamate compared to saline. The inability of LY 379268 to reduce extracellular glutamate was also seen in a prior study, where a single i.p. injection of LY 379268 improved EEG activity, reduced contusion volume, but failed to reduce extracellular glutamate; suggesting LY 379268 works through other mechanisms to provide neuroprotection than solely reducing extracellular glutamate (Stover, et al. 2003).

Glial source of extracellular glutamate (xc-)

We also examined glial glutamate release through the x_c^- , a potential non-neuronal source of extracellular glutamate, by locally applying x_c^- blocker (CPG). The x_c^- , predominantly localized to glia, is an antiporter internalizing cystine with simultaneous release of glutamate; x_c^- plays a vital role in the prevention of oxidative damage by importing cystine for the production of glutathione, a major anti-oxidant in the cell (Albrecht, et al. 2010). The x_c^- has been proposed as a major source of extracellular glutamate with CPG producing a significant ~60% decrease in extracellular glutamate sampled by microdialysis (Baker, et al. 2002). In our study, local application of CPG failed to significantly reduce extracellular glutamate compared to saline in both sham and TBI animals. Similar to our data, multiple reports have detected no significant change in extracellular glutamate with application of CPG in both anesthetized and awake animals (Melendez, et al. 2005, Hascup, et al. 2010, Lupinsky, et al. 2010). In general, the data reported here and from prior reports suggest a limited role for the x_c^- as a source of extracellular glutamate.

Glutamate uptake through EAATs regulates extracellular glutamate

In sham animals, we examined the role of EAATs on regulating extracellular glutamate by locally applying the EAAT competitive blocker, TBOA. Local application of TBOA into the extracellular space produced a robust increase in the extracellular glutamate concentration as TBOA inhibited glutamate uptake by the EAATs allowing more glutamate to escape from the synapses. Prior studies, using both microdialysis and MEAs have detected similar increases in the extracellular concentration of glutamate with inhibition of EAATs which equates to increases in extracellular glutamate ranging from ~125-800% (Montiel, et al. 2005, Day, et al. 2006, Tovar, et al. 2009, Hascup, et al. 2010). Collectively, our data and the previous reports support the importance of EAATs in regulating extracellular glutamate.

Increased glutamate spillover from the inhibition of glutamate uptake in brain-injured rats

Similar to sham animals, in brain-injured animals local application of TBOA into the extracellular space produced a robust increase in extracellular glutamate. In addition, TBI resulted in a significantly greater increase in the amount of glutamate spillover from

the synapses of brain-injured animals compared to sham. The increase in glutamate spillover when challenged with an uptake inhibitor suggests either a post-traumatic decrease in EAATs expression or function. Although we did not detect a significant decrease in the expression of GLAST and GLT-1 genes; multiple reports have detected post-traumatic reductions in the expression of EAATs in both the clinic and experimental models of TBI (Rao, et al. 1998, van Landeghem, et al. 2001, Yi, et al. 2005, van Landeghem, et al. 2006, Yi and Hazell 2006).

Decreased glutamate clearance in brain-injured rats

Rapid application of glutamate into the extracellular space allowed us to mimic endogenous glutamate release events and examine the ability of EAATs to take up glutamate *in vivo*. Here, we report significant decreases in glutamate clearance after TBI. The post-traumatic decrease in glutamate clearance seems to be due to decreases in glutamate uptake and not due to alterations in the diffusion of glutamate within the extracellular space. If TBI drastically altered the tortuosity of the extracellular space, we would expect a post-traumatic change in the diffusion of glutamate in the extracellular space (Nicholson, et al. 2000). However, we detected no significant change in the T_{rise} as glutamate diffused from the point source (micropipette) to the MEA, suggesting the decreased glutamate clearance is due to decreased glutamate uptake. Post-traumatic reductions in glutamate uptake can play a pivotal role in the pathophysiology of TBI over stimulating metabotropic and ionotropic glutamate receptors. Peri-contusional tissue exhibits decreased expression of EAATs in both the clinic and experimental models of TBI (Rao, et al. 1998, van Landeghem, et al. 2001, Yi, et al. 2005, van Landeghem, et al. 2006, Yi and Hazell 2006). Furthermore, knockdown expression of GLAST and GLT-1 produces increased neuronal damage in an experimental model of TBI (Rao, et al. 2001). These studies demonstrate the importance of maintaining proper glutamate uptake to prevent the initiation and propagation of secondary injury cascades and development of a contusion. Early post-traumatic disruptions in glutamate clearance may play a role in the development of late-onset gain-of function behavioral morbidity that is correlated with changes in glutamate hypersensitivity (Thomas, et al. 2011). Although we do not know if the disruptions in the regulation of extracellular glutamate will hold true for later time points or indefinitely, prior work has detected persistent changes

in glutamate excitability in the thalamus and somatosensory cortex (Thomas, et al. 2011).

Decreased glutamate uptake is likely the primary mechanism for increased extracellular glutamate after injury. With reduced glutamate uptake, more glutamate can spill out from the synapse increasing extracellular glutamate over time. Furthermore, reduced glutamate uptake is likely responsible for the increased KCl-evoked glutamate release seen in our prior study (Hinzman, et al. 2010). A decrease in glutamate uptake would allow more glutamate to escape from the synapse, producing larger amplitudes during evoked release. Previously, we did not detect any post-traumatic decrease in glutamate clearance parameters from KCl-evoked glutamate release most likely due to the disruptions in the electrochemical gradient required for depolarization, which is circumvented by local application of glutamate itself.

Conclusion

Using MEAs and targeted pharmacological agents, we were able to examine how neurons and glia release and regulate extracellular glutamate *in vivo*. Two days after diffuse brain injury the contribution of calcium-mediated glutamate release via the N-type calcium channel was significantly reduced. Also, TBI produced a significant decrease in glutamate clearance that was primarily due to decreases in glutamate uptake. Future work should examine if enhancing expression of the EAATs, either by viral mediated expression or stimulating expression through the use of beta-lactam antibiotics (Rothstein, et al. 2005, Harvey, et al. 2011), produces an overall improvement in glutamate regulation and behavioral outcomes in experimental models of TBI. In addition, drugs that can improve the function and/or surface expression of EAATs remain possible therapeutic targets to improve outcomes following TBI.

Chapter Three has been published in the following manuscript:

Hinzman JM, Thomas TC, Quintero JE, Gerhardt GA and Lifshitz J. (2012). Disruptions in the Regulation of Extracellular Glutamate by Neurons and Glia in the Rat Striatum Two Days after Diffuse Brain Injury.

This is a copy of an article published in the [Journal of Neurotrauma] © [2012] [copyright Mary Ann Liebert, Inc.]; [Journal of Neurotrauma] is available online at: <http://online.liebertpub.com>.

Copyright © Jason Michael Hinzman 2012

Chapter Three: Figures

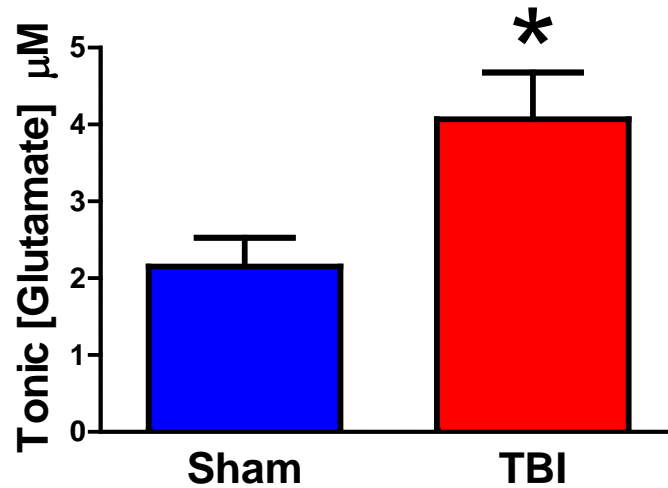


Figure 3.1 Increased extracellular glutamate in the striatum of brain-injured rats at two days after midline fluid percussion brain injury

Higher levels of extracellular glutamate in the striatum of brain-injured rats compared to sham, ($n=16$, * $p < 0.05$).

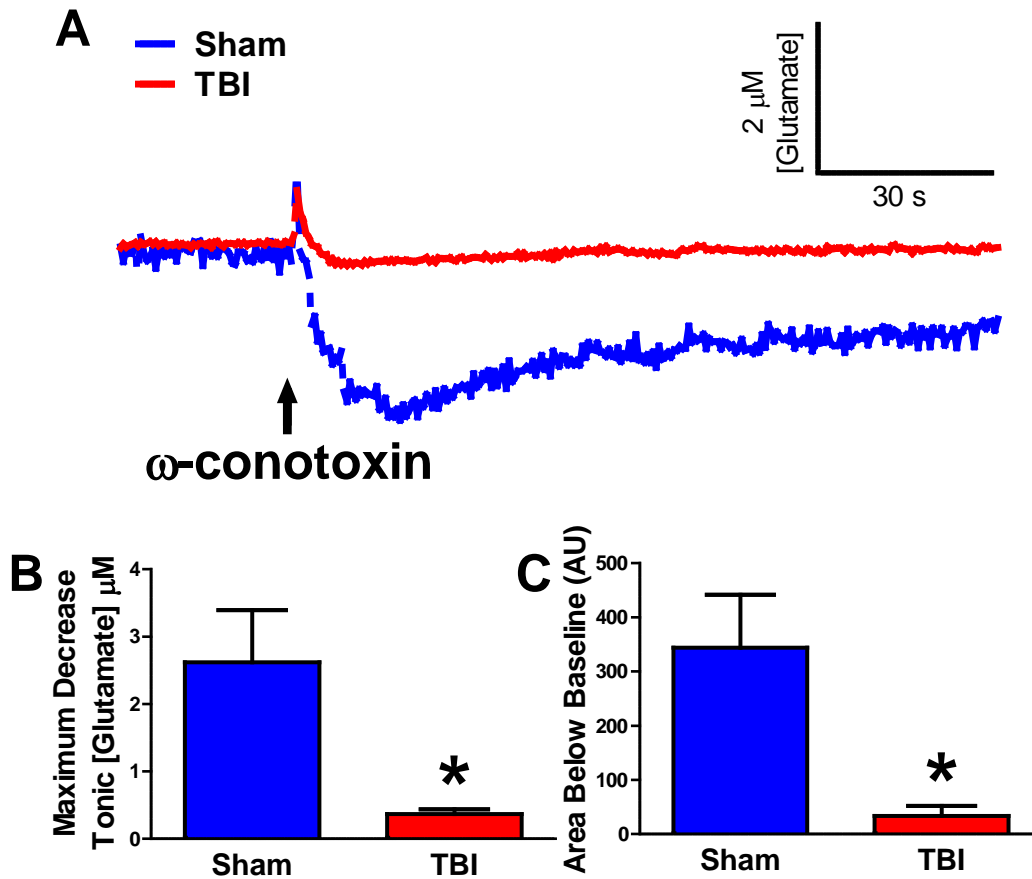


Figure 3.2 Reduced calcium channel-dependent glutamate release in the striatum of brain-injured rats

(A) Baseline-matched traces of extracellular glutamate demonstrate the average effect of 100 nL local application (↑) of 10 μM ω-conotoxin, N-type calcium channel blocker, on extracellular glutamate in sham (blue) and TBI animals (red). (B) The maximum decrease in extracellular glutamate from local application of ω-conotoxin was significantly smaller after TBI than sham. (C) The extent of reduced extracellular glutamate with respect to time (area under curve) was significantly reduced after TBI than sham (n = 4, * p < 0.05).

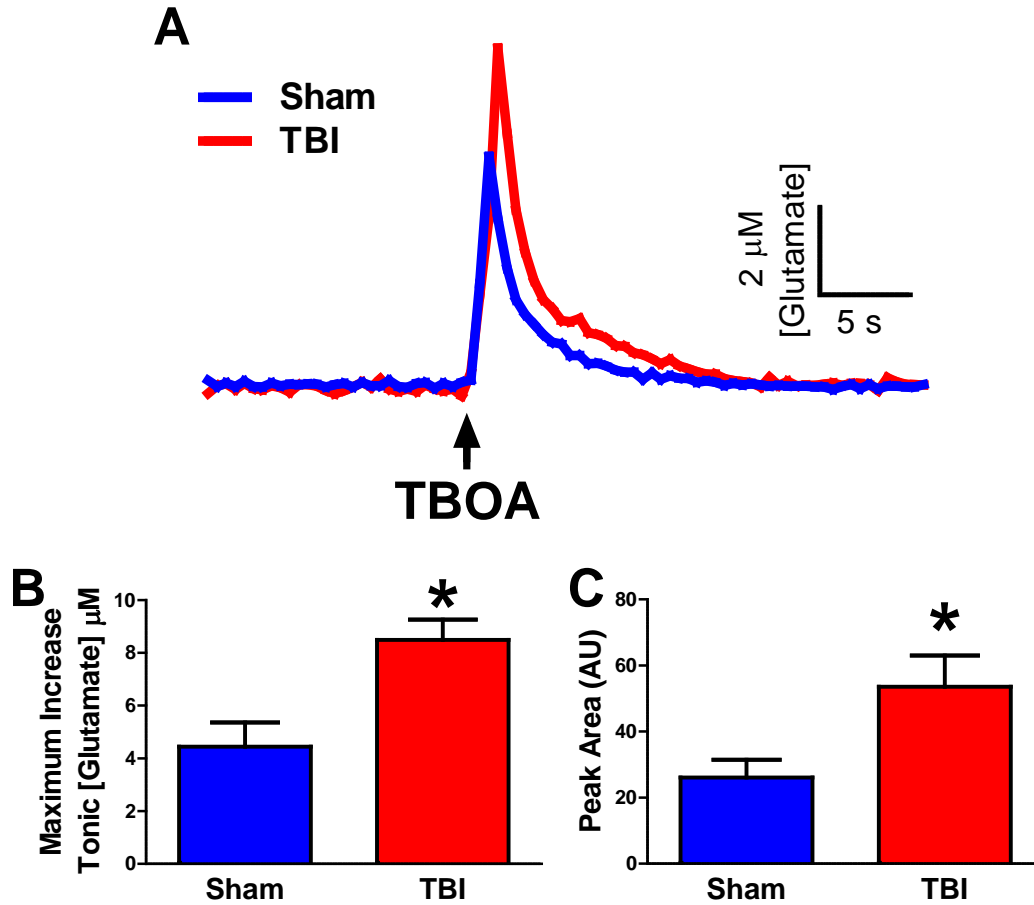


Figure 3.3 Increased glutamate spillover from inhibition of glutamate uptake in the striatum of brain-injured rats

(A) Traces of extracellular glutamate showing the average response from 100 nL local application (\uparrow) of 100 μM TBOA, excitatory amino acid transporter blocker, in sham (blue) and TBI (red). (B) The maximum increase in extracellular glutamate from local application of TBOA was significantly elevated after TBI compared to sham. (C) The extent of higher extracellular glutamate with respect to time (area under curve) was significantly increased after TBI than sham ($n = 4$, * $p < 0.05$).

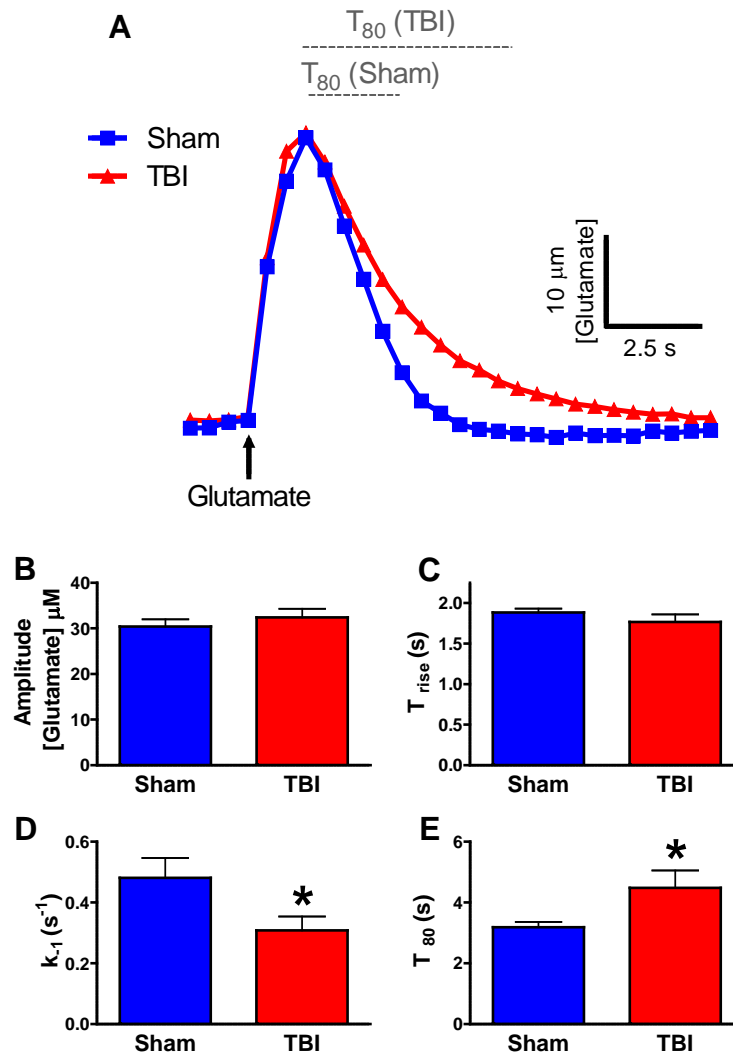


Figure 3.4 Decreased glutamate clearance in the striatum of brain-injured rats

(A) Representative glutamate signals in the striatum from local application of 500 μM glutamate (\uparrow) in sham (blue) and TBI (red) showed significant decreases in glutamate uptake parameters after TBI. (B) The amplitude of the glutamate signal was similar between sham and TBI groups. (C) T_{rise} , an indicator of glutamate diffusion, was similar between sham and TBI groups. (D) k_{-1} , an indicator of glutamate uptake rate, was significantly reduced after TBI compared to sham. (E) T_{80} , an indicator of glutamate clearance, was significantly longer after TBI compared to sham ($n = 8$, * $p < 0.05$).

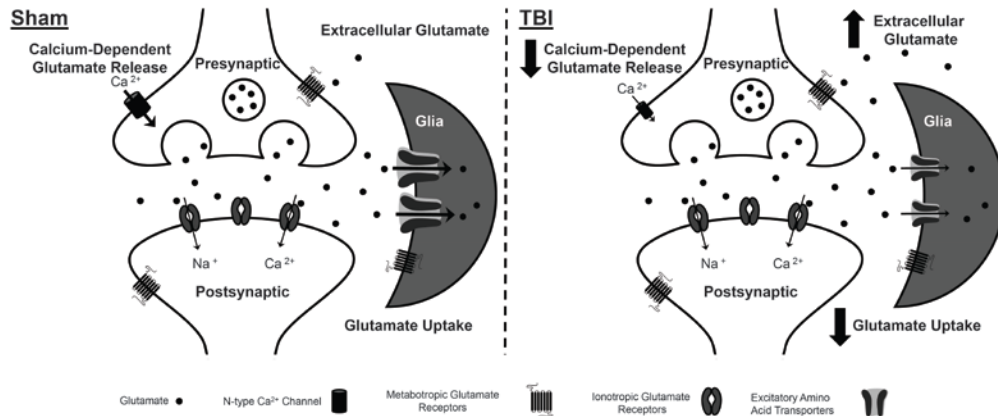


Figure 3.5 Schematic depicting the regulation of extracellular glutamate in the rat striatum in sham and brain-injured animals

In sham animals, neurons release glutamate into the extracellular space that is dependent on calcium entry through N-type calcium channels. Once in the extracellular space, glutamate acts on both metabotropic and ionotropic glutamate receptors for signal propagation. Glutamate is removed from the extracellular space by excitatory amino acid transporters, predominantly localized to glia. Glutamate uptake is the primary mechanism for removal of extracellular glutamate and is responsible for regulating the concentration extracellular glutamate. After TBI, we detected post-traumatic disruptions in the regulation of extracellular glutamate by both neurons and glia. In brain-injured animals, calcium-dependent glutamate release via N-type calcium channels was no longer a source of extracellular glutamate. Also, the uptake of glutamate by excitatory amino acid transporters was reduced in brain-injured animals. Post-traumatic decreases in glutamate uptake is likely the primary mechanism responsible for increased extracellular glutamate after TBI.

Chapter Three: Tables

Table 3.1 Effect of local application of drugs on extracellular glutamate in sham and traumatic brain injured (TBI) animals

Local Application	Maximum Change From Baseline Glutamate (μM)		Area Under Curve (AU)	
	Sham	TBI	Sham	TBI
saline	-0.7 ± 0.2	-0.4 ± 0.1	40.7 ± 21.1	11.6 ± 5.1
ω -conotoxin	$-2.6 \pm 0.8^*$	-0.4 ± 0.1	$343.8 \pm 97.8^*$	33.7 ± 18.6
saline	0.4 ± 0.4	1.0 ± 0.1	2.4 ± 2.1	2.3 ± 2.3
TBOA	$5.2 \pm 1.7^*$	$8.5 \pm 0.8^*$	$26.3 \pm 5.3^*$	$53.6 \pm 9.4^*$

Mean \pm SEM; * $p < 0.05$ (treatment vs. saline); $n=4$

Preface to Chapter Four

In the previous chapters I have demonstrated disruptions in the regulation of extracellular glutamate after diffuse brain injury. The aim of the experiments in Chapter Four was to examine a novel approach to improve the regulation of extracellular glutamate. Using a viral vector-mediated gene delivery approach, we examined if infusion of adeno-associated virus expressing glutamate transporter-1 (AAV-GLT-1) could produce targeted expression of functional GLT-1 and improve the regulation of extracellular glutamate in the rat striatum.

Chapter Four: Targeted expression of the glutamate transporter, GLT-1, in the rat striatum using a viral vector-mediated gene delivery approach

Abstract

Glutamate neurotransmission is involved in almost all aspects of neurological function. Dysregulated glutamate signaling has been implicated in a host of neurodegenerative and neuropsychiatric disorders. Increases in extracellular glutamate can excessively activate glutamate receptors producing excitotoxicity. To prevent excitotoxic accumulation of extracellular glutamate, the central nervous system has developed an abundant system of glutamate transporters to regulate extracellular glutamate. The purpose of this study was to examine if a viral vector-mediated gene delivery approach, adeno-associated virus (AAV), could target the expression of functional glutamate transporter (GLT-1) in the rat striatum. To examine the expression of functional GLT-1, glutamate-sensitive microelectrode arrays (MEAs) were used to measure clearance kinetics of locally applied glutamate into the extracellular space in rats infused with either AAV-GLT-1 or AAV-GFP (green fluorescent protein). Three weeks after viral infusion, the clearance of glutamate was significantly faster in the striatal hemisphere infused with AAV-GLT-1/RFP (red fluorescent protein) than the hemisphere infused with AAV-GFP. Thus, using a viral vector-mediated gene delivery approach, we were able to increase glutamate clearance, indicating increased expression of functional GLT-1. Overall, these data suggest a novel therapeutic strategy to improve glutamate uptake, which may improve glutamate regulation and reduce excitotoxicity.

Introduction

Glutamate, the predominant excitatory neurotransmitter in the central nervous system, is involved in almost all aspects of neurological function including cognition, motor function, memory, learning, decision making, and neuronal plasticity (McEntee and Crook 1993, Danbolt 2001). For normal neurological function, glutamate signaling must be properly regulated. Glutamate is released into the extracellular space where glutamate binds to both metabotropic and ionotropic glutamate receptors for propagation of the excitatory signal (Jabaudon, et al. 1999, Jensen, et al. 2000). Appropriate activation of glutamate receptors requires tight regulation of the extracellular concentration of glutamate. Concentrations of extracellular glutamate are maintained low by the uptake of glutamate via five high affinity sodium-dependent excitatory amino acid transporters (EAATs), GLAST, GLT-1, EAAC, EAAT4, and EAAT5 (Danbolt 2001). A majority (~90%) of glutamate uptake is performed by two glial transporters in the rat forebrain, GLAST and GLT-1 (Rothstein, et al. 1996, Tanaka, et al. 1997, Danbolt 2001).

Dysregulated glutamate signaling has been implicated in a host of neurological and neuropsychiatric disorders including TBI, stroke, Parkinson's disease, Alzheimer's disease, Huntington's disease, amyotrophic lateral sclerosis, epilepsy, schizophrenia, drug addiction, anxiety and depression (Doble 1999, Danbolt 2001, Nanitsos, et al. 2005, Mathew, et al. 2008, McNally, et al. 2008). Disruptions in the regulation of extracellular glutamate can produce increases in extracellular glutamate excessively activating glutamate receptors. Excessive stimulation of glutamate receptors can induce "excitotoxicity", a neuropathological processes involving prolonged neuronal depolarization, increases in intracellular calcium concentration, and activation of enzymatic mechanisms of cell death (Olney and de Gubareff 1978, Faden, et al. 1989, Doble 1999, Doyle, et al. 2008). Excitotoxicity is thought to be one of the predominant pathophysiological processes involved in neuronal damage and death in traumatic brain injury and stroke as excitotoxic concentrations of glutamate have been detected in stroke and TBI survivors (Bullock, et al. 1995, Davalos, et al. 2000).

Inhibiting excitotoxicity through the use of glutamate receptor antagonists has been a therapeutic strategy for the treatment of stroke and traumatic brain injury for many years (Willis, et al. 2004, Muir 2006, Garber 2007). Multiple studies have reported reduced damage and improved outcomes with the use of glutamate receptor antagonist in experimental models of stroke and traumatic brain injury (Simon, et al. 1984, Sheardown, et al. 1990, Myseros and Bullock 1995, Shen, et al. 2005, Shen, et al.

2009). However, glutamate receptor antagonists have failed to translate into positive clinical outcomes due to a lack of efficacy and/or adverse effects in the central nervous system (Bullock 1995, Ikonomidou and Turski 2002, Hoyte, et al. 2004, Villmann and Becker 2007). Taken together, these results support the examination of alternate strategies to improve the regulation of extracellular glutamate, which may produce the same beneficial effects while limiting the adverse effects observed with glutamate receptor antagonist.

Intraperitoneal administration of a beta-lactam antibiotic, ceftriaxone, has been shown to increase the expression of glutamate transporters in the rat brain, and reduce neuronal damage and improve behavioral recovery in a rat model of stroke (Rothstein, et al. 2005, Chu, et al. 2006, Chu, et al. 2007). These results suggest strategies that increase functional glutamate transporter levels can improve the regulation of extracellular glutamate and limit excitotoxicity. The purpose of this study was to examine if a novel approach, viral vector-mediated gene delivery of GLT-1 using an adeno-associated virus (AAV), could target the expression of functional GLT-1 in the rat striatum. Furthermore, we examined two different strategies of infusing the viral-vectors to determine which infusion method produced the optimal distribution and expression of GLT-1. In the first study, we examined whether a single infusion of AAV-GLT-1/RFP, expressing both the glutamate transporter and red fluorescent protein, would express functional GLT-1 in the rat striatum. In the second study, we examined whether infusing AAV-GLT-1 in multiple locations within the striatum would enhance the expression and distribution of functional GLT-1. To examine the expression of functional GLT-1, glutamate-sensitive microelectrode arrays (MEAs) measured the clearance of glutamate locally applied into the extracellular space three weeks after infusions.

Materials and Methods

Animals

In the first study, male Fischer 344 rats ($n=3$, Harlan Laboratories Inc., IN) were used, weighing 250-350 g at the time of infusion. In the second study, male Sprague-Dawley rats ($n= 12$, Harlan Laboratories Inc.) were used, weighing 250-350 g at the time of infusion. The animals were housed in a 12 h light/dark cycle with food and water available *ad libitum* and handled in accordance with guidelines from the *Guide for the*

Care and Use of Laboratory Animals (7th edition) and to the Association for Assessment and Accreditation of Laboratory Animal Care International. Animals were acclimated to their environment for at least one week before any experiments. After infusion, animals were monitored daily for post-operative care. Animal care was approved by the University of Kentucky Institutional Animal Care and Use Committee.

Construction, packaging, purification and titering of AAV vectors

The rat complimentary DNA (cDNA) for GLT-1 was first polymerase chain reaction (PCR) amplified from pc-GLT-1 (Pines, et al. 1992) (from Dr. Mike Robinson at U. Pennsylvania). The amplified PCR product contained BamHI (5' end) and XbaI (3' end) restriction enzyme sites used to insert the PCR product into pCR8/GW/TOPO (Invitrogen, CA) as an intermediate. The BamHI/XbaI fragment replaced GFP in the BamHI/XbaI digestion of pssAAV-GFP (Lowery, et al. 2009) to create pssAAV-GLT1. Viral stocks of AAV-GLT1 serotype 1 were prepared using the triple-transfection method (Xiao, et al. 1998, Howard, et al. 2008, Lowery, et al. 2009). Virus was provided by Dr. Brandon Harvery, National Institute on Drug Abuse (NIDA).

Intracerebral AAV injections

Rats were anesthetized with 3% isoflurane, and placed in a stereotaxic frame (Kopf Instruments, Tujunga, CA). Animal body temperature was maintained at 37°C with a heating pad (Braintree Scientific, Braintree, MA) and the animals' eyes were lubricated with artificial tears (The Butler Company, OH). The skin directly on top of the animal's head was cleaned with a betadine solution. Then a small incision was made over the skull to reflect the skin. Burr holes were drilled into the skull to provide access for the infusion of the virus. Before loading the syringe, the virus was sonicated for 10 s, and then loaded into a Hamilton syringe (33 gauge) (Hamilton Company, NV). The needle was stereotaxically placed into the area of interest with a two minute waiting period before starting the infusion. Virus was infused at a flow rate of 0.5 µl/min using an injection pump (UMP2; World Precision Instruments, FL) with a two minute waiting period before removal of the syringe. The burr holes were sealed with bone wax and skin sutured. Surgeries were performed with assistance from Dr. Brandon Harvey, NIDA.

For the single infusion, burr holes were drilled bilaterally for infusion of the virus into the striatum (AP: +1.0, ML: +/- 2.5, DV: -4.5). Each hemisphere received either 3 μ l of AAV-GFP or AAV-GLT-1/RFP (Fig 4.1).

For the multiple infusions, burr holes were drilled bilaterally to provide access for infusion of the virus into the striatum, and 2 μ l of virus was infused into four locations in each hemisphere (AP: +0.5, ML: 2.0 and 3.5, DV: -4.0 and -5.0). Each hemisphere received a total of 8 μ l of AAV-GFP or AAV-GLT-1 (Fig 4.2).

Enzyme-based microelectrode arrays

Ceramic-based microelectrode arrays (MEAs) consisting of four platinum recording sites (15 x 333 μ m) arranged in dual pairs were prepared and selected for *in vivo* recordings as previously described, (Burmeister, et al. 2002, Day, et al. 2006, Hascup, et al. 2007, Stephens, et al. 2009, Hinzman, et al. 2010, Hinzman, et al. 2012). Two different coatings were applied to the MEAs. One pair of recording sites was coated with glutamate-oxidase to allow for the enzymatic conversion of glutamate to α -ketoglutarate and the reporter molecule H_2O_2 . Constant potential amperometry was performed at a potential + 0.7 V versus a silver/silver chloride reference to oxidize H_2O_2 yielding two electrons. The resulting current was amplified and digitized by the FAST-16 mkII system (Fast Analytical Sensor Technology Mark II; Quanteon, L.L.C., KY). The other pair of recording sites (Sentinel sites) was coated with an insensitive protein matrix of bovine serum albumin and glutaraldehyde to measure any background current. The application of two different coatings allowed the use of a self-referencing technique, where the current from sentinel sites could be subtracted from the current from the glutamate-oxidase sites thus producing a more selective glutamate measure. A size exclusion layer of 1,3-phenylenediamine (mPD) was electroplated to the platinum recording sites blocking interferents such as ascorbic acid (AA) and dopamine (DA) from reaching the platinum recording sites (Hinzman, et al. 2010, Thomas, et al. 2011, Hinzman, et al. 2012).

MEA/micropipette assembly

For local application of glutamate into the rat brain, glass micropipettes (1 mm o.d. 0.58 mm i.d., A-M Systems, Inc., WA) were pulled (Kopf Instruments, CA), and the

tips of the micropipettes were bumped to create a tip with an i.d. of 10-15 μm . The micropipettes were placed centrally among all four platinum recording sites and mounted 50-100 μm above the MEA. Micropipettes were filled with 500 μM or 1 mM glutamate (Sigma-Aldrich, MO), dissolved in physiological saline. Solutions were sterile filtered (0.20 μm) and adjusted to a pH of 7.4. The micropipette was connected to a Picospritzer III (Parker-Hannifin, OH) with settings adjusted to consistently deliver volumes between 12.5-350 nL. Pressure was applied from 2-30 psi for 0.3-1.0 sec. Volume displacement was monitored with the use of a stereomicroscope fitted with a reticule to determine and control the volume of solution that was locally applied by pressure ejection (Friedemann and Gerhardt 1992).

***In vivo* anesthetized recordings of extracellular glutamate**

Three weeks after viral infusion, rats were anesthetized with urethane (1.25 g/kg i.p.) and prepared for *in vivo* electrochemical recordings as previously described (Day, et al. 2006, Hascup, et al. 2007, Stephens, et al. 2009, Thomas, et al. 2009, Hinzman, et al. 2010, Thomas, et al. 2011, Hinzman, et al. 2012). Briefly, MEAs were calibrated the morning of the experiment and the calibration values (sensitivity, selectivity, and limit of detection) were comparable to previous studies. Then, animals were placed in a stereotaxic frame and body temperature was maintained at $\sim 37^\circ\text{C}$ with a water pad connected to a recirculating water bath. A craniotomy was performed to provide access to the striatum. A Ag/AgCl reference wire was implanted into the lateral parietal cortex. The MEA was lowered into the striatum using a microdrive (MO-10, Narishige International, NY). All MEA recordings were performed at a frequency of 2 Hz. Glutamate recordings were performed in both hemispheres comparing the AAV-GLT-1 treated hemisphere to the AAV-GFP treated hemisphere. To examine glutamate clearance, varying volumes of 500 μM or 1 mM glutamate were applied into the extracellular space producing glutamate signals with amplitudes in the 5-200 μM range. Glutamate clearance was analyzed by the following parameters: (1) amplitude (μM); (2) T_{80} (s), the time for the signal to decay by 80% from the peak amplitude; (3) uptake rate constant k_{-1} (sec^{-1}), the slope of the linear regression of the natural log transformation of the decay over time; and (4) clearance rate T_c ($\mu\text{M}/\text{sec}$) the slope of the line between T_{20} and T_{60} (Nickell, et al. 2007, Thomas, et al. 2009, Hinzman, et al. 2010) (Fig 4.3).

In the first study, clearance of locally applied glutamate was examined 0.1 mm lateral to the infusion site of the virus (AP: +1.0, ML: \pm 2.6, DV: -4.5), represented by * (Fig 4.1). In the second study, clearance of locally applied glutamate was examined in between the two infusion tracks at multiple depths in the striatum (AP: +0.5, ML: \pm 3.3, DV: -4.0, -4.5 and -5.0), represented by *(Fig 4.2).

Data analysis

Amperometric data were analyzed using custom MATLAB[®] - based software. Data are presented as mean \pm SEM, and statistical significance was defined as $p < 0.05$. A two-tailed t-test was used for comparisons between the AAV-GFP and AAV-GLT-1 treated hemisphere, unless noted otherwise.

Histology

In the first study, after completion of the glutamate recordings, animals were transcardially perfused with physiological saline followed by 4% paraformaldehyde. Brains were removed and stored in 4% paraformaldehyde for 3 days. At the end of the 3 days, the storage solution was exchanged to 0.1m phosphate buffer with 30% sucrose. Brains were sliced on a cryostat (0.05 mm) for visualization of GFP or RFP fluorescence. Histology was performed in Dr. Brandon Harvey's Laboratory, NIDA.

Quantitative gene expression (rtPCR)

In the second study, after completion of the glutamate recordings, animals were transcardially perfused with cold saline, the brains rapidly removed from the skull, dissected into 2 mm slices using a chilled rat brain matrix, and a 2 mm diameter biopsy was removed from the dorsal striatum, approximate area represented in (Fig 4.2). The mRNA content was stabilized (RNAlater, Qiagen Corp) and stored frozen (-20°C). Isolated mRNA (RNeasy, Qiagen Corp) was quantified (NanoDrop ND-1000 spectrophotometer), converted to cDNA (High Capacity cDNA Archive Kit, Applied Biosystems Inc.) and then used as a template for selected commercially-available gene expression assays for quantitative real-time PCR (StepONE, Applied Biosystems). The Applied Biosystems TaqMan[®] Gene Expression Assays (GLT-1: Rn00568080_m1) were

used for GLT-1 gene expression. Within each animal, relative gene expression was normalized to the 18s rRNA endogenous control and the expression level in the AAV-GFP hemisphere using the $2^{-\Delta\Delta CT}$ method (Livak and Schmittgen 2001), which relates gene expression to the PCR cycle number at which the fluorescence signals exceed a threshold above baseline. Relative gene expression was compared between AAV-GFP and AAV-GLT-1 striatal punches using a two-tailed t-test.

Results

Single infusion of AAV- GLT-1/RFP increases expression of functional GLT-1 in the rat striatum

Three weeks after a single infusion of AAV-GFP or AAV-GLT-1/RFP into the rat striatum, we examined if viral-mediated expression could produce an increase in functional GLT-1. Using glutamate-sensitive MEAs we examined glutamate clearance 0.1 mm lateral to the infusion site comparing the AAV-GLT-1/RFP treated hemisphere to the AAV-GFP treated hemisphere. Local application of varying amounts of 1 mM glutamate produced reproducible glutamate signals with amplitudes ranging from 50-200 μ M. Local application of glutamate produced a rapid increase in extracellular glutamate, with the signal reaching the maximum amplitude in less than 2 seconds, followed by a decrease in the signal as glutamate uptake restored the glutamate concentration back to baseline levels (Fig 4.3). Glutamate signals with similar amplitudes were used to compare glutamate clearance between the AAV-GFP treated hemisphere to the AAV-GLT-1 treated hemisphere. Due to the small number of animals used in this study (n=3), we were only able to obtain glutamate signals with similar amplitudes in a limited range. Representative glutamate signals, in the 170-185 μ M amplitude range, highlight the faster glutamate clearance rate T_c (the slope of the line between T_{20} and T_{60}) in the AAV-GLT-1/RFP striatal hemisphere compared to the AAV-GFP treated hemisphere (Fig 4.4A). T_c was compared between AAV-GLT-1/RFP and AAV-GFP treated striatal hemispheres based on the amplitude of the glutamate signal. T_c was significantly affected by the viral treatment ANOVA [F(1,16)=31.97, $p < 0.0001$]. The AAV-GLT-1/RFP treatment produced significantly faster glutamate clearance rates than AAV-GFP treatment in the 150-165 μ M (134%) and 170-185 μ M (126%) amplitude ranges (Bonferroni post-test, * $p < 0.05$, ** $p < 0.01$, Fig 4.4B).

At the conclusion of the experiment, the brains were sectioned to visually confirm expression and distribution of the fluorescent proteins. In a coronal section of the rat striatum, we were able to confirm that infusion of AAV-GLT-1/RFP and AAV-GFP produced expression of both red and green fluorescent proteins in their respective hemispheres (Fig 4.5A). At higher magnification, we were able to visualize the expression of GFP and RFP in both cellular bodies and elongated processes (Fig 4.5B and C). Thus, using a viral vector-mediated gene delivery approach, we were able to increase the expression of functional GLT-1 into the rat striatum.

Multiple infusions of AAV- GLT-1 within the striatum failed to express functional GLT-1

Three weeks after multiple infusions of AAV-GLT-1 within the rat striatum, we examined if infusing the virus in multiple locations within the striatum would enhance the viral-mediated expression and distribution of functional GLT-1 (Fig 4.2). Glutamate-sensitive MEAs were used to examine the clearance of exogenously applied glutamate into the extracellular space in multiple depths of the striatum comparing the AAV-GLT-1 treated hemisphere to the AAV-GFP treated hemisphere. Representative glutamate signals depict a similar decay of the glutamate signal from exogenous application of glutamate between the AAV-GFP and AAV-GLT-1 treated hemispheres (Fig 4.6). Glutamate signals were sorted based on the amplitude of the signals, (<50, 50-100, >100 μ M), and parameters of glutamate clearance were compared between the AAV-GFP and AAV-GLT-1 treated hemispheres. Due to the increased number of animals in this study (n=12) we were able to obtain glutamate signals with a larger range of amplitudes for comparison. In all the amplitude ranges, we detected no significant difference in any of the clearance parameters between the AAV-GFP and AAV-GLT-1 treated hemispheres (Table 4.1). These data indicate that multiple infusion loci did not produce changes in glutamate clearance that would have been indicative of enhanced functional GLT-1 levels.

At the conclusion of the experiment, we used quantitative real-time PCR to examine the gene expression of GLT-1. In the dorsal striatum, there was no significant difference in the relative expression of GLT-1 between the AAV-GFP (0.98 ± 0.2) and AAV-GLT-1 (1.0 ± 0.1) treated hemispheres (Fig 4.7). Thus, rt-PCR results support the

conclusion that multiple injections of AAV-GLT-1 into the striatum failed to increase gene expression of GLT-1.

Discussion

The purpose of this study was to examine if a viral vector-mediated gene delivery approach (AAV-GLT-1) could target the expression of functional GLT-1 into the rat striatum and thereby improve the regulation of extracellular glutamate. In the single infusion study, infusion of AAV-GLT-1/RFP into the striatum produced significantly faster glutamate clearance compared to infusion of AAV-GFP. We were able to confirm expression of the fluorescent protein tags RFP and GFP in their respective striatal hemisphere with expression of both proteins in cell bodies and elongated processes. In the multiple infusion study, we tried to enhance the expression and distribution of GLT-1 by infusing AAV-GLT-1 into multiple locations within the striatum. Three weeks after infusion, we detected no significant difference in glutamate clearance or in the gene expression of GLT-1 between the AAV-GLT-1 and AAV-GFP treated hemispheres. Thus, using a viral vector-mediated gene delivery approach, with a single infusion of AAV-GLT-1/RFP, we were able to increase the expression of functional GLT-1 into the rat striatum.

We have yet to identify the exact reason why multiple infusions of AAV-GLT-1 failed to produce expression of functional GLT-1, while a single infusion of AAV-GLT-1/RFP produced functional expression of GLT-1 in the rat striatum. In the multiple infusion study, we used two infusion tracks to inject the virus into four separate locations within the striatum. Multiple insertions of the infusion needle may have produced an increased amount of damage and inflammation preventing transduction of the virus into the cells. However, previous work by our collaborator (Dr. Brandon Harvey), achieved viral-mediated expression of GLT-1 using a multiple infusion design within the rat cortex (Harvey, et al. 2011). Another possible reason for the lack of expression in the multiple infusion study is due to differences in the viral vectors. In the single infusion study we used AAV-GLT-1/RFP while in the multiple infusion study we used AAV-GLT-1, differences in the construction of the viral-vectors may have produced variances in the titers and/or transduction efficiency between the viral-vectors. The most likely reason for lack of expression in the multiple infusion study is a loss of viral integrity due to problems

in shipping and/or preparing the AAV-GLT-1 for infusion into the striatum. In the future, improvements in the experimental design need to include transducing primary neuron cultures using the same aliquot of virus, confirming viral integrity. Also, examining both histology for fluorescent markers and gene expression will aid in detecting problems with infusion of the virus.

In both studies, AAV serotype 1 was used, which has been shown to transduce both neurons and glia (unpublished observation, Dr. Brandon Harvey). Normally GLT-1 is only expressed on glia, so one of the overall goals of the second study was to examine how increased expression of GLT-1 in both neurons and glia would alter multiple aspects of glutamate signaling including glutamate clearance, tonic glutamate, and KCl-evoked glutamate release (Danbolt 2001). Since we were unable to increase the gene expression of GLT-1 in the second study, future work should address how neuronal expression of GLT-1 alters glutamate signaling and regulation.

The overall objective of this study was to identify a novel therapeutic strategy to improve the regulation of extracellular glutamate that may limit or reduce excitotoxicity. Recent work by our collaborator (Dr. Brandon Harvey, NIDA) has shown this approach (AAV-GLT-1) can enhance glutamate regulation, reduce damage, and improve outcomes in a rat model of stroke. Intracerebral infusions of AAV-GLT-1 into three cortical sites in the distribution of the right middle cerebral artery prior to occlusion, reduced cerebral infarction, improved functional recovery, reduced ischemia-induced glutamate overflow, and reduced tissue damage (Harvey, et al. 2011). The above study validates the theory that increasing expression of glutamate transporters can improve glutamate regulation, reduce excitotoxicity, and improve outcomes in a model of excitotoxicity.

A major advantage of using a viral vector-mediated gene delivery approach is the ability to target the expression of the glutamate transporter into the brain region of interest. Targeting the expression only in the area of interest should not alter glutamate signaling in other brain regions, thereby, limiting adverse effects seen with glutamate-receptor antagonist such as hallucinations, catatonia, ataxia, nightmares, and memory deficits (Blanke and VanDongen 2009). To date, a viral-vector mediated approach is the only known method that allows targeting the expression of a glutamate transporter into the brain region of interest. While administration of ceftriaxone may increase glutamate transporters, the increase will not be localized to a certain brain region, this may disrupt glutamate signaling in undesired brain regions producing adverse effects similar to those

observed with glutamate-receptor antagonist. Future work should thoroughly examine potential side effects from targeted over-expression of GLT-1. However, a recent study detected no significant changes in locomotor activity after multiple infusion of AAV-GLT-1 in the rat cortex (Harvey, et al. 2011).

A major disadvantage of using a viral vector-mediated gene delivery approach is the approximate three weeks needed for stable expression of the protein. In our studies, AAV-GLT-1 was infused three weeks prior to testing to allow for stable expression. The other known method to increase the expression of glutamate transporters, intraperitoneal injection of ceftriaxone, takes approximately five days of daily administration (Rothstein, et al. 2005). The relatively long period amount of time needed for stable expression of the glutamate transporters by both methods severely inhibits their potential as a viable treatment to reduce the acute excitotoxicity in stroke and TBI, which occurs within the first few days (Bullock, et al. 1995, Davalos, et al. 2000). Another disadvantage of using a viral-vector approach to increase expression of GLT-1 is the inability to modulate or stop expression after infusion, especially if unwanted side effects started to occur.

In conclusion, we have used a viral-vector mediated gene delivery approach to target the expression of functional GLT-1 into the rat striatum. Recent data supports improving glutamate regulation in pathologies where glutamate is elevated through the upregulation of glutamate transporters can protect against excitotoxicity and improve behavioral outcomes in animal models of stroke (Rothstein, et al. 2005, Chu, et al. 2006, Chu, et al. 2007, Harvey, et al. 2011). Further development of selective gene delivery may make the use of GLT-1 a more viable therapeutic strategy to treat neurological and neuropsychiatric disorders involving chronic dysregulation of extracellular glutamate in discrete brain areas. Future work is needed to identify strategies that rapidly increase the expression of glutamate transporters as this appears to be a promising therapeutic strategy to limit acute excitotoxicity and improve outcomes in traumatic brain injury and stroke survivors.

Portions of Chapter Four have been published in the following manuscript:

Harvey BK, Airavaara M, Hinzman J, Wires EM, Chiocco MJ, Howard DB, Shen H, Gerhardt G, Hoffer BJ, Wang Y. Targeted over-expression of glutamate transporter 1 (GLT-1) reduces ischemic brain injury in a rat model of stroke. PLoS One. 2011;6(8):e22135. Epub 2011 Aug 10.

Permission to publish in this thesis falls within PLoS One open access agreement.

Copyright © Jason Michael Hinzman 2012

Chapter Four: Figures

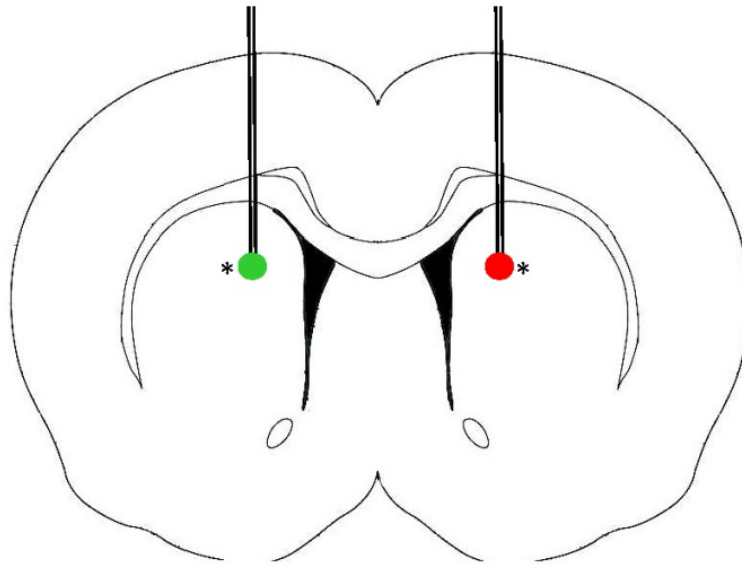


Figure 4.1 Representation of the sites for the viral infusion and glutamate recordings in the rat striatum

The diagram shows the approximate location of the viral infusion sites for AAV-GFP (green circle) and AAV-GLT-1/RFP (red circle) and the approximate location of the glutamate recording in the rat striatum (*). Bilateral recordings were conducted for glutamate clearance comparing the AAV-GFP and AAV-GLT-1/RFP treated hemispheres.

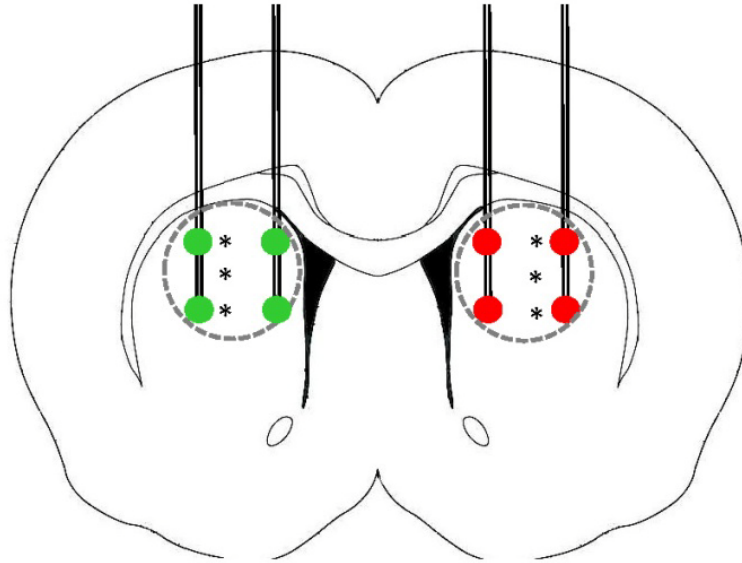


Figure 4.2 Representation of the sites for the viral infusion, glutamate recordings, and tissue punches for gene expression in the rat striatum

The diagram shows the approximate location of the viral infusion sites for AAV-GFP (green circle) and AAV-GLT-1 (red circle) and the approximate location of the glutamate recording sites in the rat striatum (*). Bilateral recordings were conducted for glutamate clearance in multiple depths of the striatum comparing the AAV-GFP and AAV-GLT-1/RFP treated hemispheres. Striatal tissue punches (grey circle) were taken to examine gene expression for GLT-1 using quantitative real-time PCR.

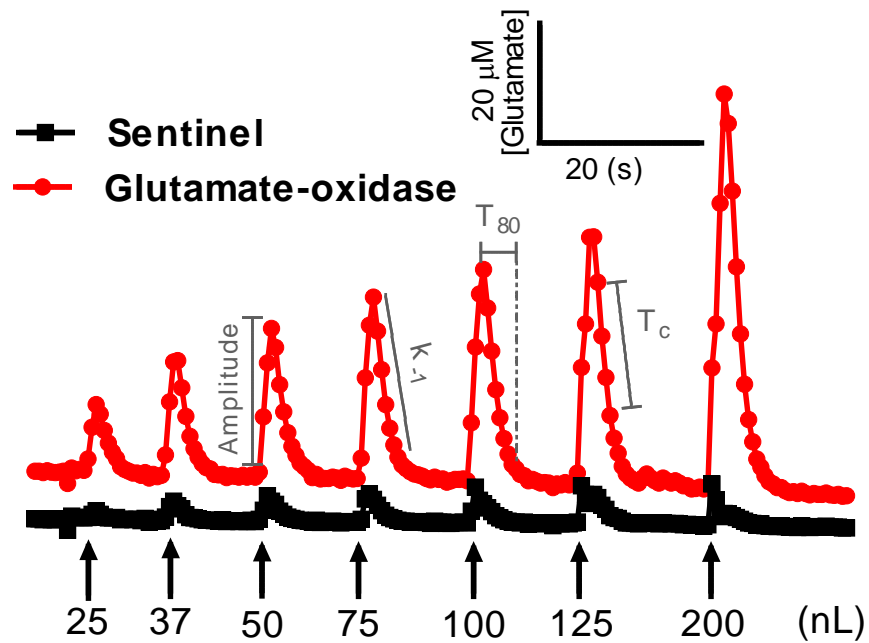


Figure 4.3 Representative in vivo recording from a glutamate-oxidase site and sentinel site of the MEA

Local application of various volumes of glutamate into the extracellular space (\uparrow) produced signals with a wide range of amplitudes. For each signal glutamate clearance was analyzed using the following parameters: amplitude, k_{-1} , T_{80} , and T_c . Parameters are shown separately for clarity.

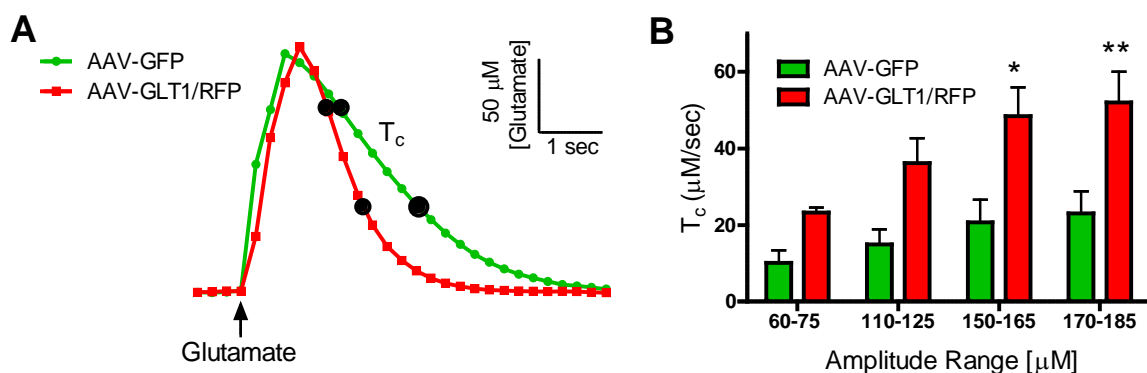


Figure 4.4 Faster glutamate clearance in AAV-GLT-1 treated hemisphere compared to AAV-GFP hemisphere

(A) Graph comparing the time course of glutamate clearance from signals with similar amplitudes in the 170-185 μM range. The GLT-1/RFP-treated hemisphere showed a faster time course of glutamate clearance compared to the GFP/RFP-treated hemisphere. Local application of 250 nL of 1 mM glutamate produced a robust increase in extracellular glutamate that returned back to baseline levels through glutamate uptake. Note that the T_c was significantly increased in the GLT-1/RFP hemisphere. (B) Faster glutamate T_c 's in the striatal hemisphere treated with GLT-1/RFP than the GFP/RFP-treated hemisphere. Glutamate signals were sorted by amplitude for comparison (* $p < 0.05$, ** $p < 0.01$, $n=3$).

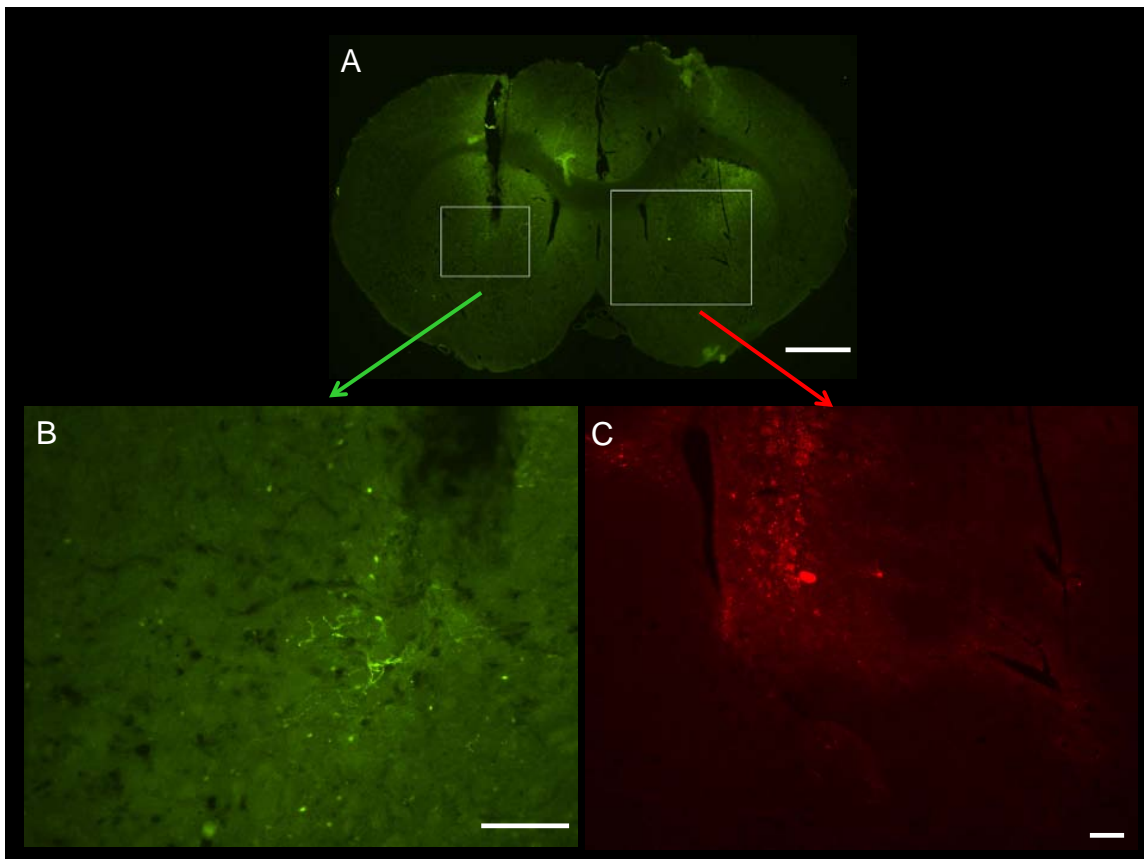


Figure 4.5 Expression of green and red fluorescent protein in the striatum three weeks after infusion of AAV-GFP and AAV-GLT-1/RFP

(A) Coronal section of the rat striatum three weeks after infusion of AAV-GFP and AAV-GLT-1/RFP depicting the recording track of the MEA (scale bar = 2 mm). (B) High magnification image of striatal hemisphere infused with AAV-GFP showing cells and elongated process expressing green fluorescent protein (scale bar = 0.2 mm). (C) High magnification image of striatal hemisphere infused with AAV-GLT-1/RFP showing cells and elongated process expressing red fluorescent protein (scale bar = 0.2 m

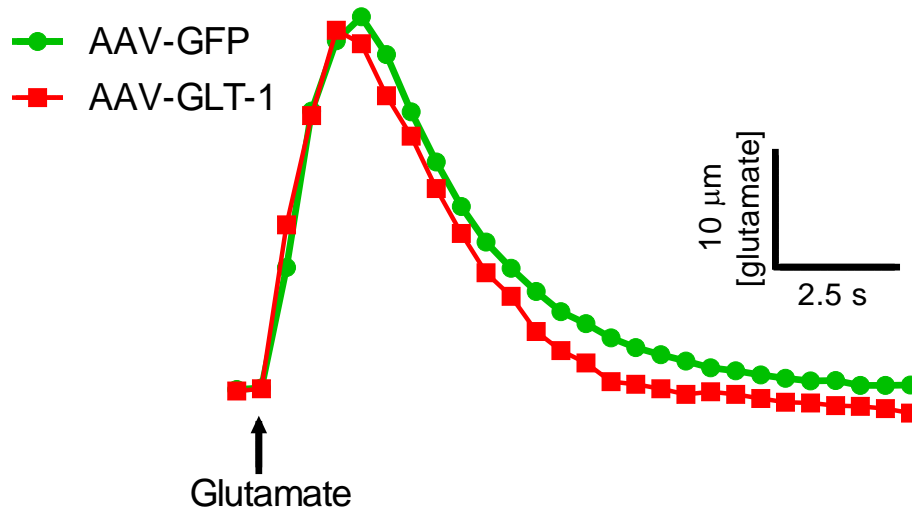


Figure 4.6 Similar rates of glutamate clearance in the AAV-GFP and AAV-GLT-1 treated hemispheres

Graph depicting glutamate signals with similar amplitudes (<50 μM) resulting from local application of glutamate (↑) at three weeks post-AAV-GFP and AAV-GLT-1 infusion. The clearance of the glutamate signal was similar between the AAV-GFP and AAV-GLT-1 treated hemispheres.

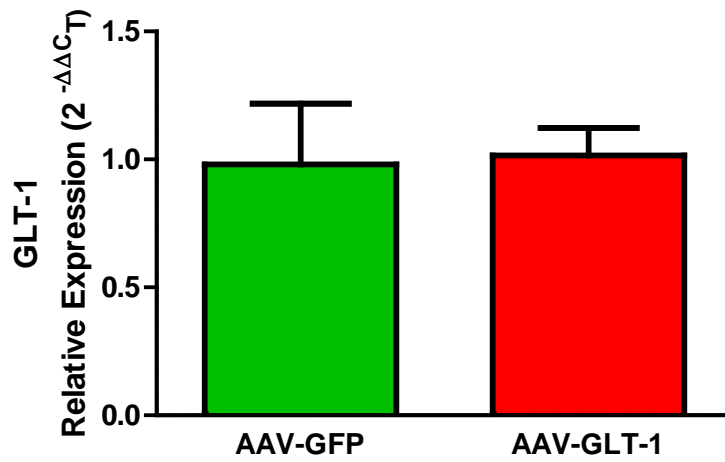


Figure 4.7 Similar amounts of GLT-1 gene expression between the AAV-GFP and AAV-GLT-1 treated hemispheres

Quantitative real-time PCR on striatal punches shows similar amounts of GLT-1 gene expressions between the AAV-GFP and AAV-GLT-1 treated hemispheres (n= 6).

Chapter Four: Tables

Table 4.1 Comparison of glutamate clearance between the AAV-GFP and AAV-GLT-1 treated hemispheres

Amplitude Range	Amplitude (μM)	k_{-1} (s^{-1})	T_{80} (s)	T_c ($\mu\text{M}/\text{s}$)
(<50μM)				
AAV-GFP (n=22)	29.4 ± 1.8	0.22 ± 0.03	5.7 ± 0.4	6.4 ± 0.8
AAV-GLT-1 (n=25)	25.1 ± 1.9	0.24 ± 0.02	5.4 ± 0.6	6.2 ± 0.6
(50-100μM)				
AAV-GFP (n=17)	72.8 ± 2.7	0.28 ± 0.04	7.0 ± 1.1	14.8 ± 1.7
AAV-GLT-1 (n=12)	70.8 ± 3.0	0.30 ± 0.04	6.3 ± 0.9	15.2 ± 2.0
(>100μM)				
AAV-GFP (n=7)	153.1 ± 6.9	0.38 ± 0.06	5.3 ± 0.7	34.7 ± 4.9
AAV-GLT-1 (n=7)	126.2 ± 3.4	0.37 ± 0.06	7.3 ± 1.6	29.3 ± 3.8

Data shown as mean \pm SEM, n= recording depth in striatum, analyzed by a two-tailed unpaired *t* test.

Preface to Chapter Five

In the previous chapters, I have demonstrated the capabilities of microelectrode arrays (MEAs) to detect disruptions in extracellular glutamate in experimental models of traumatic brain injury (TBI). Current, neurocritical care for severe traumatic brain injury patients uses a multitude of neuromonitoring devices to identify secondary insults, which are difficult to detect. We hypothesize that enzyme-based microelectrode arrays (MEAs) can provide insight into the pathophysiological mechanisms of TBI and detect potential biomarkers to guide the care and management of TBI patients. The purpose of this study was to examine the translational potential and capabilities of enzyme-based microelectrode arrays (MEAs) as a novel neuromonitoring device for clinical TBI research.

Chapter Five: Development of a novel neuromonitor for clinical TBI research: enzyme-based microelectrode arrays for real-time in vivo detection of neurochemicals

Abstract

Modern neurocritical care management uses a host of monitoring techniques to identify secondary insults and guide subsequent therapeutic interventions in an attempt to minimize the resulting secondary brain injury in severe TBI survivors. However, the onset and extent of secondary brain injury have been difficult to detect. We hypothesize that enzyme-based microelectrode arrays (MEAs) can provide insight into the pathophysiological mechanisms of TBI and detect potential biomarkers to guide the care and management of TBI patients. The purpose of this study was to examine the translational potential and capabilities of enzyme-based microelectrode arrays (MEAs) as a novel neuromonitoring device for clinical TBI research. MEAs can continuously measure extracellular glutamate during the initial 72 hours after implantation, which is the temporal window for disruptions in extracellular glutamate previously detected in TBI survivors. Second, selective coatings applied to the MEAs allow for simultaneous detection of multiple neurochemicals of interest on a single device, such as simultaneous detection of glutamate, lactate, pyruvate, and glucose. Molecules that have been previously identified as potential biomarkers in clinical microdialysis studies. Lastly, we were able to transfer a similar methodology of the MEAs onto an already

FDA-approved device, the AD-TECH[®] Epilepsy/LTM macro-micro depth electrode, for selective measures of extracellular glutamate both *in vitro* and *in vivo*.

Introduction

Current management strategies for traumatic brain injury (TBI) survivors are directed towards providing an optimal physiological environment in order to minimize secondary brain injury and maximize the body's own regenerative processes. Modern neurocritical care management uses a host of monitoring techniques to identify secondary insults and guide subsequent therapeutic interventions in an attempt to minimize the resulting secondary brain injury that occurs in severe TBI survivors (Tisdall and Smith 2007). However, the onset and extent of secondary brain injury have been difficult to detect. A multitude of invasive neuromonitoring techniques are currently being used in the intensive care unit to detect disruptions in intracranial pressure (ICP), cerebral perfusion pressure (CPP), cerebral blood flow (CBF), brain tissue oxygen tension (PbtO₂), brain temperature, markers of cerebral cellular metabolism such as glucose, lactate, pyruvate, glutamate, and glycerol, and intracranial electroencephalography (Kirkpatrick, et al. 1996, Patel, et al. 2002, Stuart, et al. 2010). However, to date, only ICP monitoring is the standard of care for management of severe TBI patients (The Brain Trauma Foundation, 2000). Other than ICP monitoring, no consensus exists regarding the selection of neuromonitoring devices for specific patient groups, the placement of devices in relation to injured brain tissue, or many of the technical aspects of inserting the devices. At present, there is a major controversy in whether the use of neuromonitoring devices leads to improved functional outcomes in severe TBI patients (Stuart, et al. 2010).

The overall goals of neuromonitoring in TBI patients is to provide insight into the pathophysiological processes of secondary brain injury, identify novel therapeutic targets, and reliably detect a biomarker to aid in the diagnosis of TBI severity, guide medical care, predict functional outcomes, and test the efficacy of therapeutics. While under development, microdialysis, a method for detecting neurochemical changes in the extracellular fluid of the central nervous system, exhibited tremendous potential as a novel tool to uncover the pathophysiological processes of secondary brain and possibly detect a biomarker for TBI (Hillered, et al. 1990). Microdialysis involves the implantation of a probe, a semi-permeable membrane, that when perfused with a physiological solution allows diffusion of small molecules into the probe to be collected and analyzed.

Cerebral microdialysis has been used clinically for the past 20 years detecting disruptions in the extracellular concentrations of neurochemicals involved in TBI pathophysiology (Hillered, et al. 1990, Hillered, et al. 2005, Goodman and Robertson 2009).

Microdialysis has been widely used clinically, primarily due to its ability to detect disruptions in the bioenergetics and metabolism of the central nervous system in severe TBI patients that includes disruptions in lactate, pyruvate, and glucose (Persson, et al. 1996, Goodman, et al. 1999, Sarrafzadeh, et al. 2000, Vespa, et al. 2005, Wang, et al. 2007, Carpenter, et al. 2008, Marcoux, et al. 2008, Meierhans, et al. 2010, Zetterling, et al. 2010, De Fazio, et al. 2011, Hejcl, et al. 2011, Nelson, et al. 2011, Timofeev, et al. 2011a, Yokobori, et al. 2011, Dizdarevic, et al. 2012, Oddo, et al. 2012). In addition, microdialysis has detected increases in the excitatory neurotransmitter, glutamate, especially in times of ischemia and energy failure (Persson and Hillered 1992, Bullock, et al. 1995, Bullock, et al. 1998, Koura, et al. 1998, Vespa, et al. 1998, Yamamoto, et al. 1999, Reinert, et al. 2000, Sarrafzadeh, et al. 2000, Hutchinson, et al. 2002, Hlatky, et al. 2004, Goodman and Robertson 2009, Chamoun, et al. 2010, Lakshmanan, et al. 2010, Timofeev, et al. 2011a). Although microdialysis provides insight into the pathophysiological processes of TBI and the corresponding neurochemical changes associated with secondary brain injury, microdialysis has failed to reliably detect a biomarker that could be used to guide the treatment and management of severe TBI patients. The inability of microdialysis to reliably detect a biomarker for TBI may be due to inherent methodological limitations of the technique. First, the large sampling area of the microdialysis probe (10 mm) and extensive damage surrounding the probe from implantation of the device limits the ability of microdialysis to sample extracellular neurochemicals that correspond to concentrations near the synapses (Borland, et al. 2005, Jaquins-Gerstl and Michael 2009). Second, the temporal resolution of microdialysis (1-20 min) is inadequate to sample the fast dynamics of neurochemical release and clearance that occurs on the order of milliseconds that likely results in the loss of relevant and critical information encoded in the regulation of the neurochemicals (Diamond 2005). Lastly, collecting and analyzing the microdialysate for the neurochemicals of interest delays examination of the data, thus limiting the usefulness of microdialysis in guiding the management and treatment of TBI patients at the bedside.

Recently developed enzyme-based MEAs have improved upon some of the methodological limitations of microdialysis for clinical monitoring of extracellular

neurochemicals. The improved spatial resolution (micrometers) and limited damage to the surrounding central nervous system during implantation of the device permits detection of neurochemicals from synaptic sources (Day, et al. 2006, Rutherford, et al. 2007, Hascup, et al. 2008, Hinzman, et al. 2012). Since MEAs use electrochemical methods, data can be collected on a sub-second time scale allowing the detection of dynamic changes in neurochemicals. In addition, electrochemical detection allows data to be collected in real-time and displayed bedside, permitting management and treatment decisions to be based on neurochemical data. We hypothesize that enzyme-based microelectrode arrays (MEAs) can provide insight into the pathophysiological mechanisms of TBI and detect potential biomarkers to guide the care and management of TBI patients. The purpose of this study was to examine the translational potential and capabilities of enzyme-based MEAs as a novel neuromonitoring device for clinical TBI research.

Materials and Methods

Animals

Male Sprague-Dawley rats were used for all experiments. The animals were housed in a 12 h light/dark cycle with food and water *ad libitum* according to the Association for Assessment and Accreditation of Laboratory Animal Care International. Animals were acclimated to their environment for at least 1 week before any experiments. After surgery, animals were monitored daily for post-operative care. Animal care was approved by the University of Kentucky Institutional Animal Care and Use Committee.

Continuous recordings of extracellular glutamate for 72 hours in awake animals

Ceramic-based MEAs, consisting of four platinum recording sites (15 x 333 μm) arranged in dual pairs, were prepared and selected for *in vivo* recordings (Burmeister, et al. 2002, Day, et al. 2006). MEAs were prepared and coated for glutamate measures similar to previous work with one modification (Burmeister and Gerhardt 2001, Burmeister, et al. 2002, Rutherford, et al. 2007, Hinzman, et al. 2010). On the sentinel

recording sites, inactivated glutamate-oxidase was used using the same procedure and concentrations as the active glutamate-oxidase. Glutamate-oxidase was inactivated by autoclaving ~1.0 μ L aliquot of active enzyme. Inactivated glutamate-oxidase was used to ensure similar diffusion layers on all recording sites. The two different coatings allowed the use of a self-referencing technique, in which the background current of the sentinel sites can be subtracted from the current of the glutamate-oxidase sites, thereby producing a more selective glutamate measure (Burmeister and Gerhardt 2001, Burmeister, et al. 2002). MEA pedestals were fabricated and constructed for chronic glutamate measures similar to previous studies (Rutherford, et al. 2007).

Before implantation of the MEA pedestal, MEAs were calibrated to test the capability of the MEA to measure glutamate and generate a standard curve for the conversion of current to glutamate concentration (Hinzman, et al. 2010). Before implanting the MEA pedestal, rats underwent a sham injury (Lifshitz 2008, Hinzman, et al. 2010, Thomas, et al. 2011). Upon completion of the sham surgery, animals were implanted with the MEA pedestal (Rutherford, et al. 2007). MEAs were stereotaxically placed in the striatum (AP: +1.0, ML: + 2.5, DV: -4.0). Animals were then placed in the recording chamber, 21 x 11 inch plexiglass rectangle, and connected to the FAST-16 mkII system via hammerhead-type pre-amplifier. Data was collected at a frequency of 4 Hz. Animals were provided with food and water *ad libitum* and remained on their 12 hour light/dark cycle.

Amperometric data were analyzed using custom MATLAB[®] - based software. Extracellular glutamate was calculated using the self-referencing method (Burmeister and Gerhardt 2001, Burmeister, et al. 2002). Data were filtered using a fourier low pass filter (0.14) and wavelet low pass filter (3). Extracellular glutamate levels were averaged per hour.

Multiple Analyte Calibrations

MEAs were prepared and coated for the analyte of interest (Burmeister, et al. 2004) with one modification. Polyurethane was coated by hand onto selected sites instead of dipping all sites into polyurethane. Polyurethane was only coated only on the platinum recording sites coated with lactate-oxidase and pyruvate-oxidase. Calibrations were conducted to test the capability of the MEA to selectively measure the analyte of interest. The parameters tested were limit of detection (three times the standard

deviation of the baseline noise), sensitivity to the analyte (slope), and the linear increase in current due to additions of the analyte (R^2). Constant potential amperometry was performed with the MEAs using the FAST-16 mkII system. A potential of +0.7 V versus an Ag/AgCl reference was applied to oxidize the reporter molecule, H_2O_2 . The resulting current was amplified and digitized by the FAST-16 mkII system.

Modification of FDA-approved device (AD-TECH[®] Epilepsy/LTM macro-micro depth electrode) for *in vivo* detection of glutamate

AD-TECH[®] Epilepsy/LTM macro-micro depth electrodes were provided by AD-TECH[®] (AD-TECH Medical Instruments, Racine, WI). Probes were prepared and coated for glutamate measures (Hinzman, et al. 2010) with minor modifications. A 10 μ L solution of 2% bovine serum albumin (BSA), 0.25% glutaraldehyde, and 1% glutamate-oxidase was prepared. Using a dissecting microscope, a microsyringe was used to manually apply a small drop ($\sim 0.1\mu$ L) of the glutamate-oxidase solution onto the micro-depth electrodes. The increased percentage of BSA and glutaraldehyde compared to methods described in Chapters 2, 3, and 4 was used to aid in the adherence of the coatings onto the micro-depth electrode. Multiple coats were applied to the micro-depth electrodes until the whole electrode was encapsulated. The same procedure was used to coat sentinel sites, micro-depth electrodes coated with a solution containing 2 % BSA and 0.25% glutaraldehyde. After coating, the probes were cured for at least 48 hours in a low humidity environment. The coated probes were connected to the FAST-16 mk II system and the micro-depth electrodes were placed in a 5 mM mPD solution. Electroplating software was used to apply a potential as a triangular wave with an offset of -0.5V, peak to peak amplitude equal to 0.25V, at a frequency of 0.05 Hz, for a period of 25 minutes to electroplate the mPD on the micro-depth electrodes. Probes were cured for an additional 24 hours in a low humidity environment before use.

Calibrations were conducted to test the capability of the probe to measure glutamate and generate a standard curve for the conversion of current to glutamate concentration. The AD-TECH[®] Epilepsy/LTM macro-micro depth electrode was placed in a continuously stirred 40 ml solution of 0.05 M phosphate buffered saline (PBS) maintained at 37 °C with a re-circulating water bath. The probes were exposed to final concentrations of 250 μ M AA, 20, 40, 60 μ M glutamate, 2 μ M DA, and 8.8 μ M H_2O_2 .

Parameters tested were limit of detection (LOD), selectivity for glutamate over ascorbic acid, slope of the electrode (sensitivity), and linearity of the glutamate response (R²).

Animals were anesthetized with isoflurane and prepared for *in vivo* electrochemical recordings (Burmeister, et al. 2002, Pomerleau, et al. 2003, Day, et al. 2006). Briefly, animals were placed in a stereotaxic frame and body temperature was maintained at 37 °C with a water pad connected to a re-circulating water bath. A craniotomy was performed to provide access to the striatum. A Ag/AgCl reference wire was implanted into the lateral parietal cortex in the opposite hemisphere from the recording areas. The AD-TECH[®] Epilepsy/LTM macro-micro depth electrode was lowered into the brain using a microdrive. All recordings were performed at a frequency of 4 Hz using constant potential amperometry. Glutamate was locally applied into the striatum using a 30 gauge Hamilton needle. While the animal was under isoflurane anesthesia, urethane was administered (1.25 g/kg i.p.).

Amperometric data were analyzed using custom MATLAB[®] - based software. Extracellular glutamate was calculated using the self-referencing method (Burmeister and Gerhardt 2001, Burmeister, et al. 2002). For local application of glutamate, data were filtered using a fourier low pass filter (0.14). For analysis of the decrease in extracellular glutamate from injection of urethane, data were filtered with a fourier low pass filter (0.14) and with a 10 sec boxcar average. The data collected five minutes prior to urethane injection and minutes 5-10 after the urethane injection were compared.

Results

MEAs can continuously measure extracellular glutamate for the initial 72 hours after implantation

Disruptions in extracellular glutamate have been detected in traumatic brain injury survivors using microdialysis, with a vast majority of these disruptions being detected within the first 72 hours of implantation of the microdialysis probe (Persson and Hillered 1992, Bullock, et al. 1995, Bullock, et al. 1998, Koura, et al. 1998, Vespa, et al. 1998, Yamamoto, et al. 1999, Reinert, et al. 2000, Sarrafzadeh, et al. 2000, Hutchinson, et al. 2002, Hlatky, et al. 2004, Chamoun, et al. 2010, Lakshmanan, et al. 2010, Timofeev, et al. 2011a). To test the ability of MEAs to continuously record extracellular

glutamate for the initial 72 hours after implantation, we implanted rats with a MEA and recorded extracellular glutamate levels continuously in the rats for the initial 72 hours after implantation (Fig 5.1A).

In the first animal, we recorded extracellular glutamate levels continuously for 74 hours. In the first hour, extracellular glutamate averaged 0.4 μM with a gradual rise in extracellular glutamate over the next 10 hours reaching a maximum of 10.5 μM . Then, extracellular glutamate levels slowly fell over the next 30 hours where the extracellular glutamate concentration remained stable around ~ 1.0 μM for the remainder of the recording (Fig 5.1B). In the second animal, we record extracellular glutamate levels continuously for 75 hours. Similar to the first animal, there was an initial rise in extracellular glutamate rising from 4.5 μM in the first hour to 28.2 μM thirteen hours later. Unlike the first animal, extracellular glutamate exhibited a diurnal rhythm with sharp increases in extracellular glutamate levels at the start of the second and third dark cycles. The hour prior to the start of the second dark cycle, extracellular glutamate averaged 14.4 μM sharply rising to a maximum of 22.8 μM six hours later. The hour prior to the start of the third dark cycle, extracellular glutamate averaged 12.4 μM sharply rising to a maximum of 17.1 μM three hours later. In the second animal, extracellular glutamate exhibited a potential diurnal rhythm but did not reach a stable baseline during the 75 hours of recording (Fig 5.1C). Thus, MEAs can continuously record extracellular glutamate for at least the initial 72 hours after implantation.

Detection of multiple analytes of interest using a single MEA (glutamate, lactate, pyruvate, or glucose)

Microdialysis studies in TBI survivors have identified certain compounds that could be potential biomarkers for TBI, with extracellular levels of these compounds correlating with injury severity and functional outcomes. The four molecules that have been consistently disrupted in TBI survivors are glutamate (Persson and Hillered 1992, Bullock, et al. 1995, Bullock, et al. 1998, Koura, et al. 1998, Vespa, et al. 1998, Yamamoto, et al. 1999, Reinert, et al. 2000, Sarrafzadeh, et al. 2000, Hutchinson, et al. 2002, Hlatky, et al. 2004, Chamoun, et al. 2010, Lakshmanan, et al. 2010, Timofeev, et al. 2011a), lactate and pyruvate (Persson, et al. 1996, Goodman, et al. 1999, Sarrafzadeh, et al. 2000, Vespa, et al. 2005, Wang, et al. 2007, Carpenter, et al. 2008, Marcoux, et al. 2008, Meierhans, et al. 2010, Zetterling, et al. 2010, De Fazio, et al.

2011, Hejcl, et al. 2011, Nelson, et al. 2011, Timofeev, et al. 2011a, Yokobori, et al. 2011, Dizdarevic, et al. 2012, Oddo, et al. 2012), and glucose (Caspari, et al. 1992, Persson, et al. 1996, Alessandri, et al. 2000, Vespa, et al. 2003, Meierhans, et al. 2010, Timofeev, et al. 2011a, Timofeev, et al. 2011b, Yokobori, et al. 2011, Dizdarevic, et al. 2012).

Previous work in our laboratory has shown that MEAs can detect glutamate, lactate, and glucose (Burmeister, et al. 2004). However, the ability of MEAs to detect multiple analytes on a single MEA was unknown. The purpose of this experiment was to examine the ability of a single MEA to detect multiple compounds of interest. A major obstacle for detection of multiple compounds on a single device is the potential vast concentration differences between the compounds. Extracellular concentrations of glutamate and pyruvate are in the micromolar range. While extracellular concentrations of lactate and glucose are in the millimolar range. Another obstacle for the detection of lactate and glucose is the saturation of their corresponding oxidase enzymes. These enzymes saturate at ~1 mM limiting the ability of the MEAs to detect physiological concentrations. To overcome saturation of the enzymes polyurethane coatings were developed to produce a diffusion barrier preventing saturation of the enzymes and shifting the detectable range into the millimolar range.

The first MEA was configured for the detection of glutamate and lactate. The *in vitro* calibration demonstrated the ability of the MEA to simultaneously measure glutamate and lactate (Fig 5.2A). Additions of 20 μM glutamate produced a step-wise increase in current on the platinum recording site coated with glutamate-oxidase with no response on the recording sites coated with lactate-oxidase. For the glutamate-oxidase recording site, the sensitivity to glutamate was 7.3 pA/ μM (slope), detection limit of 1.0 μM (LOD), and linearity of response equal to 0.99 (R^2). Additions of 2 mM lactate produced a robust step-wise increase in current on the recording site coated with lactate-oxidase with no response on the glutamate-oxidase site despite the large increase in current corresponding to the high concentrations of lactate. For the lactate-oxidase recording site, the sensitivity to lactate was 0.3 pA/ μM (slope), detection limit of 20 μM (LOD), and linearity of response equal to 0.99 (R^2). Using the polyurethane coating, we were able to measure up to 10 mM lactate with a linear response.

The second MEA was configured for the detection of glutamate and pyruvate. The *in vitro* calibration demonstrated the ability of the MEA to simultaneously measure glutamate and pyruvate (Fig 5.2B). Additions of 20 μM and 100 μM pyruvate produced a

corresponding step-wise increase in current on the recording site coated with pyruvate-oxidase with minimal response on the glutamate-oxidase site during additions of the pyruvate. For the pyruvate-oxidase recording site, the sensitivity to pyruvate was 1 pA/ μ M (slope), detection limit of 0.6 μ M (LOD), and linearity of response equal to 0.98 (R^2) up to 500 μ M. Additions of 20 μ M glutamate produced a step-wise increase in current on the platinum recording site coated with glutamate-oxidase with no response on the recording site coated with pyruvate-oxidase. For the glutamate-oxidase recording site, the sensitivity to glutamate was 11 pA/ μ M (slope), detection limit of 0.1 μ M (LOD), and linearity of response equal to 0.99 (R^2).

The third MEA was configured for the detection of glucose and lactate. Polyurethane was coated on the recording sites coated with glucose-oxidase and lactate-oxidase. The *in vitro* calibration demonstrated the ability of the MEA to simultaneously measure glucose and lactate (Fig 5.2C). Additions of 4 mM glucose produced a robust step-wise increase in current on the platinum recording site coated with glucose-oxidase with no response on the recording sites coated with lactate-oxidase. For the glucose-oxidase recording site, the sensitivity to glucose was 0.18 pA/ μ M (slope), detection limit of 12 μ M (LOD), and linearity of response equal to 0.95 (R^2). Additions of 4 mM lactate produced a step-wise increase in current on the recording sites coated with lactate-oxidase with no response on the glucose-oxidase site. For the lactate-oxidase recording site, the sensitivity to lactate was 0.022 pA/ μ M (slope), detection limit of 64 μ M (LOD), and linearity of response equal to 0.99 (R^2). Using the polyurethane coating, we were able to measure up to 20 mM glucose and 8 mM lactate concentrations with a reasonable linear response. Thus, with the use of polyurethane and selective enzyme coatings, MEAs exhibit the ability to detect multiple analytes (glutamate, pyruvate, lactate, and glucose) on a single device. MEA coatings and calibrations were performed in collaboration with Jason Burmiester.

Modification of FDA approved device (AD-TECH[®] Epilepsy/LTM macro-micro depth electrode) for *in vivo* detection of glutamate

The AD-TECH[®] Epilepsy/LTM macro-micro depth electrode provides up to 16 micro-electrodes (38 μ M platinum wire) that could be coated similar to the MEAs for detection of neurochemicals. The AD-TECH[®] Epilepsy/LTM macro-micro depth electrode has four macro-depth electrodes with multiple rows of four micro-depth electrodes

residing above the macro-depth electrodes (Fig 5.3A). Some of the micro-depth electrodes were coated with glutamate-oxidase for the detection of glutamate while other micro-depth electrodes were coated with an inactive protein matrix (sentinel sites) to allow for self-referencing (see methods for details). Using similar coating procedures, we were able to adhere enzyme onto the micro-depth electrodes (Fig 5.3B). The *in vitro* calibration demonstrated the ability of the AD-TECH[®] Epilepsy/LTM macro-micro depth electrode to selectively measure glutamate (Fig 5.3C). Addition of a major interferent (250 μ M ascorbic acid) produced little response on the glutamate-oxidase and sentinel micro-depth electrodes. Additions of 20 μ M glutamate produced a step-wise increase in current on the micro-depth electrodes coated with glutamate-oxidase with minimal response on the sentinel micro-depth electrode. Addition of 8.8 μ M H₂O₂ produced an increase in current on both the glutamate-oxidase and sentinel micro-depth electrodes. For the micro-depth electrode coated with glutamate-oxidase, the sensitivity to glutamate was 15 pA/ μ M (slope), detection limit of 0.9 μ M (LOD), selectivity for glutamate over ascorbic acid (91:1), and linearity of response equal to 0.99 (R²). Thus, we were able to modify an AD-TECH[®] Epilepsy/LTM macro-micro depth electrode to selectively measure glutamate *in vitro*.

Next, we examined the ability of the AD-TECH[®] Epilepsy/LTM macro-micro depth electrode to measure extracellular glutamate *in vivo*. The AD-TECH[®] Epilepsy/LTM macro-micro depth electrode was implanted into the striatum of a rat under isoflurane anesthesia (Fig 5.4A). Local application of 500 μ M glutamate into the rat striatum produced a robust and rapid increase in extracellular glutamate that rapidly returned to baseline (Fig 5.4 B). Prior to injection of glutamate, the baseline value of glutamate was 9.0 μ M. Local application of 500 μ M glutamate produced a glutamate signal with a maximum amplitude of 109.3 μ M that decayed back to baseline levels through glutamate uptake and diffusion from the probe. The time for the signal to decay 80 % (T₈₀) was 11.75 s, with an uptake rate of 9.58 μ M/s. In a second experiment, we examined if we could modulate extracellular glutamate levels. Injection of urethane has been shown to reduce extracellular glutamate levels in awake rats (Rutherford, et al. 2007). While the rat was under isoflurane anesthesia, 1.25 mg/kg of urethane was injected i.p. Under isoflurane anesthesia, extracellular glutamate levels averaged 1.8 μ M, five minutes after injection of urethane extracellular glutamate levels decreased by ~75% to 0.4 μ M (five minute average of extracellular glutamate) (Fig 5.5C). Thus, a modified AD-TECH[®] Epilepsy/LTM macro-micro depth electrode can measure extracellular glutamate *in vivo*.

Discussion

The purpose of this study was to examine the translational potential of MEAs as a novel neuromonitoring device for clinical TBI research. Here, we report MEAs exhibit the properties and capabilities to be a useful tool for clinical TBI research. First, MEAs can continuously measure extracellular glutamate for the initial 72 hours after implantation, which is the temporal window for disruptions in extracellular glutamate in TBI survivors. Second, MEAs can detect multiple potential biomarkers (glutamate, lactate, pyruvate, or glucose) on a single device, molecules that have been previously shown to correlate with injury severity and functional outcomes. Lastly, we were able to transfer a similar methodology of the MEAs onto an already FDA-approved device, AD-TECH[®] Epilepsy/LTM macro-micro depth electrode, for selective measures of extracellular glutamate both *in vitro* and *in vivo*.

The use of an enzyme-based system with constant potential amperometry has certain methodological advantages over microdialysis, currently the only *in vivo* method to detect dynamic extracellular changes in neurochemicals clinically. Since constant potential amperometry measures the current from the oxidation of H₂O₂ generated from specific oxidase enzymes, data are collected at a sub-second scale with real-time data readout at the bedside possible. Although improvements are being made for online analysis of microdialysis samples, most studies require collection and analysis of the microdialysate to obtain neurochemical values. Recent methodological advancements with bedside analyzers such as the CMA ISCUS^{flex} (CMA/Microdialysis, Sweden) permits analysis, monitoring, and time trend display of neurochemicals that interfaces with commonly used intensive care unit systems. However, this approach permits only analysis of glucose, pyruvate, lactate, glycerol and glutamate (Goodman and Robertson 2009). Also, the improved spatial resolution of MEAs and limited damage to the surrounding tissue allows sampling of neurochemicals from the synaptic pool (Day, et al. 2006, Rutherford, et al. 2007, Hascup, et al. 2008, Hinzman, et al. 2012). In contrast, the large sampling area of the microdialysis membrane (10 mm length) and extensive damage from implantation of the microdialysis probe, which limits the ability of microdialysis to sample neurochemicals from the synaptic pool (Borland, et al. 2005, Jaquins-Gerstl and Michael 2009). Furthermore, the low temporal resolution of microdialysis (1-20 min) is inadequate to sample the fast dynamics of neurochemical release and clearance that occurs on the order of milliseconds to seconds (Diamond

2005). Thus, due to these methodological improvements MEAs exhibit tremendous potential as a clinical research tool for TBI.

Our laboratory has developed multiple MEA prototypes for clinical use. The first prototype, Spencer-Gerhardt (SG1), embeds a S2-style MEA onto the surface of a FDA-approved device (Fig 5.5A). Embedding the MEA on the surface of an AD-TECH[®] Spencer[®] probe provides certain advantages for clinical use. The MEAs would be able to gain access to the central nervous system to detect extracellular neurochemicals without the need for additional surgeries or implantations of devices. Also, embedding the MEA on a currently used device such as the AD-TECH[®] Spencer[®] probe would reduce the need for additional training on handling or implanting the device by neurosurgeons. However, permanently embedding the device produces certain disadvantages such as the inability to remove the MEA independently of the AD-TECH[®] Spencer[®] probe. Also, placement of the MEA into the central nervous system will be limited to placement of the AD-TECH[®] Spencer[®] probe. The second prototype, Spencer-Gerhardt (SG2), was developed as an independent device. The SG2 has a S2-style MEA placed on the tip of a long thin polyimide tubing (Fig 5.5B). This prototype allows the MEA to be implanted independently and can be placed in the brain region of interest. Since the device is independent, additional surgery and procedures will be required for implantation. However, this will allow for independent removal of the device. Recent designs of MEAs provide better configurations for the detection of multiple analytes. The DS-PR-8 is a double sided MEA with 16 platinum recording sites, eight on each side arranged in pairs (Fig 5.3C). The configuration of the DS-PR-8 could potentially allow for the simultaneous detection of glutamate, lactate, pyruvate, and glucose on a single device. Further work is needed to examine the capability of the DS-PR-8 to simultaneously measure all four analytes of interest. Lastly, a third clinical prototype is in development, which combines features of the SG1 and SG2. The third generation prototype would consist of an FDA-approved device, such as the AD-TECH[®] Epilepsy/LTM Behnke fried depth electrode that has a central open lumen with an opening at the tip allowing a MEA to be inserted through the middle of the device and extended out of the tip and into the tissue. This strategy would reduce the need for additional surgeries and implantations while retaining the ability to remove the device independently. Ongoing work is proceeding to evaluate and improve clinical designs for translation of MEA technology into the clinic.

Extracellular glutamate recordings in awake animals for the initial 72 hours after implantation revealed a substantial initial increase in extracellular glutamate in the first

10-13 hours after implantation. The inflammatory response from implantation of electrodes into the central nervous systems activates microglia and signals migration of microglia to the injury site, which secrete reactive oxygen species, inflammatory cytokines, and release extracellular glutamate (Turner, et al. 1999, Block and Hong 2005, Polikov, et al. 2005, Block, et al. 2007, McConnell, et al. 2007, Rutherford, et al. 2007). However, these responses are thought to occur over days and weeks after implantation of the device (Turner, et al. 1999). Initial implantation of the device damages multiple structures including capillaries, extracellular matrix, cells, and permits blood-borne macrophage entry into the CNS (Polikov, et al. 2005). The initial damage and subsequent cellular responses may be responsible for the initial increase in extracellular glutamate during the initial 10-13 hours after injury. A likely source of extracellular glutamate is from activated microglia. Also, the cytokine release from the initial damage during implantation may produce cellular swelling and edema, shrinking the extracellular space; thereby, increasing the extracellular glutamate concentration. Future work, should examine if pre-treatment with an anti-inflammatory, such as Rimadyl[®] (carprofen), could reduce or prevent the initial rise in extracellular glutamate.

The ability of the MEAs to simultaneously detect multiple analytes is a significant milestone for MEA technology. Detection of only a single compound of interest was a major disadvantage of MEAs compared to microdialysis, where multiple compounds could be detected and analyzed. Unexpectedly, the MEAs configured for detection of multiple analytes exhibited a similar performance for the detection of the compounds of interest compared to MEAs configured to detect only a single analyte (Burmeister, et al. 2002, Burmeister, et al. 2004, Burmeister, et al. 2005, Hinzman, et al. 2010). Current work on newer configurations of MEAs, such as the DS-PR-8, will allow simultaneous detection of multiple compounds of interest. The newer designs of the MEAs with platinum recordings sites on the front and the back of the ceramic shank will allow the coating of oxidase enzyme on one side and the corresponding sentinel site on the other side. The front/back design should prevent crosstalk where peroxide generated from the oxidase enzyme diffuses to the sentinel site providing a false signal. Also, the eight pairs of platinum recording sites arranged vertically on the ceramic shank will allow the bottom recording sites to be “dip” coated with polyurethane, which is easier and more reproducible than the hand coating of polyurethane onto the individual platinum recording sites, which is necessary for the detection of lactate and glucose. Further work is needed to optimize configurations and a coating on the newer electrode designs

for the simultaneous detection of glutamate, lactate, pyruvate, and glucose on a single device.

An easier path into the clinic may be modifying an already FDA-approved device for detection of the molecules of interest. In this report, we were able to modify an AD-TECH[®] Epilepsy/LTM macro-micro depth electrode to measure extracellular glutamate both *in vitro* and *in vivo*. Using a similar methodology to the MEAs, we were able to coat the microelectrode with glutamate-oxidase and an inactive protein matrix to allow for self-referencing. The modified AD-TECH[®] Epilepsy/LTM macro-micro depth electrode was able to selectively measure glutamate with similar selectivity, limit of detection, and linearity compared to MEAs (Burmeister, et al. 2002, Hinzman, et al. 2010). However, the sensitivity to glutamate (slope) was substantially lower on the AD-TECH[®] Epilepsy/LTM macro-micro depth electrode compared to MEAs. Increasing the sensitivity of the probe could be achieved by increasing the active surface area of the micro-depth electrodes. One option is to increase the diameter of the platinum wire, such as the AD-TECH[®] Epilepsy/LTM macro-micro depth electrode (MM14A-SP05X-000) with 50 μm platinum wires for the micro-depth electrodes. Another option is pooling multiple micro-depth electrodes into a single channel; however, this option would increase the background current and could reduce the spatial ability of the channel to detect glutamate, especially if glutamate release is localized to a single micro-depth electrode. Another way to improve the performance is to move the preamplifier closer to the Epilepsy/LTM macro-micro depth electrode, which should reduce the noise and improve signal detection of the probes. Future work should examine these improvements and further evaluate the ability of FDA-approved devices for the detection of neurochemicals.

In conclusion, MEAs have tremendous potential as a clinical tool to help understand the pathophysiology of TBI and possibly detect a reliable biomarker(s) to aid in the diagnosis of TBI severity, guide management and care of the patient, predict functional outcomes, and test the efficacy of therapeutics. TBI offers a unique platform for translation of this technology into the clinic due to the large number of devices already implanted into the central nervous system of TBI patients. Future work should determine what enzyme/exclusion coatings would be permitted for use in the clinic, develop a final clinical prototype, ensure performance of sterilized probes both *in vitro* and *in vivo*, and examine damage to the central nervous system from implantation of the device compared to other currently used devices, preferably in larger animal models. Advancement of MEAs or MEA technology into the clinic may provide a better

understanding of TBI pathophysiology leading to the development of novel drugs, and/or provide an improved tool to test the efficacy of therapeutics, which could lead to improved outcomes in TBI survivors.

Copyright © Jason Michael Hinzman 2012

Chapter Five: Figures

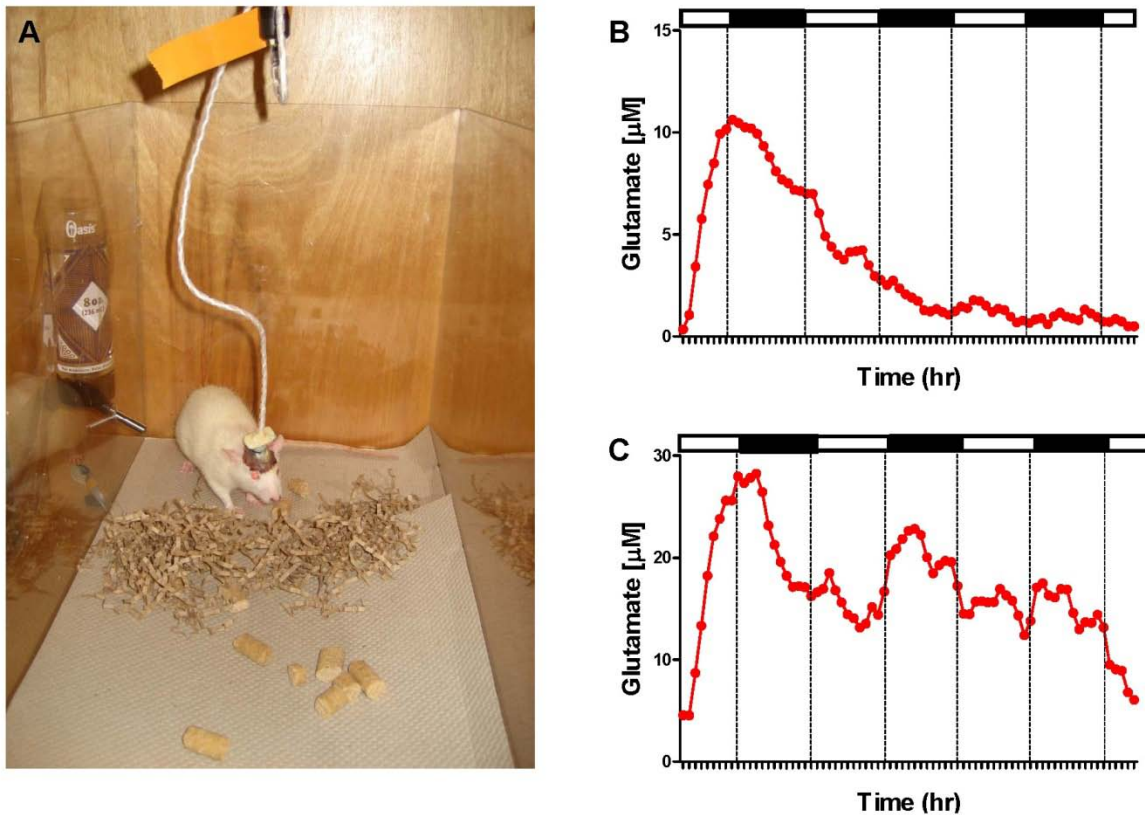


Figure 5.1 MEAs can continuously measure extracellular glutamate for the initial 72 hours after implantation

(A) Rat in the recording chamber was implanted with a MEA pedestal connected to the FAST-16 recording system via a hammerhead-type pre-amplifier. (B) Extracellular glutamate levels in the rat striatum during the initial 72 hours after implantation, open/closed blocks correspond to the day/night cycle. Note the initial rise in extracellular glutamate in the first 10-13 hours that subsides over the next 24-36 hours (glutamate averaged per hour, $n=1$). (C) Extracellular glutamate levels in the rat striatum during the initial 72 hours after implantation, open/closed blocks correspond to the day/night cycle. Note the initial rise in extracellular glutamate in the first 10 hours and subsequent increases in extracellular glutamate that correspond with start of the night cycle on the second and third nights (glutamate averaged per hour, $n=1$).

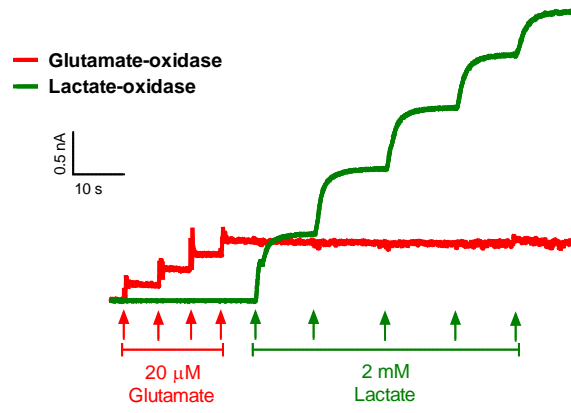
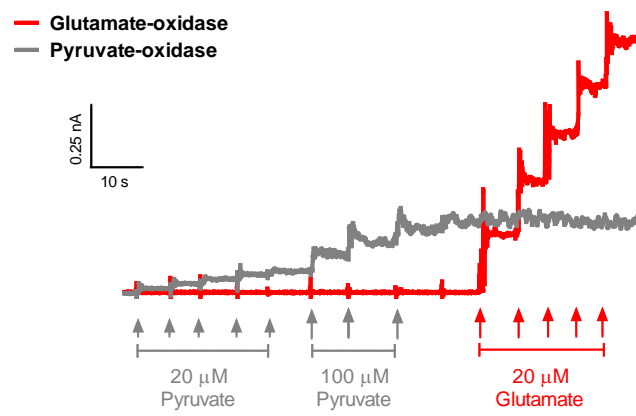
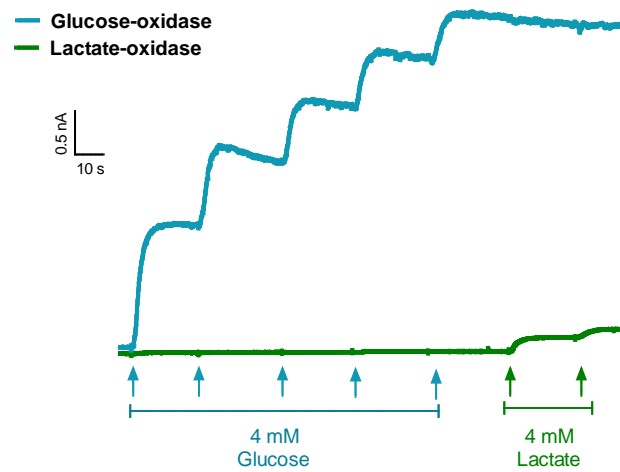
A**Glutamate/Lactate MEA Calibration****B****Glutamate/Pyruvate MEA Calibration****C****Glucose/Lactate MEA Calibration**

Figure 5.2 MEAs can detect multiple analytes of interest on a single device (glutamate, lactate, pyruvate, and glucose)

(A) Calibration of a MEA coated with glutamate-oxidase and lactate-oxidase. Four additions of 20 μM glutamate (\uparrow) produced a stepwise increase in current on the recording site coated with glutamate-oxidase (red). Five additions of 2mM lactate (\uparrow) produced a stepwise increase in current on the recording site coated with lactate-oxidase (green). Note the lack of cross talk between the glutamate-oxidase and lactate-oxidase sites despite the robust signals and concentration differences between the analytes. (B) Calibration of a MEA coated with glutamate-oxidase and pyruvate-oxidase. Five additions of 20 μM pyruvate (small \uparrow) and three additions of 100 μM pyruvate (large \uparrow) produced a proportional stepwise increase in current on the recording site coated with pyruvate-oxidase (grey). Five additions of 20 μM glutamate (\uparrow) produced a stepwise increase in current on the recording site of the MEA coated with glutamate-oxidase (red). (C) Calibration of a MEA coated with glucose-oxidase and lactate-oxidase. Five additions of 4 mM glucose (\uparrow) produced an increase in current on the recording site of the MEA coated with glucose-oxidase (blue). Two additions of 4mM lactate (\uparrow) produced an increase in current on the recording site coated with lactate-oxidase (green). Results obtained in collaboration with Jason Burmeister.

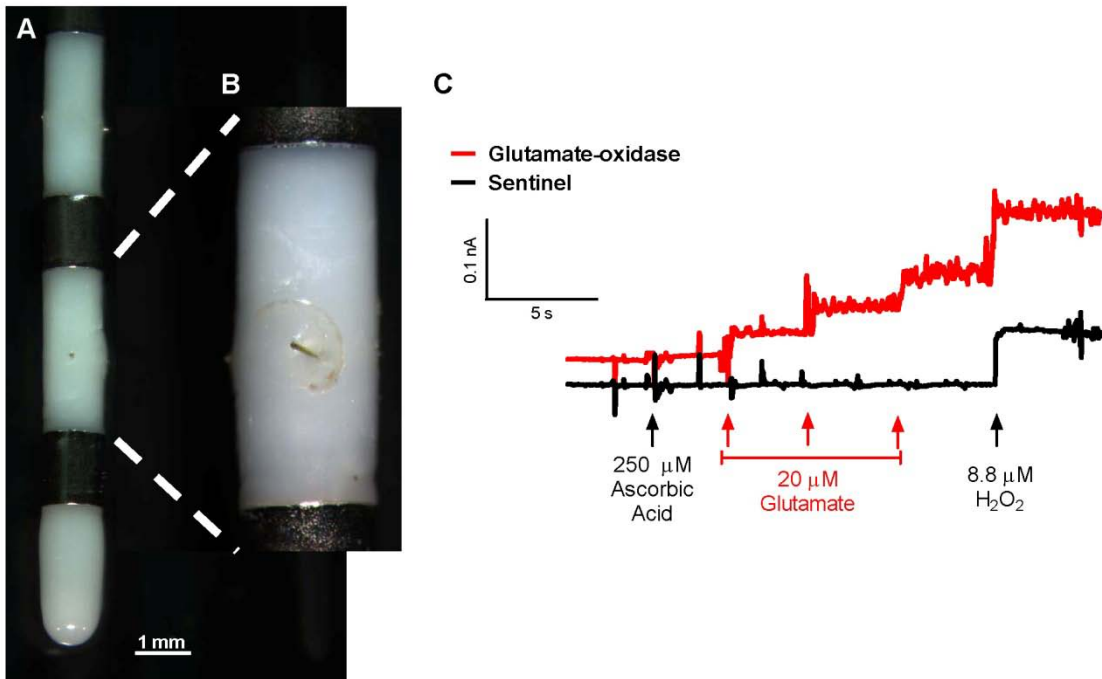


Figure 5.3 Modification of FDA-approved device AD-TECH® Epilepsy/LTM macro-micro depth electrode for real-time glutamate measures using constant potential amperometry

(A) Picture of AD-TECH® Epilepsy/LTM macro-micro depth electrode. (B) Inset, depicting a micro-electrode in between two macro-electrodes that has been coated with glutamate-oxidase for detection of glutamate. (C) *In vitro* calibration measuring the change in current on the micro-electrode coated with glutamate-oxidase (red) and micro-electrode coated with inactive protein matrix (sentinel, black). Addition of an interferent (↑) ascorbic acid produced no change in current on the glutamate-oxidase or sentinel sites. Three glutamate additions (↑) showed a stepwise increase of current on the glutamate-oxidase site with no response on the sentinel site. Addition of H₂O₂ (↑) produced an increase in current on both the glutamate-oxidase and sentinel site.

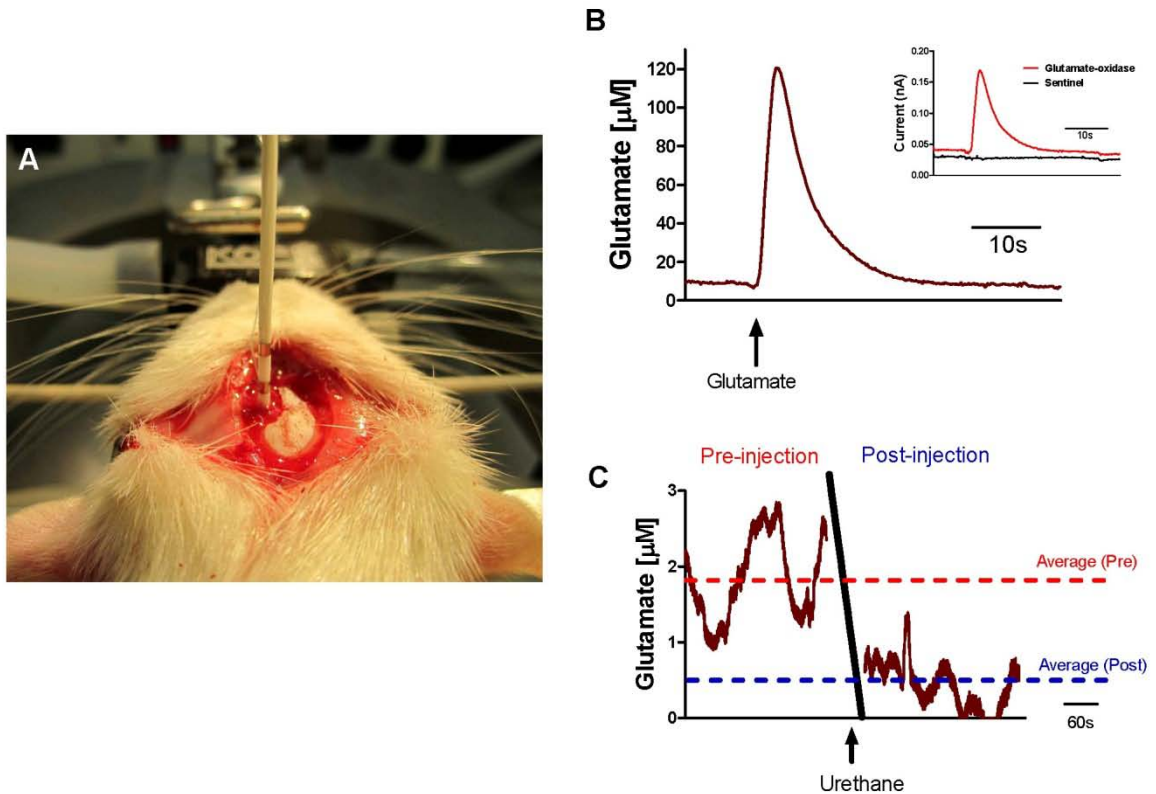


Figure 5.4 *In vivo* detection of extracellular glutamate using modified AD-TECH® Epilepsy/LTM macro-micro depth electrode

(A) Picture showing the AD-TECH® Epilepsy/LTM macro-micro depth electrode implanted in the striatum of an anesthetized rat. (B) Local application of 500 μM glutamate (\uparrow) into the rat striatum produced a robust and rapid increase in extracellular glutamate that rapidly returned to baseline. Inset, depicts the change in current from local application of 500 μM glutamate on a micro-electrode coated with glutamate-oxidase and a micro-electrode coated with an inactive protein matrix (sentinel). Note the lack of response on the sentinel channel. (C) Extracellular glutamate levels decreased after an injection of urethane. While the animal was under isoflurane anesthesia 1.25 mg/kg of urethane was injected i.p. Under isoflurane anesthesia extracellular glutamate levels averaged 1.8 μM , five minutes after injection of urethane extracellular glutamate levels decreased by $\sim 75\%$ to 0.4 μM (five minute average of extracellular glutamate).

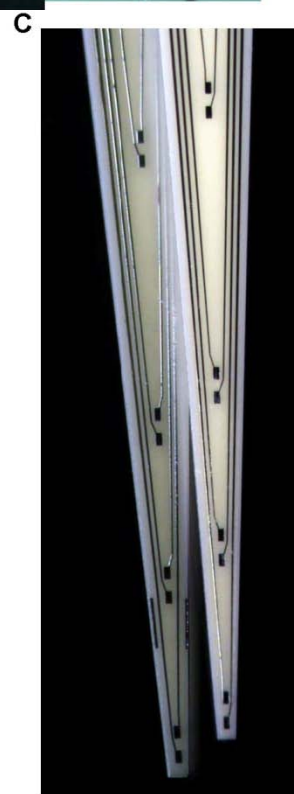
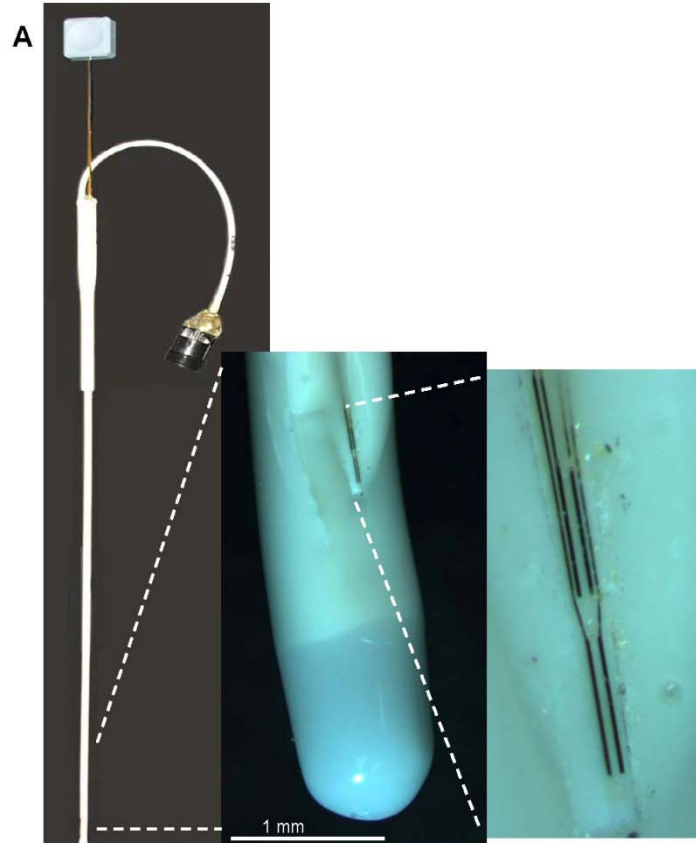


Figure 5.5 MEA prototypes for clinical use

(A,) Picture of Spencer-Gerhardt (SG1) electrode, a modified AD-TECH[®] Spencer[®] probe with a S2-style MEA embedded on the surface of the probe. Higher magnification images show the S2-style MEA embedded on the surface of the AD-TECH[®] Spencer[®] probe. (D) Picture of second generation of the Spencer-Gerhardt (SG2) electrode with a S2-style MEA placed on the tip of a polyimide tubing to allow for implantation into deeper brain structures. (E) Double-sided MEA (DS-PR-8) with 16 platinum recording sites, eight on each side, to allow for the detection of multiple analytes of interest on a single device. Images courtesy Peter Huettl.

Chapter Six: Overall Conclusions

In summary, we have detected several disruptions in the regulation of extracellular glutamate in the rat striatum two days after a diffuse brain injury. First, we detected significant increases in tonic glutamate with tonic glutamate levels correlating with the severity of injury. Second, we determined the contribution of pre-synaptic calcium channel-dependent neuronal glutamate release to extracellular glutamate was significantly decreased in brain-injured animals compared to uninjured animals. Third, the amplitude of glutamate released from local stimulation with KCl was significantly greater in the striatum of brain-injured animals compared to uninjured animals. Fourth, brain-injured animals exhibited slower clearance of extracellular glutamate compared to uninjured animals, due primarily to decreases in glutamate uptake. These results are depicted in schematic format to highlight the disruptions in the regulation of extracellular glutamate in the rat striatum two days after diffuse brain injury (Fig 6.1).

Although tonic glutamate levels were significantly increased in the dentate gyrus and striatum two days after diffuse brain injury, the extracellular concentrations of glutamate do not appear to reach excitotoxic levels as a continuous infusion of 1.8 M glutamate at 0.5 $\mu\text{L/hr}$ was insufficient to produce a neuropathological lesion (Mangano and Schwarcz 1983). However, the post-traumatic increases in tonic glutamate may play a role in a slower, indirect form of excitotoxicity that is mediated by physiological concentrations of glutamate and is thought to be involved in chronic neurodegenerative disorders such as Parkinson's disease, Huntington's disease, amyotrophic lateral sclerosis, and Alzheimer's disease (Albin and Greenamyre 1992, Beal 1992b). "Slow excitotoxicity" involves mitochondrial damage producing an overall reduction in intracellular ATP that impairs the ability of the Na^+/K^+ ATPase to maintain the resting membrane potential (Greene and Greenamyre 1996, Doble 1999). The loss of a stable membrane potential leads to cellular depolarization, removal of the magnesium block from the NMDA receptor, and opening of voltage-gated calcium channels. With cellular depolarization and removal of the magnesium block, the NMDA receptor is more susceptible to activation by ambient or even slightly elevated levels of extracellular glutamate (Beal 1992a, Greene and Greenamyre 1996, Doble 1999). Over prolonged periods of time, slight increases in the activation of the NMDA receptors can activate the same pathophysiological processes of acute excitotoxicity responsible for neuronal death (Olney and de Gubareff 1978, Doble 1999). Slow excitotoxicity may be the

pathophysiological mechanism responsible for the increased risk of epilepsy, Parkinson's disease, and Alzheimer's disease in TBI survivors (Masel and DeWitt 2010). Persistent changes in glutamate regulation in the thalamus and somatosensory cortex have been detected up to 28 days post-injury, suggesting long-term disruptions in glutamate regulation (Thomas, et al. 2011). Further work is needed to determine if disruptions in the regulation of extracellular glutamate will hold true for later time points or indefinitely, providing further evidence for "slow excitotoxicity" as a chronic pathophysiological mechanism of TBI.

Damage from the mechanical forces of the primary brain injury and resulting secondary injury leads to neuronal death and disruption of functional neuronal circuits. The plasticity of the central nervous system facilitates re-connections of synapses and reformation of neuronal networks (Wieloch and Nikolich 2006). This plasticity can be adaptive, re-establishing functional connections or bypassing the damaged area, resulting in normal neurological function; or the plasticity can be maladaptive, forming dysfunctional connections and circuits responsible for producing neurological deficits. Post-traumatic increases in extracellular glutamate may aid maladaptive plasticity forming dysfunctional neuronal connections. Pro-inflammatory cytokines, which are released after TBI, alter the composition, trafficking, and distribution of glutamate receptors leading to increased expression of receptors on the cell surface (Beattie, et al. 2010). The increased surface expression of glutamate receptors in combination with increased extracellular glutamate levels may lead to activation of receptors under ambient conditions. Also, post-traumatic increases in extracellular glutamate could lead to the activation of glutamate receptors extrasynaptically or on neighboring synapses, disrupting neuronal signalling. Activation of extrasynaptic NMDA receptors alters the trafficking, surface expression, and function of NMDA receptors, which can result in epileptogenesis (Luhmann, et al. 1995, Frasca, et al. 2011). Further work is needed to determine if improved glutamate regulation after a TBI prevents or reduces the neurological deficits associated with maladaptive plasticity, such as post-traumatic epilepsy or sensory sensitivity observed in animal models (D'Ambrosio, et al. 2004, McNamara, et al. 2010, Thomas, et al. 2011).

Tonic glutamate levels in the striatum of brain-injured rats were insensitive to the calcium channel blocker ω -conotoxin compared to uninjured animals, suggesting a limited contribution of calcium-dependent vesicular glutamate release to tonic glutamate. This could be explained by either a post-traumatic decrease in neuronal glutamate

release with a concurrent increase in non-neuronal sources of glutamate, or a post-traumatic alteration in the mechanism of vesicular glutamate release that is independent of calcium entry through the calcium channel. Regardless of the mechanism, our data would suggest sodium or calcium channel blockers, may be ineffective in reducing extracellular levels of glutamate. Although we did not detect a significant decrease in extracellular glutamate from transient activation of mGluR_{2/3}, future studies should examine if long-term activation of the glutamate autoreceptors mGluR_{2/3}, which inhibit presynaptic glutamate release and increase expression of the glutamate transporters, can improve the regulation of extracellular glutamate (Nakanishi 1994, Di Iorio, et al. 1996, Battaglia, et al. 1997, Allen, et al. 1999, Schoepp 2001, Zhou, et al. 2006).

Glutamate clearance was significantly slower in the striatum of brain-injured rats compared to uninjured rats, with the decrease in glutamate clearance primarily due to decreases in glutamate uptake. Post-traumatic decreases in glutamate uptake are likely responsible for the increases in tonic glutamate levels and evoked glutamate release detected in the striatum of brain-injured rats. Decreased expression of the glutamate transporters (EAATs) has been detected both clinically and in experimental models of TBI, suggesting post-traumatic reductions in glutamate uptake plays a pivotal role in the pathophysiology of secondary brain injury (Rao, et al. 1998, van Landeghem, et al. 2001, Yi, et al. 2005, van Landeghem, et al. 2006, Yi and Hazell 2006). Reduced glutamate uptake may lead to increased activation of glutamate receptors and fail to contain glutamate release within a single synapse permitting glutamate spillover to neighboring synapses. Further work is needed to pinpoint the mechanism responsible for decreased glutamate uptake in brain-injured rats; biotinylation of the EAATs could examine the surface expression of the receptors and possible oxidative damage to the receptors to determine if reduced glutamate uptake is due to lower expression of the EAATs and/or a decrease in the function of the EAATs (Trotti, et al. 1998, Nickell, et al. 2007).

Since we detected decreases in glutamate uptake in the striatum of brain-injured rats, we wanted to examine therapeutic strategies to increase glutamate uptake and improve glutamate regulation. At the time, intraperitoneal administration of a beta-lactam antibiotic (ceftriaxone) was the only known method to increase the expression of glutamate transporters in the rat brain (Rothstein, et al. 2005). Furthermore, administration of ceftriaxone was shown to reduce neuronal damage and improve behavioral outcomes in a rat model of stroke, providing evidence that increasing

glutamate transporters is a viable approach to prevent/reduce excitotoxicity (Chu, et al. 2006, Chu, et al. 2007). However, this approach was unable to target the expression of the glutamate transporters into the brain region of interest, which may disrupt glutamate signaling in undesired regions producing similar adverse effects seen with glutamate receptor antagonist (Blanke and VanDongen 2009). The overall goal of our viral studies was to identify a novel therapeutic approach that could target the expression of glutamate transporters into the brain region of interest to prevent/limit excitotoxicity while limiting adverse effects. Using a viral-vector mediated gene delivery approach (AAV-GLT-1) we were able to increase the expression of functional GLT-1 into the rat striatum. Work by our collaborator (Dr. Brandon Harvey) showed that intracerebral infusions of AAV-GLT-1 into three cortical sites in the distribution of the right middle cerebral artery prior to occlusion, reduced cerebral infarction, improved functional recovery, reduced ischemia-induced glutamate overflow, and reduced tissue damage (Harvey, et al. 2011). This work further validates the theory that increasing expression of glutamate transporters can improve glutamate regulation, reduce excitotoxicity, and improve outcomes in a model of excitotoxicity. With further development, viral-vector mediated gene delivery of glutamate transporters may be a viable therapeutic strategy to treat neurological disorders involving chronic dysregulation of glutamate. However, the amount of time needed for stable expression of the glutamate transporters (~ 3 weeks) limits the ability of this technique to treat acute excitotoxicity seen in stroke and TBI. Recently, novel activators of GLT-1 have been identified that produce a rapid increase in the expression of the transporter within 24 hours (Xing, et al. 2011). Further work should examine the potential of these compounds to prevent/limit acute excitotoxicity in stroke and TBI animal models.

Presently, there are no approved therapeutics for the treatment of TBI, instead current medical care focuses on maintaining proper physiological parameters such as blood pressure and intracranial pressure (ICP) (Wang, et al. 2006). A major problem hindering the development of successful therapies into the clinic is an inability to model the severity and complexity of severe TBI, which may explain why therapies developed and tested in animal models of TBI have failed to show a clinical benefit (Bullock, et al. 1999). To gain better insight into the physiology of a severe TBI, a multitude of invasive neuromonitors have been developed in the past 20 years. These neuromonitors are currently being used to detect the pathophysiological mechanisms of severe TBI and find a reliable biomarker that could aid in the diagnosis of TBI severity, guide patient care

and management, predict functional outcomes, and test the efficacy of therapeutics (Kirkpatrick, et al. 1996, Patel, et al. 2002, Stuart, et al. 2010). However, only ICP monitoring is currently in the standard of care for management of severe TBI patients (The Brain Trauma Foundation, 2000); emphasizing the need for improved tools to detect the pathophysiological mechanisms of TBI.

We hypothesize that enzyme-based microelectrode arrays (MEAs) can provide insight into the pathophysiological mechanisms of TBI and detect potential biomarkers to guide the care of TBI patients. In chapter Five, we demonstrated the potential of MEAs as a novel neuromonitoring device for severe TBI to help understand the pathophysiology of TBI and possibly detect a reliable biomarker(s). TBI offers a unique platform for translation of MEA technology into the clinic for a variety of reasons. First, there is a large amount of evidence from clinical microdialysis studies confirming glutamate, lactate, pyruvate, and glucose as potential biomarkers for TBI, neurochemicals that MEAs can reliably detect. Second, MEA technology exhibits certain methodological advantages compared to microdialysis for *in vivo* detection of neurochemicals in a clinical setting, such as improved spatial and temporal resolution, limited damage to the central nervous system, and real-time data readouts at the bedside. Third, a multitude of invasive neuromonitors are already being used in severe TBI patients, providing a clear path into the clinic with the rationale, protocols, and procedures already in place for implantation and recording from these devices. Overall, there is a substantial amount of evidence that the care and management of severe TBI patients may benefit from translation of MEA technology into the clinic.

A tremendous amount of work is still needed to make the translational leap into the clinic. We need to design a final clinical prototype with consultation from neurosurgeons to ensure practical functionality of the device. Once the devices are manufactured, we need to ensure that the probes will remain functional after sterilization. Previous work in our lab by Dr. Michelle Stephens has already identified a viable sterilization procedure that should be successful (Stephens, et al. 2010). In addition, we need to determine if we can improve the reliability of the enzyme coatings allowing the performance of the MEAs to be predicted from the initial H₂O₂ calibration. Using the H₂O₂ calibration prior to enzyme coatings, instead of the traditional glutamate calibration that is used prior to implantation in animals, would negate the need for pre-calibrations prior to implantation into the central nervous system, which may not be possible in the clinical situation. With advice from neurosurgeons and researchers, we need to develop

implantation procedures and protocols with a major focus on determining the placement of the probe (white/grey matter, normal/peri-lesional tissue) in the various types of brain injuries (diffuse, focal, subarachnoid hemorrhage, etc.). Furthermore, parameters or tests need to be developed to ensure proper functioning of the device. Lastly, the software for readout and analysis of the data needs to be compatible with currently used ICU equipment and software. Overall, advancement of MEA technology into the clinic may provide insights into the pathophysiology of TBI leading to the development of novel drugs, and/or provide a tool that can reliably detect a biomarker to aide in the diagnosis of TBI severity, guide patient care and management, predict functional outcomes, and test the efficacy of therapeutics, which may lead to improvements in the outcomes of TBI survivors.

Chapter Six: Figures

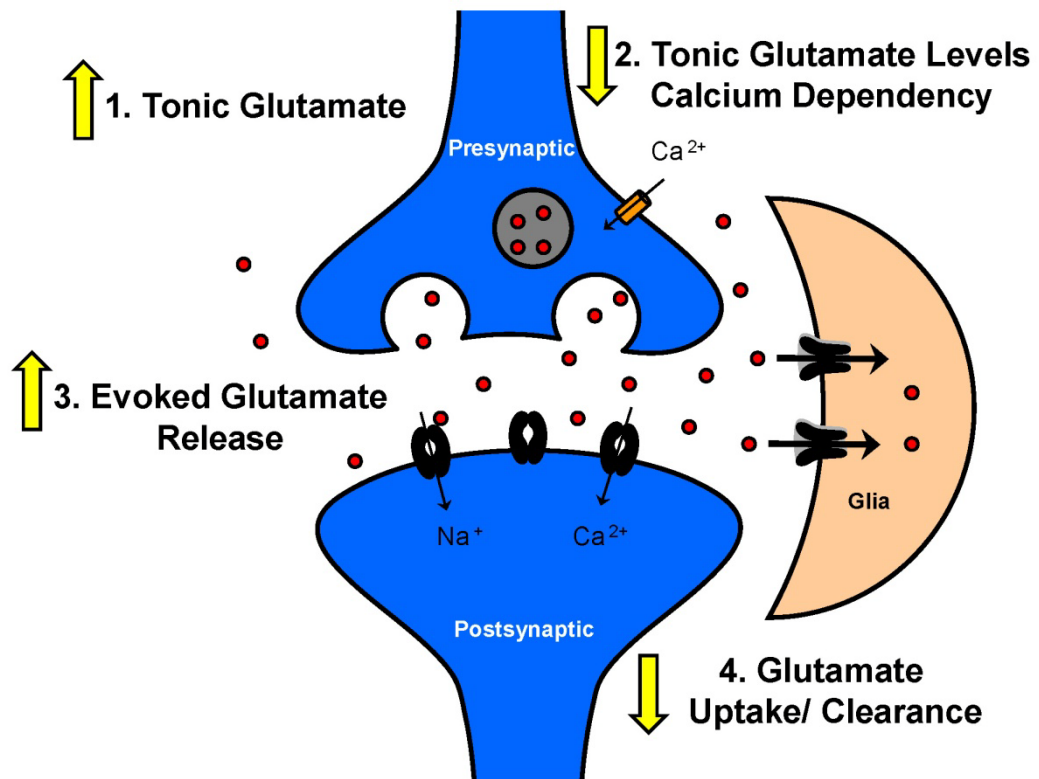


Figure 6.1 Schematic depicting the disruptions in the regulation of extracellular glutamate in the rat striatum two days after diffuse brain injury

In brain-injured rats, we detected post-traumatic disruptions in the regulation of extracellular glutamate that include (1) increased tonic glutamate levels, (2) reduced contribution of calcium-dependent glutamate release to tonic glutamate, (3) increased amplitudes of evoked glutamate release, (4) slower glutamate clearance primarily due to decreases in glutamate.

References

- (2000). The Brain Trauma Foundation. The American Association of Neurological Surgeons. The Joint Section on Neurotrauma and Critical Care. Indications for intracranial pressure monitoring. *J Neurotrauma*. 17:479-491.
- Albin RL and Greenamyre JT. (1992). Alternative excitotoxic hypotheses. *Neurology*. 42:733-738.
- Albrecht P, Lewerenz J, Dittmer S, Noack R, Maher P and Methner A. (2010). Mechanisms of oxidative glutamate toxicity: the glutamate/cystine antiporter system xc⁻ as a neuroprotective drug target. *CNS Neurol Disord Drug Targets*. 9:373-382.
- Alessandri B, Reinert M, Young HF and Bullock R. (2000). Low extracellular (ECF) glucose affects the neurochemical profile in severe head-injured patients. *Acta Neurochir Suppl*. 76:425-430.
- Allen JW, Ivanova SA, Fan L, Espey MG, Basile AS and Faden AI. (1999). Group II metabotropic glutamate receptor activation attenuates traumatic neuronal injury and improves neurological recovery after traumatic brain injury. *J Pharmacol Exp Ther*. 290:112-120.
- Andersen P. 2007. *The hippocampus book*. Oxford University Press: Oxford ; New York.
- Arundine M and Tymianski M. (2004). Molecular mechanisms of glutamate-dependent neurodegeneration in ischemia and traumatic brain injury. *Cell Mol.Life Sci*. 61:657-668.
- Baddeley A. (1992). Working memory. *Science*. 255:556-559.
- Baker DA, Xi ZX, Shen H, Swanson CJ and Kalivas PW. (2002). The origin and neuronal function of in vivo nonsynaptic glutamate. *J Neurosci*. 22:9134-9141.
- Barger SW, Goodwin ME, Porter MM and Beggs ML. (2007). Glutamate release from activated microglia requires the oxidative burst and lipid peroxidation. *J Neurochem*. 101:1205-1213.
- Battaglia G, Monn JA and Schoepp DD. (1997). In vivo inhibition of veratridine-evoked release of striatal excitatory amino acids by the group II metabotropic glutamate receptor agonist LY354740 in rats. *Neurosci Lett*. 229:161-164.
- Beal MF. (1992a). Mechanisms of excitotoxicity in neurologic diseases. *FASEB J*. 6:3338-3344.
- Beal MF. (1992b). Role of excitotoxicity in human neurological disease. *Curr Opin Neurobiol*. 2:657-662.
- Beattie MS, Ferguson AR and Bresnahan JC. (2010). AMPA-receptor trafficking and injury-induced cell death. *Eur J Neurosci*. 32:290-297.

- Blanke ML and VanDongen AMJ. (2009). Activation Mechanisms of the NMDA Receptor.
- Block ML and Hong JS. (2005). Microglia and inflammation-mediated neurodegeneration: multiple triggers with a common mechanism. *Prog Neurobiol.* 76:77-98.
- Block ML, Zecca L and Hong JS. (2007). Microglia-mediated neurotoxicity: uncovering the molecular mechanisms. *Nat Rev Neurosci.* 8:57-69.
- Bond A, Jones NM, Hicks CA, Whiffin GM, Ward MA, O'Neill MF, Kingston AE, Monn JA, Ornstein PL, Schoepp DD, Lodge D and O'Neill MJ. (2000). Neuroprotective effects of LY379268, a selective mGlu2/3 receptor agonist: investigations into possible mechanism of action in vivo. *J Pharmacol Exp Ther.* 294:800-809.
- Bond A, Ragumoorthy N, Monn JA, Hicks CA, Ward MA, Lodge D and O'Neill MJ. (1999). LY379268, a potent and selective Group II metabotropic glutamate receptor agonist, is neuroprotective in gerbil global, but not focal, cerebral ischaemia. *Neurosci Lett.* 273:191-194.
- Borland LM, Shi G, Yang H and Michael AC. (2005). Voltammetric study of extracellular dopamine near microdialysis probes acutely implanted in the striatum of the anesthetized rat. *J Neurosci Methods.* 146:149-158.
- Braugher JM and Hall ED. (1992). Involvement of lipid peroxidation in CNS injury. *J Neurotrauma.* 9 Suppl 1:S1-7.
- Brown GC and Neher JJ. (2010). Inflammatory neurodegeneration and mechanisms of microglial killing of neurons. *Mol Neurobiol.* 41:242-247.
- Bullock MR, Lyeth BG and Muizelaar JP. (1999). Current status of neuroprotection trials for traumatic brain injury: lessons from animal models and clinical studies. *Neurosurgery.* 45:207-217; discussion 217-220.
- Bullock R. (1995). Strategies for neuroprotection with glutamate antagonists. Extrapolating from evidence taken from the first stroke and head injury studies. *Ann N Y Acad Sci.* 765:272-278; discussion 298.
- Bullock R, Zauner A, Myseros JS, Marmarou A, Woodward JJ and Young HF. (1995). Evidence for prolonged release of excitatory amino acids in severe human head trauma. Relationship to clinical events. *Ann N Y Acad Sci.* 765:290-297; discussion 298.
- Bullock R, Zauner A, Woodward JJ, Myseros J, Choi SC, Ward JD, Marmarou A and Young HF. (1998). Factors affecting excitatory amino acid release following severe human head injury. *J Neurosurg.* 89:507-518.
- Burmeister JJ, Coates TD and Gerhardt GA. (2004). Multisite microelectrode arrays for measurements of multiple neurochemicals. *Conf Proc IEEE Eng Med Biol Soc.* 7:5348-5351.

- Burmeister JJ and Gerhardt GA. (2001). Self-referencing ceramic-based multisite microelectrodes for the detection and elimination of interferences from the measurement of L-glutamate and other analytes. *Anal.Chem.* 73:1037-1042.
- Burmeister JJ, Palmer M and Gerhardt GA. (2005). L-lactate measures in brain tissue with ceramic-based multisite microelectrodes. *Biosens Bioelectron.* 20:1772-1779.
- Burmeister JJ, Pomerleau F, Palmer M, Day BK, Huettl P and Gerhardt GA. (2002). Improved ceramic-based multisite microelectrode for rapid measurements of L-glutamate in the CNS. *J.Neurosci.Methods.* 119:163-171.
- Cai Z, Xiao F, Fratkin JD and Rhodes PG. (1999). Protection of neonatal rat brain from hypoxic-ischemic injury by LY379268, a Group II metabotropic glutamate receptor agonist. *Neuroreport.* 10:3927-3931.
- Canales JJ, Capper-Loup C, Hu D, Choe ES, Upadhyay U and Graybiel AM. (2002). Shifts in striatal responsivity evoked by chronic stimulation of dopamine and glutamate systems. *Brain.* 125:2353-2363.
- Capruso DX and Levin HS. (1992). Cognitive impairment following closed head injury. *Neurol Clin.* 10:879-893.
- Carbonell WS and Grady MS. (1999). Evidence disputing the importance of excitotoxicity in hippocampal neuron death after experimental traumatic brain injury. *Ann N Y Acad Sci.* 890:287-298.
- Carpenter KL, Timofeev I, Al-Rawi PG, Menon DK, Pickard JD and Hutchinson PJ. (2008). Nitric oxide in acute brain injury: a pilot study of NO(x) concentrations in human brain microdialysates and their relationship with energy metabolism. *Acta Neurochir Suppl.* 102:207-213.
- Caspari D, Wappler M and Bellaire W. (1992). [Treatment of delirium tremens--a comparison between clomethiazole and clorazepate with reference to effectiveness and rate of side effects]. *Psychiatr Prax.* 19:23-27.
- Chamoun R, Suki D, Gopinath SP, Goodman JC and Robertson C. (2010). Role of extracellular glutamate measured by cerebral microdialysis in severe traumatic brain injury. *J Neurosurg.* 113:564-570.
- Chu K, Lee ST, Jung KH, Kim M and Roh JK. (2006). Upregulation of glutamate transporter-1 by ceftriaxone induces prolonged ischemic tolerance. *Stroke.* 37:730-730.
- Chu K, Lee ST, Sinn DI, Ko SY, Kim EH, Kim JM, Kim SJ, Park DK, Jung KH, Song EC, Lee SK, Kim M and Roh JK. (2007). Pharmacological induction of ischemic tolerance by glutamate transporter-1 (EAAT2) upregulation. *Stroke.* 38:177-182.
- Cooper JR, Bloom FE and Roth RH. 2003. The biochemical basis of neuropharmacology. 8th ed. Oxford University Press: Oxford ; New York.

- Corrigan JD, Selassie AW and Orman JA. (2010). The epidemiology of traumatic brain injury. *J Head Trauma Rehabil.* 25:72-80.
- D'Ambrosio R, Fairbanks JP, Fender JS, Born DE, Doyle DL and Miller JW. (2004). Post-traumatic epilepsy following fluid percussion injury in the rat. *Brain.* 127:304-314.
- Danbolt NC. (2001). Glutamate uptake. *Prog.Neurobiol.* 65:1-105.
- Davalos A, Shuaib A and Wahlgren NG. (2000). Neurotransmitters and pathophysiology of stroke: evidence for the release of glutamate and other transmitters/mediators in animals and humans. *J Stroke Cerebrovasc Dis.* 9:2-8.
- Day BK, Pomerleau F, Burmeister JJ, Huettl P and Gerhardt GA. (2006). Microelectrode array studies of basal and potassium-evoked release of L-glutamate in the anesthetized rat brain. *J.Neurochem.* 96:1626-1635.
- De Fazio M, Rammo R, O'Phelan K and Bullock MR. (2011). Alterations in cerebral oxidative metabolism following traumatic brain injury. *Neurocrit Care.* 14:91-96.
- Delahunty TM, Jiang JY, Gong QZ, Black RT and Lyeth BG. (1995). Differential consequences of lateral and central fluid percussion brain injury on receptor coupling in rat hippocampus. *J Neurotrauma.* 12:1045-1057.
- Delatour B and Gisquet-Verrier P. (2000). Functional role of rat prelimbic-infralimbic cortices in spatial memory: evidence for their involvement in attention and behavioural flexibility. *Behav Brain Res.* 109:113-128.
- Di Iorio P, Battaglia G, Ciccarelli R, Ballerini P, Giuliani P, Poli A, Nicoletti F and Caciagli F. (1996). Interaction between A1 adenosine and class II metabotropic glutamate receptors in the regulation of purine and glutamate release from rat hippocampal slices. *J Neurochem.* 67:302-309.
- Diamond JS. (2005). Deriving the glutamate clearance time course from transporter currents in CA1 hippocampal astrocytes: transmitter uptake gets faster during development. *J.Neurosci.* 25:2906-2916.
- Dixon CE, Lyeth BG, Povlishock JT, Findling RL, Hamm RJ, Marmarou A, Young HF and Hayes RL. (1987). A fluid percussion model of experimental brain injury in the rat. *J.Neurosurg.* 67:110-119.
- Dizdarevic K, Hamdan A, Omerhodzic I and Kominlija-Smajic E. (2012). Modified Lund concept versus cerebral perfusion pressure-targeted therapy: a randomised controlled study in patients with secondary brain ischaemia. *Clin Neurol Neurosurg.* 114:142-148.
- Doble A. (1999). The role of excitotoxicity in neurodegenerative disease: implications for therapy. *Pharmacol Ther.* 81:163-221.

- Domercq M, Sanchez-Gomez MV, Sherwin C, Etxebarria E, Fern R and Matute C. (2007). System xc- and glutamate transporter inhibition mediates microglial toxicity to oligodendrocytes. *J Immunol.* 178:6549-6556.
- Doyle KP, Simon RP and Stenzel-Poore MP. (2008). Mechanisms of ischemic brain damage. *Neuropharmacology.* 55:310-318.
- Faden AI, Demediuk P, Panter SS and Vink R. (1989). The role of excitatory amino acids and NMDA receptors in traumatic brain injury. *Science.* 244:798-800.
- Farkas O, Lifshitz J and Povlishock JT. (2006). Mechanoporation induced by diffuse traumatic brain injury: an irreversible or reversible response to injury? *J. Neurosci.* 26:3130-3140.
- Fonnum F, Storm-Mathisen J and Divac I. (1981). Biochemical evidence for glutamate as neurotransmitter in corticostriatal and corticothalamic fibres in rat brain. *Neuroscience.* 6:863-873.
- Frasca A, Aalbers M, Frigerio F, Fiordaliso F, Salio M, Gobbi M, Cagnotto A, Gardoni F, Battaglia GS, Hoogland G, Di Luca M and Vezzani A. (2011). Misplaced NMDA receptors in epileptogenesis contribute to excitotoxicity. *Neurobiol Dis.* 43:507-515.
- Friedemann MN and Gerhardt GA. (1992). Regional effects of aging on dopaminergic function in the Fischer-344 rat. *Neurobiol. Aging.* 13:325-332.
- Gaetz M. (2004). The neurophysiology of brain injury. *Clin Neurophysiol.* 115:4-18.
- Garber K. (2007). Stroke treatment--light at the end of the tunnel? *Nat Biotechnol.* 25:838-840.
- Gardoni F and Di Luca M. (2006). New targets for pharmacological intervention in the glutamatergic synapse. *Eur J Pharmacol.* 545:2-10.
- Geddes JW and Saatman KE. (2010). Targeting individual calpain isoforms for neuroprotection. *Exp Neurol.* 226:6-7.
- Gemba T, Oshima T and Ninomiya M. (1994). Glutamate efflux via the reversal of the sodium-dependent glutamate transporter caused by glycolytic inhibition in rat cultured astrocytes. *Neuroscience.* 63:789-795.
- Globus MY, Alonso O, Dietrich WD, Busto R and Ginsberg MD. (1995). Glutamate release and free radical production following brain injury: effects of posttraumatic hypothermia. *J Neurochem.* 65:1704-1711.
- Goodman JC and Robertson CS. (2009). Microdialysis: is it ready for prime time? *Curr Opin Crit Care.* 15:110-117.
- Goodman JC, Valadka AB, Gopinath SP, Uzura M and Robertson CS. (1999). Extracellular lactate and glucose alterations in the brain after head injury measured by microdialysis. *Crit Care Med.* 27:1965-1973.

- Grady MS, Charleston JS, Maris D, Witgen BM and Lifshitz J. (2003). Neuronal and glial cell number in the hippocampus after experimental traumatic brain injury: analysis by stereological estimation. *J Neurotrauma*. 20:929-941.
- Greene JG and Greenamyre JT. (1996). Bioenergetics and glutamate excitotoxicity. *Prog Neurobiol*. 48:613-634.
- Hall ED, Andrus PK, Yonkers PA, Smith SL, Zhang JR, Taylor BM and Sun FF. (1994). Generation and detection of hydroxyl radical following experimental head injury. *Ann.N.Y.Acad.Sci*. 738:15-24.
- Hamann M, Rossi DJ, Marie H and Attwell D. (2002). Knocking out the glial glutamate transporter GLT-1 reduces glutamate uptake but does not affect hippocampal glutamate dynamics in early simulated ischaemia. *Eur.J.Neurosci*. 15:308-314.
- Hamm RJ. (2001). Neurobehavioral assessment of outcome following traumatic brain injury in rats: an evaluation of selected measures. *J Neurotrauma*. 18:1207-1216.
- Hamm RJ, Lyeth BG, Jenkins LW, O'Dell DM and Pike BR. (1993). Selective cognitive impairment following traumatic brain injury in rats. *Behav Brain Res*. 59:169-173.
- Harvey BK, Airavaara M, Hinzman J, Wires EM, Chiocco MJ, Howard DB, Shen H, Gerhardt G, Hoffer BJ and Wang Y. (2011). Targeted Over-Expression of Glutamate Transporter 1 (GLT-1) Reduces Ischemic Brain Injury in a Rat Model of Stroke. *PLoS One*. 6:e22135.
- Hascup ER, af Bjerken S, Hascup KN, Pomerleau F, Huettl P, Stromberg I and Gerhardt GA. (2009). Histological studies of the effects of chronic implantation of ceramic-based microelectrode arrays and microdialysis probes in rat prefrontal cortex. *Brain Res*. 1291:12-20.
- Hascup ER, Hascup KN, Stephens M, Pomerleau F, Huettl P, Gratton A and Gerhardt GA. (2010). Rapid microelectrode measurements and the origin and regulation of extracellular glutamate in rat prefrontal cortex. *J Neurochem*. 115:1608-1620.
- Hascup KN, Hascup ER, Pomerleau F, Huettl P and Gerhardt GA. (2008). Second-by-second measures of L-glutamate in the prefrontal cortex and striatum of freely moving mice. *J.Pharmacol.Exp.Ther*. 324:725-731.
- Hascup KN, Rutherford EC, Quintero JE, Day BK, Nickell JR, Pomerleau F, Huettl P, Burmeister JJ and Gerhardt GA. (2007). Second-by-Second Measures of L-Glutamate and Other Neurotransmitters Using Enzyme-Based Microelectrode Arrays.
- Hejcl A, Bolcha M, Prochazka J, Huskova E and Sames M. (2011). Elevated Intracranial Pressure, Low Cerebral Perfusion Pressure, and Impaired Brain Metabolism Correlate with Fatal Outcome after Severe Brain Injury. *Cen Eur Neurosurg*.

- Hillered L, Persson L, Ponten U and Ungerstedt U. (1990). Neurometabolic monitoring of the ischaemic human brain using microdialysis. *Acta Neurochir (Wien)*. 102:91-97.
- Hillered L, Vespa PM and Hovda DA. (2005). Translational neurochemical research in acute human brain injury: the current status and potential future for cerebral microdialysis. *J.Neurotrauma*. 22:3-41.
- Hinzman J, Thomas TC, Quintero J, Gerhardt G and Lifshitz J. (2012). Disruptions in the Regulation of Extracellular Glutamate by Neurons and Glia in the Rat Striatum Two Days after Diffuse Brain Injury. *J Neurotrauma*.
- Hinzman JM, Thomas TC, Burmeister JJ, Quintero JE, Huettl P, Pomerleau F, Gerhardt GA and Lifshitz J. (2010). Diffuse brain injury elevates tonic glutamate levels and potassium-evoked glutamate release in discrete brain regions at two days post-injury: an enzyme-based microelectrode array study. *J Neurotrauma*. 27:889-899.
- Hlatky R, Valadka AB, Goodman JC, Contant CF and Robertson CS. (2004). Patterns of energy substrates during ischemia measured in the brain by microdialysis. *J Neurotrauma*. 21:894-906.
- Howard D, Powers K, Wang Y and Harvey B. (2008). Tropism and toxicity of adeno-associated viral vector serotypes 1, 2, 5, 6, 7, 8, and 9 in rat neurons and glia in vitro. *Virology*. 372:24-34.
- Hoyte L, Barber PA, Buchan AM and Hill MD. (2004). The rise and fall of NMDA antagonists for ischemic stroke. *Curr Mol Med*. 4:131-136.
- Hutchinson PJ, O'Connell MT, Al-Rawi PG, Kett-White CR, Gupta AK, Maskell LB, Pickard JD and Kirkpatrick PJ. (2002). Increases in GABA concentrations during cerebral ischaemia: a microdialysis study of extracellular amino acids. *J Neurol Neurosurg Psychiatry*. 72:99-105.
- Ikonomidou C and Turski L. (2002). Why did NMDA receptor antagonists fail clinical trials for stroke and traumatic brain injury? *Lancet Neurol*. 1:383-386.
- Jabaudon D, Shimamoto K, Yasuda-Kamatani Y, Scanziani M, Gahwiler BH and Gerber U. (1999). Inhibition of uptake unmasks rapid extracellular turnover of glutamate of nonvesicular origin. *Proc Natl Acad Sci U S A*. 96:8733-8738.
- Jaquins-Gerstl A and Michael AC. (2009). Comparison of the brain penetration injury associated with microdialysis and voltammetry. *J Neurosci Methods*. 183:127-135.
- Jensen JB, Pickering DS and Schousboe A. (2000). Depolarization-induced release of [(3)H]D-aspartate from GABAergic neurons caused by reversal of glutamate transporters. *Int J Dev Neurosci*. 18:309-315.
- Kalivas PW. (2009). The glutamate homeostasis hypothesis of addiction. *Nat Rev Neurosci*. 10:561-572.

- Katayama Y, Becker DP, Tamura T and Hovda DA. (1990). Massive increases in extracellular potassium and the indiscriminate release of glutamate following concussive brain injury. *J.Neurosurg.* 73:889-900.
- Katoh H, Sima K, Nawashiro H, Wada K and Chigasaki H. (1997). The effect of MK-801 on extracellular neuroactive amino acids in hippocampus after closed head injury followed by hypoxia in rats. *Brain Res.* 758:153-162.
- Kawamata T, Katayama Y, Hovda DA, Yoshino A and Becker DP. (1995). Lactate accumulation following concussive brain injury: the role of ionic fluxes induced by excitatory amino acids. *Brain Res.* 674:196-204.
- Kelley BJ, Lifshitz J and Povlishock JT. (2007). Neuroinflammatory responses after experimental diffuse traumatic brain injury. *J Neuropathol Exp Neurol.* 66:989-1001.
- Kew JN and Kemp JA. (2005). Ionotropic and metabotropic glutamate receptor structure and pharmacology. *Psychopharmacology (Berl).* 179:4-29.
- Khan F, Baguley IJ and Cameron ID. (2003). 4: Rehabilitation after traumatic brain injury. *Med J Aust.* 178:290-295.
- Kirkpatrick PJ, Czosnyka M and Pickard JD. (1996). Multimodal monitoring in neurointensive care. *J Neurol Neurosurg Psychiatry.* 60:131-139.
- Kobori N, Clifton GL and Dash PK. (2006). Enhanced catecholamine synthesis in the prefrontal cortex after traumatic brain injury: implications for prefrontal dysfunction. *J.Neurotrauma.* 23:1094-1102.
- Kobori N and Dash PK. (2006). Reversal of brain injury-induced prefrontal glutamic acid decarboxylase expression and working memory deficits by D1 receptor antagonism. *J Neurosci.* 26:4236-4246.
- Koizumi H, Fujisawa H, Ito H, Maekawa T, Di X and Bullock R. (1997). Effects of mild hypothermia on cerebral blood flow-independent changes in cortical extracellular levels of amino acids following contusion trauma in the rat. *Brain Res.* 747:304-312.
- Koura SS, Doppenberg EM, Marmarou A, Choi S, Young HF and Bullock R. (1998). Relationship between excitatory amino acid release and outcome after severe human head injury. *Acta Neurochir Suppl.* 71:244-246.
- Lakshmanan R, Loo JA, Drake T, Leblanc J, Ytterberg AJ, McArthur DL, Etchepare M and Vespa PM. (2010). Metabolic crisis after traumatic brain injury is associated with a novel microdialysis proteome. *Neurocrit Care.* 12:324-336.
- Levine B, Cabeza R, McIntosh AR, Black SE, Grady CL and Stuss DT. (2002). Functional reorganisation of memory after traumatic brain injury: a study with H(2)(15)O positron emission tomography. *J Neurol Neurosurg Psychiatry.* 73:173-181.

- Lifshitz J. 2008. Fluid Percussion Injury In: *Animal Models of Acute Neurological Injuries*. In J Chen ZX, X-M Xu and J Zhang (ed). The Humana Press Inc.: Totowa, NJ.
- Lifshitz J, Sullivan PG, Hovda DA, Wieloch T and McIntosh TK. (2004). Mitochondrial damage and dysfunction in traumatic brain injury. *Mitochondrion*. 4:705-713.
- Liu S, Lyeth BG and Hamm RJ. (1994). Protective effect of galanin on behavioral deficits in experimental traumatic brain injury. *J Neurotrauma*. 11:73-82.
- Livak KJ and Schmittgen TD. (2001). Analysis of relative gene expression data using real-time quantitative PCR and the 2(-Delta Delta C(T)) Method. *Methods*. 25:402-408.
- Lowery R, Zhang Y, Kelly E, Lamantia C, Harvey B and Majewska A. (2009). Rapid, long-term labeling of cells in the developing and adult rodent visual cortex using double-stranded adeno-associated viral vectors. *Dev Neurobiol*. 69:674-688.
- Lucas DR and Newhouse JP. (1957). The toxic effect of sodium L-glutamate on the inner layers of the retina. *AMA Arch Ophthalmol*. 58:193-201.
- Luhmann HJ, Mudrick-Donnon LA, Mittmann T and Heinemann U. (1995). Ischaemia-induced long-term hyperexcitability in rat neocortex. *Eur J Neurosci*. 7:180-191.
- Lupinsky D, Moquin L and Gratton A. (2010). Interhemispheric regulation of the medial prefrontal cortical glutamate stress response in rats. *J Neurosci*. 30:7624-7633.
- Lyeth BG, Jenkins LW, Hamm RJ, Dixon CE, Phillips LL, Clifton GL, Young HF and Hayes RL. (1990). Prolonged memory impairment in the absence of hippocampal cell death following traumatic brain injury in the rat. *Brain Res*. 526:249-258.
- Makoroff KL, Cecil KM, Care M and Ball WS, Jr. (2005). Elevated lactate as an early marker of brain injury in inflicted traumatic brain injury. *Pediatr Radiol*. 35:668-676.
- Mangano RM and Schwarcz R. (1983). Chronic infusion of endogenous excitatory amino acids into rat striatum and hippocampus. *Brain Res Bull*. 10:47-51.
- Mao L and Wang JQ. (2002). Glutamate cascade to cAMP response element-binding protein phosphorylation in cultured striatal neurons through calcium-coupled group I metabotropic glutamate receptors. *Mol Pharmacol*. 62:473-484.
- Marcoux J, McArthur DA, Miller C, Glenn TC, Villablanca P, Martin NA, Hovda DA, Alger JR and Vespa PM. (2008). Persistent metabolic crisis as measured by elevated cerebral microdialysis lactate-pyruvate ratio predicts chronic frontal lobe brain atrophy after traumatic brain injury. *Crit Care Med*. 36:2871-2877.
- Marmarou A. (2004). The pathophysiology of brain edema and elevated intracranial pressure. *Cleve Clin J Med*. 71 Suppl 1:S6-8.
- Masel BE and DeWitt DS. (2010). Traumatic brain injury: a disease process, not an event. *J Neurotrauma*. 27:1529-1540.

- Mathew SJ, Price RB and Charney DS. (2008). Recent advances in the neurobiology of anxiety disorders: implications for novel therapeutics. *Am J Med Genet C Semin Med Genet.* 148C:89-98.
- Matsushita Y, Shima K, Nawashiro H, Wada K, Tsuzuki N and Miyazawa T. (2000). Real time monitoring of glutamate following fluid percussion brain injury with hypoxia in the rat. *Acta Neurochir.Suppl.* 76:207-212.
- McAllister TW. (1992). Neuropsychiatric sequelae of head injuries. *Psychiatr Clin North Am.* 15:395-413.
- McConnell GC, Schneider TM, Owens DJ and Bellamkonda RV. (2007). Extraction force and cortical tissue reaction of silicon microelectrode arrays implanted in the rat brain. *IEEE Trans Biomed Eng.* 54:1097-1107.
- McEntee WJ and Crook TH. (1993). Glutamate: its role in learning, memory, and the aging brain. *Psychopharmacology (Berl).* 111:391-401.
- McGinn MJ, Kelley BJ, Akinyi L, Oli MW, Liu MC, Hayes RL, Wang KK and Povlishock JT. (2009). Biochemical, structural, and biomarker evidence for calpain-mediated cytoskeletal change after diffuse brain injury uncomplicated by contusion. *J Neuropathol Exp Neurol.* 68:241-249.
- McIntosh TK, Noble L, Andrews B and Faden AI. (1987). Traumatic brain injury in the rat: characterization of a midline fluid-percussion model. *Cent.Nerv.Syst.Trauma.* 4:119-134.
- McIntosh TK, Smith DH, Meaney DF, Kotapka MJ, Gennarelli TA and Graham DI. (1996). Neuropathological sequelae of traumatic brain injury: relationship to neurochemical and biomechanical mechanisms. *Lab Invest.* 74:315-342.
- McNally L, Bhagwagar Z and Hannestad J. (2008). Inflammation, glutamate, and glia in depression: a literature review. *CNS Spectr.* 13:501-510.
- McNamara KC, Lisembee AM and Lifshitz J. (2010). The whisker nuisance task identifies a late-onset, persistent sensory sensitivity in diffuse brain-injured rats. *J Neurotrauma.* 27:695-706.
- Meierhans R, Bechir M, Ludwig S, Sommerfeld J, Brandi G, Haberthur C, Stocker R and Stover JF. (2010). Brain metabolism is significantly impaired at blood glucose below 6 mM and brain glucose below 1 mM in patients with severe traumatic brain injury. *Crit Care.* 14:R13.
- Melendez RI, Vuthiganon J and Kalivas PW. (2005). Regulation of extracellular glutamate in the prefrontal cortex: focus on the cystine glutamate exchanger and group I metabotropic glutamate receptors. *J Pharmacol Exp Ther.* 314:139-147.
- Montiel T, Camacho A, Estrada-Sanchez AM and Massieu L. (2005). Differential effects of the substrate inhibitor l-trans-pyrrolidine-2,4-dicarboxylate (PDC) and the non-substrate inhibitor DL-threo-beta-benzyloxyaspartate (DL-TBOA) of glutamate

- transporters on neuronal damage and extracellular amino acid levels in rat brain in vivo. *Neuroscience*. 133:667-678.
- Movsesyan VA and Faden AI. (2006). Neuroprotective effects of selective group II mGluR activation in brain trauma and traumatic neuronal injury. *J Neurotrauma*. 23:117-127.
- Muir KW. (2006). Glutamate-based therapeutic approaches: clinical trials with NMDA antagonists. *Curr Opin Pharmacol*. 6:53-60.
- Myseros JS and Bullock R. (1995). The rationale for glutamate antagonists in the treatment of traumatic brain injury. *Ann N Y Acad Sci*. 765:262-271; discussion 298.
- Nakanishi S. (1994). Metabotropic glutamate receptors: synaptic transmission, modulation, and plasticity. *Neuron*. 13:1031-1037.
- Nanitsos EK, Nguyen KT, St'astny F and Balcar VJ. (2005). Glutamatergic hypothesis of schizophrenia: involvement of Na⁺/K⁺-dependent glutamate transport. *J Biomed Sci*. 12:975-984.
- Narayan RK, Michel ME, Ansell B, Baethmann A, Biegon A, Bracken MB, Bullock MR, Choi SC, Clifton GL, Contant CF, Coplin WM, Dietrich WD, Ghajar J, Grady SM, Grossman RG, Hall ED, Heetderks W, Hovda DA, Jallo J, Katz RL, Knoller N, Kochanek PM, Maas AI, Majde J, Marion DW, Marmarou A, Marshall LF, McIntosh TK, Miller E, Mohberg N, Muizelaar JP, Pitts LH, Quinn P, Riesenfeld G, Robertson CS, Strauss KI, Teasdale G, Temkin N, Tuma R, Wade C, Walker MD, Weinrich M, Whyte J, Wilberger J, Young AB and Yurkewicz L. (2002). Clinical trials in head injury. *J Neurotrauma*. 19:503-557.
- Nasr P, Gursahani HI, Pang Z, Bondada V, Lee J, Hadley RW and Geddes JW. (2003). Influence of cytosolic and mitochondrial Ca²⁺, ATP, mitochondrial membrane potential, and calpain activity on the mechanism of neuron death induced by 3-nitropropionic acid. *Neurochem Int*. 43:89-99.
- Neher E and Sakaba T. (2008). Multiple roles of calcium ions in the regulation of neurotransmitter release. *Neuron*. 59:861-872.
- Nelson DW, Thornquist B, MacCallum RM, Nystrom H, Holst A, Rudehill A, Wanecek M, Bellander BM and Weitzberg E. (2011). Analyses of cerebral microdialysis in patients with traumatic brain injury: relations to intracranial pressure, cerebral perfusion pressure and catheter placement. *BMC Med*. 9:21.
- Nicholls DG and Budd SL. (2000). Mitochondria and neuronal survival. *Physiol Rev*. 80:315-360.
- Nicholson C, Chen KC, Hrabetova S and Tao L. (2000). Diffusion of molecules in brain extracellular space: theory and experiment. *Prog Brain Res*. 125:129-154.

- Nickell J, Salvatore MF, Pomerleau F, Apparsundaram S and Gerhardt GA. (2007). Reduced plasma membrane surface expression of GLAST mediates decreased glutamate regulation in the aged striatum. *Neurobiol Aging*. 28:1737-1748.
- Nilsson P, Hillered L, Ponten U and Ungerstedt U. (1990). Changes in cortical extracellular levels of energy-related metabolites and amino acids following concussive brain injury in rats. *J.Cereb.Blood Flow Metab*. 10:631-637.
- Obrenovitch TP. (1999). High extracellular glutamate and neuronal death in neurological disorders. Cause, contribution or consequence? *Ann.N.Y.Acad.Sci*. 890:273-286.
- Obrenovitch TP, Urenjak J, Zilkha E and Jay TM. (2000). Excitotoxicity in neurological disorders--the glutamate paradox. *Int.J.Dev.Neurosci*. 18:281-287.
- Oddo M, Levine JM, Frangos S, Maloney-Wilensky E, Carrera E, Daniel RT, Levivier M, Magistretti PJ and Leroux PD. (2012). Brain Lactate Metabolism in Humans With Subarachnoid Hemorrhage. *Stroke*.
- Okonkwo DO, Buki A, Siman R and Povlishock JT. (1999). Cyclosporin A limits calcium-induced axonal damage following traumatic brain injury. *Neuroreport*. 10:353-358.
- Olney JW and de Gubareff T. (1978). Glutamate neurotoxicity and Huntington's chorea. *Nature*. 271:557-559.
- Palmer AM, Marion DW, Botscheller ML, Swedlow PE, Styren SD and DeKosky ST. (1993). Traumatic brain injury-induced excitotoxicity assessed in a controlled cortical impact model. *J.Neurochem*. 61:2015-2024.
- Patel HC, Menon DK, Tebbs S, Hawker R, Hutchinson PJ and Kirkpatrick PJ. (2002). Specialist neurocritical care and outcome from head injury. *Intensive Care Med*. 28:547-553.
- Pellegrini-Giampietro DE, Cherici G, Alesiani M, Carla V and Moroni F. (1990). Excitatory amino acid release and free radical formation may cooperate in the genesis of ischemia-induced neuronal damage. *J Neurosci*. 10:1035-1041.
- Persson L and Hillered L. (1992). Chemical monitoring of neurosurgical intensive care patients using intracerebral microdialysis. *J Neurosurg*. 76:72-80.
- Persson L, Valtysson J, Enblad P, Warne PE, Cesarini K, Lewen A and Hillered L. (1996). Neurochemical monitoring using intracerebral microdialysis in patients with subarachnoid hemorrhage. *J Neurosurg*. 84:606-616.
- Phillis JW, Ren J and O'Regan MH. (2000). Transporter reversal as a mechanism of glutamate release from the ischemic rat cerebral cortex: studies with DL-threo-beta-benzyloxyaspartate. *Brain Res*. 880:224.
- Pines G, Danbolt N, Bjørås M, Zhang Y, Bendahan A, Eide L, Koepsell H, Storm-Mathisen J, Seeberg E and Kanner B. (1992). Cloning and expression of a rat brain L-glutamate transporter. *Nature*. 360:464-467.

- Polikov VS, Tresco PA and Reichert WM. (2005). Response of brain tissue to chronically implanted neural electrodes. *J Neurosci Methods*. 148:1-18.
- Pomerleau F, Day BK, Huettl P, Burmeister JJ and Gerhardt GA. (2003). Real time in vivo measures of L-glutamate in the rat central nervous system using ceramic-based multisite microelectrode arrays. *Ann.N.Y.Acad.Sci*. 1003:454-457.
- Rao VL, Baskaya MK, Dogan A, Rothstein JD and Dempsey RJ. (1998). Traumatic brain injury down-regulates glial glutamate transporter (GLT-1 and GLAST) proteins in rat brain. *J.Neurochem*. 70:2020-2027.
- Rao VL, Dogan A, Bowen KK, Todd KG and Dempsey RJ. (2001). Antisense knockdown of the glial glutamate transporter GLT-1 exacerbates hippocampal neuronal damage following traumatic injury to rat brain. *Eur.J.Neurosci*. 13:119-128.
- Reeves TM, Lyeth BG and Povlishock JT. (1995). Long-term potentiation deficits and excitability changes following traumatic brain injury. *Exp Brain Res*. 106:248-256.
- Reilly P and Bullock R. 1997. Head injury : pathophysiology and management of severe closed injury. Chapman & Hall Medical: London ; New York.
- Reinert M, Khaldi A, Zauner A, Doppenberg E, Choi S and Bullock R. (2000). High extracellular potassium and its correlates after severe head injury: relationship to high intracranial pressure. *Neurosurg Focus*. 8:e10.
- Rose ME, Huerbin MB, Melick J, Marion DW, Palmer AM, Schiding JK, Kochanek PM and Graham SH. (2002). Regulation of interstitial excitatory amino acid concentrations after cortical contusion injury. *Brain Res*. 943:15-22.
- Rothstein JD, Dykes-Hoberg M, Pardo CA, Bristol LA, Jin L, Kuncl RW, Kanai Y, Hediger MA, Wang Y, Schielke JP and Welty DF. (1996). Knockout of glutamate transporters reveals a major role for astroglial transport in excitotoxicity and clearance of glutamate. *Neuron*. 16:675-686.
- Rothstein JD, Patel S, Regan MR, Haenggeli C, Huang YH, Bergles DE, Jin L, Dykes Hoberg M, Vidensky S, Chung DS, Toan SV, Bruijn LI, Su ZZ, Gupta P and Fisher PB. (2005). Beta-lactam antibiotics offer neuroprotection by increasing glutamate transporter expression. *Nature*. 433:73-77.
- Rutherford EC, Pomerleau F, Huettl P, Stromberg I and Gerhardt GA. (2007). Chronic second-by-second measures of L-glutamate in the central nervous system of freely moving rats. *J.Neurochem*. 102:712-722.
- Ryglewski S, Pflueger HJ and Duch C. (2007). Expanding the neuron's calcium signaling repertoire: intracellular calcium release via voltage-induced PLC and IP3R activation. *PLoS Biol*. 5:e66.
- Saatman KE, Creed J and Raghupathi R. (2010). Calpain as a therapeutic target in traumatic brain injury. *Neurotherapeutics*. 7:31-42.

- Saatman KE, Duhaime AC, Bullock R, Maas AI, Valadka A and Manley GT. (2008). Classification of traumatic brain injury for targeted therapies. *J Neurotrauma*. 25:719-738.
- Sarrafzadeh AS, Sakowitz OW, Callsen TA, Lanksch WR and Unterberg AW. (2000). Bedside microdialysis for early detection of cerebral hypoxia in traumatic brain injury. *Neurosurg Focus*. 9:e2.
- Sattler R and Tymianski M. (2000). Molecular mechanisms of calcium-dependent excitotoxicity. *J Mol Med*. 78:3-13.
- Schmidt RH and Grady MS. (1993). Regional patterns of blood-brain barrier breakdown following central and lateral fluid percussion injury in rodents. *J Neurotrauma*. 10:415-430.
- Schoepp DD. (2001). Unveiling the functions of presynaptic metabotropic glutamate receptors in the central nervous system. *J Pharmacol Exp Ther*. 299:12-20.
- Sheardown MJ, Nielsen EO, Hansen AJ, Jacobsen P and Honore T. (1990). 2,3-DIHYDROXY-6-NITRO-7-SULFAMOYL-BENZO(F)QUINOXALINE - A NEUROPROTECTANT FOR CEREBRAL-ISCHEMIA. *Science*. 247:571-574.
- Shen H, Chen G, Harvey B, Bickford P and Wang Y. (2005). Inosine reduces ischemic brain injury in rats. *Stroke*. 36:654-659.
- Shen H, Kuo CC, Chou J, Delvolve A, Jackson SN, Post J, Woods AS, Hoffer BJ, Wang Y and Harvey BK. (2009). Astaxanthin reduces ischemic brain injury in adult rats. *FASEB J*. 23:1958-1968.
- Simon RP, Swan JH, Griffiths T and Meldrum BS. (1984). BLOCKADE OF N-METHYL-D-ASPARTATE RECEPTORS MAY PROTECT AGAINST ISCHEMIC DAMAGE IN THE BRAIN. *Science*. 226:850-852.
- Singh IN, Sullivan PG, Deng Y, Mbye LH and Hall ED. (2006). Time course of post-traumatic mitochondrial oxidative damage and dysfunction in a mouse model of focal traumatic brain injury: implications for neuroprotective therapy. *J Cereb Blood Flow Metab*. 26:1407-1418.
- Steketee JD. (2003). Neurotransmitter systems of the medial prefrontal cortex: potential role in sensitization to psychostimulants. *Brain Res Brain Res Rev*. 41:203-228.
- Stephens ML, Pomerleau F, Huettl P, Gerhardt GA and Zhang Z. (2010). Real-time glutamate measurements in the putamen of awake rhesus monkeys using an enzyme-based human microelectrode array prototype. *J Neurosci Methods*. 185:264-272.
- Stephens ML, Quintero JE, Pomerleau F, Huettl P and Gerhardt GA. (2009). Age-related changes in glutamate release in the CA3 and dentate gyrus of the rat hippocampus. *Neurobiol Aging*.

- Stoffel M, Eriskat J, Plesnila M, Aggarwal N and Baethmann A. (1997). The penumbra zone of a traumatic cortical lesion: a microdialysis study of excitatory amino acid release. *Acta Neurochir Suppl.* 70:91-93.
- Stoffel M, Plesnila N, Eriskat J, Furst M and Baethmann A. (2002). Release of excitatory amino acids in the penumbra of a focal cortical necrosis. *J Neurotrauma.* 19:467-477.
- Stover JF, Sakowitz OW, Beyer TF, Dohse NK, Kroppenstedt SN, Thomale UW, Schaser KD and Unterberg AW. (2003). Effects of LY379268, a selective group II metabotropic glutamate receptor agonist on EEG activity, cortical perfusion, tissue damage, and cortical glutamate, glucose, and lactate levels in brain-injured rats. *J Neurotrauma.* 20:315-326.
- Stuart RM, Schmidt M, Kurtz P, Waziri A, Helbok R, Mayer SA, Lee K, Badjatia N, Hirsch LJ, Connolly ES and Claassen J. (2010). Intracranial multimodal monitoring for acute brain injury: a single institution review of current practices. *Neurocrit Care.* 12:188-198.
- Sullivan PG, Rabchevsky AG, Waldmeier PC and Springer JE. (2005). Mitochondrial permeability transition in CNS trauma: cause or effect of neuronal cell death? *J.Neurosci.Res.* 79:231-239.
- Sullivan PG, Springer JE, Hall ED and Scheff SW. (2004). Mitochondrial uncoupling as a therapeutic target following neuronal injury. *J Bioenerg Biomembr.* 36:353-356.
- Sun DA, Deshpande LS, Sombati S, Baranova A, Wilson MS, Hamm RJ and DeLorenzo RJ. (2008). Traumatic brain injury causes a long-lasting calcium (Ca²⁺)-plateau of elevated intracellular Ca levels and altered Ca²⁺ homeostatic mechanisms in hippocampal neurons surviving brain injury. *Eur J Neurosci.* 27:1659-1672.
- Swanson CJ, Bures M, Johnson MP, Linden AM, Monn JA and Schoepp DD. (2005). Metabotropic glutamate receptors as novel targets for anxiety and stress disorders. *Nat.Rev.Drug Discov.* 4:131-144.
- Takamori S. (2006). VGLUTs: 'exciting' times for glutamatergic research? *Neurosci Res.* 55:343-351.
- Tanaka K, Watase K, Manabe T, Yamada K, Watanabe M, Takahashi K, Iwama H, Nishikawa T, Ichihara N, Kikuchi T, Okuyama S, Kawashima N, Hori S, Takimoto M and Wada K. (1997). Epilepsy and exacerbation of brain injury in mice lacking the glutamate transporter GLT-1. *Science.* 276:1699-1702.
- Tate DF and Bigler ED. (2000). Fornix and hippocampal atrophy in traumatic brain injury. *Learn Mem.* 7:442-446.
- Tavalin SJ, Ellis EF and Satin LS. (1997). Inhibition of the electrogenic Na pump underlies delayed depolarization of cortical neurons after mechanical injury or glutamate. *J Neurophysiol.* 77:632-638.

- Thomas TC, Grandy DK, Gerhardt GA and Glaser PE. (2009). Decreased dopamine D4 receptor expression increases extracellular glutamate and alters its regulation in mouse striatum. *Neuropsychopharmacology*. 34:436-445.
- Thomas TC, Hinzman J, Gerhardt GA and Lifshitz J. (2012). Hypersensitive glutamate signaling correlates with the development of late-onset behavioral morbidity in diffuse brain-injured circuitry. *J Neurotrauma*.
- Timmerman W and Westerink BH. (1997). Brain microdialysis of GABA and glutamate: what does it signify? *Synapse*. 27:242-261.
- Timofeev I, Carpenter KL, Nortje J, Al-Rawi PG, O'Connell MT, Czosnyka M, Smielewski P, Pickard JD, Menon DK, Kirkpatrick PJ, Gupta AK and Hutchinson PJ. (2011a). Cerebral extracellular chemistry and outcome following traumatic brain injury: a microdialysis study of 223 patients. *Brain*. 134:484-494.
- Timofeev I, Czosnyka M, Carpenter KL, Nortje J, Kirkpatrick PJ, Al-Rawi PG, Menon DK, Pickard JD, Gupta AK and Hutchinson PJ. (2011b). Interaction between brain chemistry and physiology after traumatic brain injury: impact of autoregulation and microdialysis catheter location. *J Neurotrauma*. 28:849-860.
- Tisdall MM and Smith M. (2007). Multimodal monitoring in traumatic brain injury: current status and future directions. *Br J Anaesth*. 99:61-67.
- Tovar YRLB, Santa-Cruz LD, Zepeda A and Tapia R. (2009). Chronic elevation of extracellular glutamate due to transport blockade is innocuous for spinal motoneurons in vivo. *Neurochem Int*. 54:186-191.
- Trotti D, Danbolt NC and Volterra A. (1998). Glutamate transporters are oxidant-vulnerable: a molecular link between oxidative and excitotoxic neurodegeneration? *Trends Pharmacol Sci*. 19:328-334.
- Turner JN, Shain W, Szarowski DH, Andersen M, Martins S, Isaacson M and Craighead H. (1999). Cerebral astrocyte response to micromachined silicon implants. *Exp Neurol*. 156:33-49.
- van Landeghem FK, Stover JF, Bechmann I, Bruck W, Unterberg A, Buhner C and von Deimling A. (2001). Early expression of glutamate transporter proteins in ramified microglia after controlled cortical impact injury in the rat. *Glia*. 35:167-179.
- van Landeghem FK, Weiss T, Oehmichen M and von DA. (2006). Decreased expression of glutamate transporters in astrocytes after human traumatic brain injury. *J Neurotrauma*. 23:1518-1528.
- Vespa P, Bergsneider M, Hattori N, Wu HM, Huang SC, Martin NA, Glenn TC, McArthur DL and Hovda DA. (2005). Metabolic crisis without brain ischemia is common after traumatic brain injury: a combined microdialysis and positron emission tomography study. *J Cereb Blood Flow Metab*. 25:763-774.
- Vespa P, Prins M, Ronne-Engstrom E, Caron M, Shalmon E, Hovda DA, Martin NA and Becker DP. (1998). Increase in extracellular glutamate caused by reduced

cerebral perfusion pressure and seizures after human traumatic brain injury: a microdialysis study. *J Neurosurg.* 89:971-982.

- Vespa PM, McArthur D, O'Phelan K, Glenn T, Etchepare M, Kelly D, Bergsneider M, Martin NA and Hovda DA. (2003). Persistently low extracellular glucose correlates with poor outcome 6 months after human traumatic brain injury despite a lack of increased lactate: a microdialysis study. *J Cereb Blood Flow Metab.* 23:865-877.
- Villmann C and Becker CM. (2007). On the hypes and falls in neuroprotection: Targeting the NMDA receptor. *Neuroscientist.* 13:594-615.
- Wagner AK, Sokoloski JE, Ren D, Chen X, Khan AS, Zafonte RD, Michael AC and Dixon CE. (2005). Controlled cortical impact injury affects dopaminergic transmission in the rat striatum. *J. Neurochem.* 95:457-465.
- Wang KK, Larner SF, Robinson G and Hayes RL. (2006). Neuroprotection targets after traumatic brain injury. *Curr Opin Neurol.* 19:514-519.
- Wang Q, Li AL, Zhi DS and Huang HL. (2007). Effect of mild hypothermia on glucose metabolism and glycerol of brain tissue in patients with severe traumatic brain injury. *Chin J Traumatol.* 10:246-249.
- Wieloch T and Nikolich K. (2006). Mechanisms of neural plasticity following brain injury. *Curr Opin Neurobiol.* 16:258-264.
- Willis C, Lybrand S and Bellamy N. (2004). Excitatory amino acid inhibitors for traumatic brain injury. *Cochrane Database Syst Rev.* CD003986.
- Wu Y, Pearl SM, Zigmond MJ and Michael AC. (2000). Inhibitory glutamatergic regulation of evoked dopamine release in striatum. *Neuroscience.* 96:65-72.
- Xiao X, Li J and Samulski RJ. (1998). Production of high-titer recombinant adeno-associated virus vectors in the absence of helper adenovirus. *J Virol.* 72:2224-2232.
- Xing X, Chang LC, Kong Q, Colton CK, Lai L, Glicksman MA, Lin CL and Cuny GD. (2011). Structure-activity relationship study of pyridazine derivatives as glutamate transporter EAAT2 activators. *Bioorg Med Chem Lett.* 21:5774-5777.
- Yamamoto T, Rossi S, Stiefel M, Doppenberg E, Zauner A, Bullock R and Marmarou A. (1999). CSF and ECF glutamate concentrations in head injured patients. *Acta Neurochir Suppl.* 75:17-19.
- Yi JH and Hazell AS. (2006). Excitotoxic mechanisms and the role of astrocytic glutamate transporters in traumatic brain injury. *Neurochem.Int.* 48:394-403.
- Yi JH, Pow DV and Hazell AS. (2005). Early loss of the glutamate transporter splice-variant GLT-1v in rat cerebral cortex following lateral fluid-percussion injury. *Glia.* 49:121-133.

- Yokobori S, Watanabe A, Matsumoto G, Onda H, Masuno T, Fuse A, Kushimoto S and Yokota H. (2011). Lower extracellular glucose level prolonged in elderly patients with severe traumatic brain injury: a microdialysis study. *Neurol Med Chir (Tokyo)*. 51:265-271.
- Zetterling M, Hallberg L, Hillered L, Karlsson T, Enblad P and Ronne Engstrom E. (2010). Brain energy metabolism in patients with spontaneous subarachnoid hemorrhage and global cerebral edema. *Neurosurgery*. 66:1102-1110.
- Zhou F, Yao HH, Wu JY, Yang YJ, Ding JH, Zhang J and Hu G. (2006). Activation of Group II/III metabotropic glutamate receptors attenuates LPS-induced astroglial neurotoxicity via promoting glutamate uptake. *J.Neurosci.Res.* 84:268-277.

VITA

Name: Jason Michael Hinzman
Date of Birth: 11/17/1983
Birthplace: Lexington, Kentucky, USA

Education

- 2007-2012 Expected Ph.D., University of Kentucky, Department of Anatomy and Neurobiology (G.P.A. 3.71).
- 2002-2006 B.S., Biology, University of Kentucky (Magna Cum Laude with Honors, G.P.A. 3.75).
- 1999-2002 High School Diploma, Holy Cross High School, Covington, KY.

Professional Experience

2012- Ph.D. Thesis Research

My thesis project under the supervision of Dr. Greg Gerhardt and Dr. Jonathan Lifshitz uses recently developed microelectrode arrays to examine post-traumatic alterations in glutamate signaling after diffuse brain injury. My overall research goal is to identify the specific mechanisms responsible for disrupting glutamate signaling after brain injury, and to examine whether targeted therapeutics can improve glutamate regulation and behavioral outcomes after brain injury.

2006 Integrated Biomedical Sciences Rotations

Research under Dr. Jim Geddes and Dr. Greg Gerhardt focused on recording glutamate signaling using a ceramic based microelectrode array in both white and grey matter of the spinal cord. Using the same technology, I developed a method to record real-time glutamate release during spinal cord injury.

2006-2004 Undergraduate Research

Four semesters at the University of Kentucky under Dr. Greg Gerhardt. My specific projects involved optimizing microelectrode arrays to measure dopamine and record dopamine signaling in the striatum of awake freely moving animals using microelectrode arrays. During these rotations I was responsible for learning basic lab duties, animal handling, sterile surgery, and data collection.

Summer research project at the University of Cincinnati under Dr. Winston Kao. My research project involved expressing keratocan in the cornea of keratocan-null mice using a bone marrow stem cell injection. During this rotation I became familiar with genotyping using PCR and gel electrophoresis, sectioning of the cornea, and immunohistochemistry.

Awards and Recognition

2010	Murray Goldstein Award of Excellence (National Neurotrauma Symposium).
2010	Top Student Poster (National Neurotrauma Symposium).
2005, 2009, 2010	Outstanding Student Poster Presentation (Bluegrass Chapter of the Society for Neuroscience).
2005	Outstanding Summer Undergraduate Poster Presentation (Capstone Poster Presentation, University of Cincinnati).
2002-2006	Dean's List (six semesters) University of Kentucky

Poster Presentations

J.M. Hinzman, T.C. Thomas, J.E. Quintero, J. Lifshitz, G.A. Gerhardt. Diffuse Brain Injury Disrupts Glutamate Regulation in the Rat Striatum. Neurotrauma 2011, Fort Lauderdale, FL, July 2011.

J.M. Hinzman, T.C. Thomas, J.E. Quintero P. Huettl, F. Pomerleau, J. Lifshitz, G.A. Gerhardt. Disrupted Glutamate Regulation in the Rat Striatum Two Days after Diffuse Brain Injury. Bluegrass Chapter of the Society for Neuroscience, Lexington, Kentucky, March 2011.

J.M. Hinzman, T.C. Thomas, J.E. Quintero P. Huettl, F. Pomerleau, J. Lifshitz, G.A. Gerhardt. Diffuse Brain Injury Disrupts Glutamate Signaling in the Rat Striatum Two Days Post-Injury: An Enzyme Based Microelectrode Array Study. Society for Neuroscience 40th Annual Meeting 2010, San Diego, CA, Nov 2010.

J.M. Hinzman, T.C. Thomas, J.E. Quintero P. Huettl, F. Pomerleau, J. Lifshitz, G.A. Gerhardt. Injury Severity-Dependent Disruptions in Glutamate Signaling in the Rat Striatum Two Days after Diffuse Brain Injury. Neurotrauma 2010, Las Vegas, NV, June 2010.

J.M. Hinzman, T.C. Thomas, J.E. Quintero P. Huettl, F. Pomerleau, J. Lifshitz, G.A. Gerhardt. Subsecond Glutamate Dynamics Reveal Alterations in Glutamate Signaling in the Rat Striatum Two Days after Diffuse Brain Injury. Kentucky Spinal Cord and Head Injury Research Trust, Lexington, Kentucky, June 2010.

J.M. Hinzman, T.C. Thomas, J.E. Quintero P. Huettl, F. Pomerleau, J. Lifshitz, G.A. Gerhardt. Subsecond Glutamate Dynamics Reveal Alterations in Glutamate Signaling in the Rat Striatum Two Days after Diffuse Brain Injury. Center for Clinical and Translational Science, Lexington, Kentucky, March 2010.

J.M. Hinzman, T.C. Thomas, J.E. Quintero P. Huettl, F. Pomerleau, J. Lifshitz, G.A. Gerhardt. Subsecond Glutamate Dynamics Reveal Alterations in Glutamate Signaling in the Rat Striatum Two Days after Diffuse Brain Injury. Bluegrass Chapter of the Society for Neuroscience, Lexington, Kentucky, March 2010.

J.M. Hinzman, A. Lisembee, P. Huettl, F. Pomerleau, J. Lifshitz, G.A. Gerhardt. Subsecond Glutamate Dynamics Reveal Increases in Tonic Glutamate Levels and Evoked Glutamate Release After Diffuse Brain Injury in the Rat. The Second Joint Symposium of the International and National Neurotrauma Societies, Santa Barbara, California, September, 2009.

J.M. Hinzman, A. Lisembee, P. Huettl, F. Pomerleau, J. Lifshitz, G.A. Gerhardt. Increased Resting Glutamate Levels and Altered Potassium-evoked Glutamate Release after Traumatic Brain Injury in the Rat. Kentucky Spinal Cord and Head Injury Research Trust, Louisville, Kentucky, June 2009.

J.M. Hinzman, A. Lisembee, P. Huettl, F. Pomerleau, J. Lifshitz, G.A. Gerhardt. Increased Resting Glutamate Levels and Altered Potassium-evoked Glutamate Release after Traumatic Brain Injury in the Rat. Bluegrass Chapter of the Society for Neuroscience, Lexington, Kentucky, March 2009.

J.M. Hinzman, A. Lisembee, P. Huettl, F. Pomerleau, J. Lifshitz, G.A. Gerhardt. Alterations in Glutamate Neurotransmission After Traumatic Brain Injury: Study Using Enzyme-Based Microelectrode Arrays. 12th International Conference on In Vivo Methods, Vancouver, Canada, August 2008.

J.M. Hinzman, A. Lisembee, P. Huettl, F. Pomerleau, J. Lifshitz, G.A. Gerhardt. Increased Resting Glutamate Levels and Altered Potassium-evoked Glutamate Release after Traumatic Brain Injury in the Rat. Kentucky Spinal Cord and Head Injury Research Trust, Lexington, Kentucky, June 2008.

J.M. Hinzman, A. Lisembee, P. Huettl, F. Pomerleau, J. Lifshitz, G.A. Gerhardt. Increased Resting Glutamate Levels and Altered Potassium-evoked Glutamate Release after Traumatic Brain Injury in the Rat. Bluegrass Chapter of the Society for Neuroscience, Lexington, Kentucky, March 2008.

J.M. Hinzman, O.M. Littrell, P. Huettl, F. Pomerleau, C.G. Yu, J.W. Geddes, G.A. Gerhardt. Second-by-Second Recordings of L-Glutamate in a Rat Spinal Cord and Injury Model Using Enzyme-Based Microelectrode Arrays. Bluegrass Chapter of the

Society for Neuroscience, Lexington, Kentucky, March 2007.

J.M. Hinzman, H. Liu, W.W. Kao. Expression of keratocan in the cornea of keratocan-null mice following injection of bone marrow stem cells . Capstone Presentation, Cincinnati, Ohio, August 2005.

Manuscripts

Jason M. Hinzman, T.C. Thomas, J.J. Burmeister, J.E. Quintero P. Huettl, F. Pomerleau, G.A. Gerhardt, J. Lifshitz. Diffuse Brain Injury Produces Regional Increases in Tonic Glutamate Levels and Potassium-Evoked Glutamate Release Two Days after Injury in the Rat Central Nervous System. Journal of Neurotrauma. 2010 May;27(5):889-99. PMC 2943939.

B.K. Harvey, M.T. Airavaara, Jason M. Hinzman, E.M. Simons, M.C. Chiocco, D.B. Howard, H. Shen, G.A. Gerhardt, Y. Wang. Over-expression of glutamate transporter 1(GLT-1) reduces ischemic brain injury in rodent model of stroke. PLoS One. 2011;6(8):e22135. Epub 2011 Aug 10. PMC 3154194

DR van Breght, T.C. Thomas, Jason M. Hinzman, T. Cao, G.A. Gerhardt, J.R. Pauly, J. Lifshitz, Substantia Nigra Vulnerability after a Single Moderate Diffuse Brain Injury in the Rat. Experimental Neurology. Epub December 9, 2011.

Jason M. Hinzman, T.C. Thomas, J.E. Quintero, G.A. Gerhardt, J. Lifshitz. Disruptions in the Regulation of Extracellular Glutamate by Neurons and Glia in the Rat Striatum Two Days after Diffuse Brain Injury. Journal of Neurotrauma. Epub 2012 Jan 10.

T.C. Thomas, Jason M. Hinzman, T. Cao, G.A. Gerhardt, J. Lifshitz. Hypersensitive Glutamate Signaling Correlates with the Development of Late-Onset Behavioral Morbidity in Diffuse Brain-injured Circuitry. Journal of Neurotrauma. 2012 Jan: 29 (2): 187-200.

Fellowships

- 2010-2012 Predoctoral Ruth L. Kirschstein National Research Service Award (F31) "Alterations in Glutamate Neurotransmission after Experimental Brain Injury". F31NS067899.
- 2009-2010 Predoctoral Training Program, T32 "Cellular and Molecular Aspects of Brain Aging". T32AG000242.
- 2006-2007 Academic Fellowship: Graduate School, University of Kentucky.
- 2005 Summer Undergraduate Research Fellowship, University of Cincinnati.